Multiparametric Analysis of Tumor Immune Environment

Zipei Feng

Table of Contents

Tables and Figures

List of Abbreviations

ACT	Adoptive cellular therapy	**LMP10**	large multifunctional peptidase 10
APM	antigen processing machinery	**mAb**	monoclonal antibody
b2-m	beta-2-microglobulin	**MDSC**	myeloid-derived suppressor cells
CA	cancer antigen	**MHC**	major histocompatibility complex
CD	Cluster of differentiation	**NBF**	neutral-buffered 10% formalin
CEA	cancer embryonic antigen	**NPV**	Negative-predictive value
CM	Complete medium	**OS**	overall survival
CRC	colorectal carcinoma	**OSCC**	oral squamous cell carcinoma
CSI	cumulative SI	**OSR**	overall survival rate
CTL	cytotoxic T lymphocytes	**OX40**	Tumor necrosis factor receptor superfamily, member 4 (TNFRSF4), also known as CD134
DC	dendritic cell	**PBMC**	peripheral blood mononuclear cells
ddH2O	double-distilled H2O	**PD-1**	Programmed cell death protein 1, also known as CD279
EGFI	epidermal growth factor	**PD-L1**	Programmed death-ligand 1 also known as CD 274 or B7 homolog 1 (B7-H1)
FFPE	Formalin-fixed paraffin-embedded	**PLP**	periodate–lysine–paraformaldehyde
FoxP3	Forkhead box P3 also known as scurfin	**PPMC**	Providence Portland Medical Center
FSC	Frozen section controls	**PPV**	Positive-predictive value
GITR	Tumor necrosis factor receptor superfamily member 18 (TNFRSF18) also known as activation-inducible TNFR family receptor (AITR)	**REP**	Rapid expansion protocol
GM	granulocyte macrophage	**RR**	relative risk
H&E	Hematoxylin and eosin	**RT**	room temperature
HAL	Human applications laboratory	**RT**	room temperature
HC10	MHC heavy chain	**SCC**	squamous cell carcinoma
HIF	hypoxia inducible factor	**SI**	suppression index
HNSCC	head and neck squamous cell carcinoma	**TA**	tumor antigen
HPV	human papilloma virus	**TAM**	tumor-associated macrophage
HRE	hypoxia responsive element	**TAP**	transporter associated with antigen processing
HRP	horse radish peroxidase	**TCR**	T cell receptor
IFN	Interferon	**TIL**	Tumor-infiltrating lymphocytes
IHC	Immunohistochemistry	**TNF**	tumor necrosis factor
IM	invasive margin	**TNM**	tumor, node, metastasis

iNOS	Calcium-insensitive Nitric oxide synthases	**Tregs**	regulatory T cells
IRS	international rating score	**TSA**	tyramide
IU	International unit	**WT**	wild-type

Acknowledgement

I would like to thank my mentor Bernie Fox for introducing me to the world of immunotherapy and facilitating a wonderful experience over the course of my PhD work. I would like to thank members of the Fox Laboratory: Shawn, Sachin, Carmen, Tarsem, Dave, Michael, Christopher, Keith and Tyler for supporting me and teaching me different techniques over the years. I would like to thank Bryan Bell, Rom Leidner and Carlo Bifulco for clinical and translational mentorship. I would also like to thank other members of the Earle A. Chiles Research Institute including Michel Gough, Marka Crittenden, Andy Weinberg, Will Redmond, Hong-Ming Hu, and the Institute director Walter Urba for an integrative and excellent training experience for me.

I thank my thesis committee: Ann Hill, Daniel Clayburgh, Summer Gibbs, Lisa Butterfield, Andy Weinberg and Bernie Fox for all your great support and insight throughout my candidature.

Thanks to the MD/PhD program: David Jacoby, Dan Marks, Johanna Colgrove for the great support over the years. Special thanks to Johanna for editing of the thesis.

Thanks to the CANB program, especially Lola Bichler who has helped me tremendously over the years.

Thanks to my friends and family for supporting me over the years.

Special thanks to our collaborators from PerkinElmer (Cliff, Kent, Kristin, Chi, Ed), Univ. of Halle (Daniel, Barbara, Claudia, Matthias, Alexander), ACD (Emily, Ming-Xiao, Xiao-Jun), the Coussens Lab, ISB (Ilya, Vesteinn, Fred), for making the various projects discussed in each chapter possible.

Special thanks to my funding sources: OCTRI OSLER TL-1 Training Grant, Tartar Trust Fund, for your support.

Abstract

Failure to develop an effective anti-tumor immune response is recognized to be central to the progression of cancer. Patients who are able to mount a strong anti-tumor T cell response – sometimes manifested through increased T cell densities – not only demonstrate improved prognosis, but also respond better to standard and experimental therapies. Conventional single-color immuno-histochemistry approaches are useful in stratifying patients based on the degree of their CD3 and CD8 T cell infiltrate, but are unable to capture important suppressive mechanisms within the tumor microenvironment. We established a technique that allows for studying multiple parameters simultaneously in both human and mice. Using this technique we can show evidence that the interactions between different immune populations can be used as a better prognostic tool compared to CD8 T cell density alone. Furthermore, integrating this tool with clinical trials, as described in the appendices, could be important in understanding the mechanisms of action of the therapies and to develop predictive biomarkers that will allow for better directed therapy.

Chapter 1: Introduction

Improved understanding of the complexity of the tumor microenvironment has led to advances in therapies for patients with cancer. The immune system, in particular, has been demonstrated to be a critical component in the recognition and elimination of neoplastic cells. The prognostic impact of T cell infiltrates was described as early as the 1960s, when Lloyd et al. observed an inverse correlation between the density of lymphocytic infiltrate and stages of cutaneous melanoma[1]. In the past twenty years, work from Schreiber and others elegantly cemented a framework for immune surveillance with the three stages of immunoediting: elimination, equilibrium, and escape. Following the neoplastic transformation of cells, rapid elimination by immune cells almost always occurs; in some circumstances, however, certain tumor cells avoid immune elimination and exist in a state that's kept in check by the immune system. This "equilibrium" stage can last for many years until the neoplastic cells gain additional immunosuppressive advantages, thereby escaping immune surveillance and emerging as clinically evident cancer[2-7]. Antigenic loss and/or aberrant expression of key molecules such as PD-L1 and IDO within the tumor are thought to facilitate T cell anergy and immune escape. In the microenvironment, a network of T cells, B cells, macrophages, dendritic cells, natural killer (NK) cells, neutrophils, eosinophils, endothelial cells and mast cells can all exist within the tumor with little to no beneficial immune function, which ultimately leads to tumor growth. Specifically, it is thought that an enrichment of suppressive immune factors such as TGF-beta, IL-4, IL-10, IL-13, arginase and IDO are

expressed within the tumor microenvironment and can limit anti-tumor immune response[8-12]. Therapies that specifically target the immune escape phase such as anti-CTLA-4 and anti-PD-1 are designed to reverse T cell immunosuppression and restore the immune surveillance to equilibrium or elimination phases where high levels of pro-inflammatory cytokines include IFN-gamma, IL-2, IL-12 and TNF-alpha dictate a strong type I anti-tumor T cell response. In humans, however, great diversity – not only within the cancer cells, but more importantly the immune environment in both the tumor and stroma – accompanies the escaped tumors, resulting in variable responses to surgery, chemotherapy, radiation, and immunotherapy. To identify who will respond better to different therapies and stratify patients, novel tools that allow for objective assessment of immune diversity are much needed.

Objective Immunohistochemistry

Immunohistochemistry has been established as one of the seminal tools for the study of tissue morphology and architecture. Compared to genomics and flow cytometry approaches, immunohistochemistry offers important contextual and positional information of different immune subsets within the tumor and allows for assessment of spatial interactions between these populations[13]. For almost all types of cancer, pathologists examine the tissue under the microscope for the density of various immune populations and grade them as brisk, non-brisk, or absent. On the extreme ends of the spectrum, brisk lymphocytic infiltrate into the tumor, or a “hot” tumor, is frequently associated with more pro-inflammatory

tumor milieu, better response to therapies, and improved outcome. An absence of lymphocytic infiltrate, or a “cold” tumor, is associated with rapid progression of disease[14, 15]. However, for the majority of patients with an intermediate T cell infiltrate, the prognostic accuracy using conventional grading is less clear, as the interpretation is subject to day-to-day bias that decreases the consistency and reliability of the test[16]. Objective assessment using digitized slides and computer software is a critical step towards addressing the subjectivity. Developed by Jerome Galon and colleagues, quantitative assessment of CD3+ and CD8+ T cells at the invasive margin and tumor center has been shown to be highly prognostic, and remarkably more so than conventional AJCC TNM staging[17, 18]. This revolutionized the field of predictive and prognostic biomarker discovery of immune subsets within the tumor, and encouraged the use of digital pathology tools for biomarker discover and validation. Currently, CD8 T cell infiltrates have been shown to have prognostic value in various types of cancer, including melanoma, NSCLC, RCC and bladder cancer[19]. Quantitative IHC assessment can also be predictive, as high densities of CD8 and PD-L1 staining correlate with response to anti-PD-1 immunotherapy agents[20, 21]. However, many patients, with high levels of T cell infiltrates in their tumors, rapidly progress, and other patients, with tumors that have high PD-L1 expression, don’t respond to anti-PD-L1 therapy[22]. *Therefore, we hypothesize that the tumor harbors a complex microenvironment that is difficult to encapsulate with single markers such as CD8 and PD-L1, and that the utilization of multiparametric analysis to study the interactions between cell types could capture a more comprehensive landscape*

of the tumor microenvironment that can help us to more accurately stratify the patients compared to CD8 alone. This central hypothesis is the basis for the work in subsequent chapters.

Multiparametric Immunohistochemistry

Limitations in single marker conventional IHC pose a significant challenge for the development of effective prognostic, as well as predictive biomarkers for cancer immunotherapy. The introduction of novel techniques, such as multiplex IHC, helps overcome some of the obstacles[23]. Compared to single color IHC, the main advantage of multiplex IHC is 2 fold. First, because it allows for the analysis of multiple parameters simultaneously on a single slide, it significantly decreases the amount of tissue required for assessment. Second, perhaps more importantly, the simultaneously analysis of multiple immune cells allows for the study of their spatial relationship, which is valuable information that could be a surrogate for their relative function[23, 24].

The methods for multiplex imaging falls into 2 categories: brightfield and florescent. Brightfield utilizes chromogen deposition such as DAB and AEC, which produces distinct colors for visualization. Compared to other multiplex methodologies, brightfield multiplexing allows for fast visualization of multiple markers on a single tissue stained in an automated platform. On a single slide, it's possible to image up to 5 distinct colors using the conventional method (Figure 1.1).

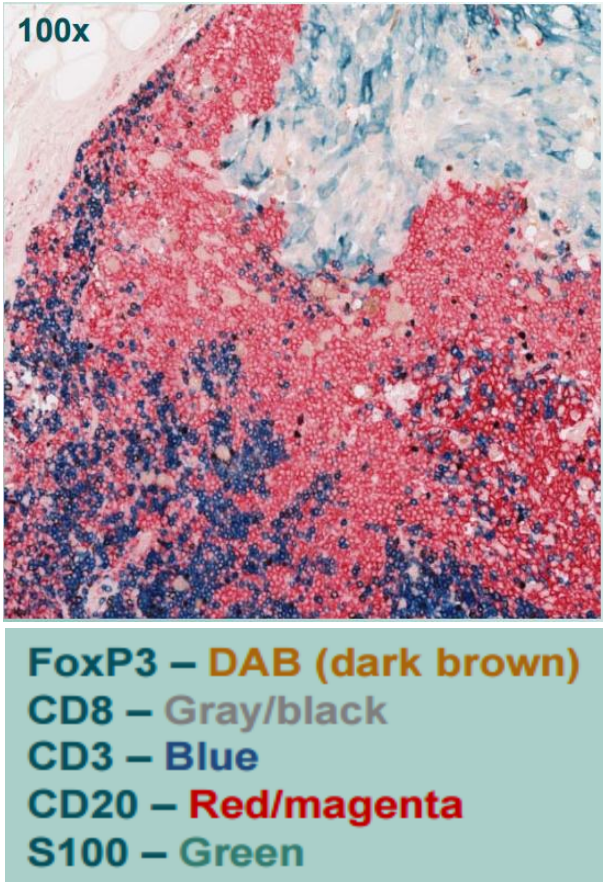

Figure 1.1: 5-plex Brightfield Imaging utilizing Ventana platform. Adapted from Capone et al, SITC 2014

However, subsequent image analysis is limited, as in its current state, the software is inadequate to separate each marker for an objective assessment. Methods with more advanced image alignment and antigen stripping allows for quantitative evaluation of 12 or more markers stained sequentially[25], however, this method is extremely time consuming in both image acquisition and analysis, and can cause antigen loss after multiple rounds of stripping.

Florescent multiplex imaging has long been the standard approach, utilizing the difference in fluorophore emission spectra to establish simultaneous detection of 3 or even 4 markers. However, detection of more than 4 markers simultaneously

has been extremely difficult, due to the inability to effectively strip the previous antigen without affecting the sensitive fluorophore, as well as problems with photobleaching[23]. Recently, advanced imaging technologies utilizing tyramide-based fluorophores as a backbone demonstrated the ability to effectively detect 7 different markers on a single slide. This technology has the potential to be used in an automated process that could increase reproducibility and could find clinical application. Capabilities and drawbacks of this particular method will be extensively discussed in Chapters 2, 3, and 4 in the context of adoptive T cell therapy, murine tumor and spleen studies, and staining of head and neck squamous cell cancer.

Adoptive T cell therapy

In certain cancers such as melanoma and HNSCC, the tumor-infiltrating T cells (TILs) can be isolated from the tumor and expanded *ex vivo* using high dose IL-2. The cytolytic capacity of these T cells against autologous tumor serves as a functional indicator of a pre-existing anti-tumor immune response; more importantly, these tumor-specific T cells can be used for adoptive cell therapy (ACT), a promising treatment strategy for patients with metastatic melanoma. The process involves harvesting T cells from autologous tumor resection or biopsy, expanding them *ex vivo* with IL-2, testing them for tumor-specificity using cytokine production as a functional readout, and ultimately rapidly expanding the tumor-specific TIL for re-infusion into the patients. Non-myeloablative lymphodepletion using chemotherapy is performed prior to infusion to allow for

spaces the T cells can expand into, and high dose IL-2 is administered to support the *in vivo* expansion of transferred T cells[26, 27]. CD8 T cells often constitute the majority of the tumor-specific T cells in culture, other cells such as CD4 T cells, NK cells, and gamma-delta T cells are also present in these cultures and have been shown to possess significant anti-tumor activity[27]. Regulatory T cells are also present and depletion of them prior to re-infusion has positively correlated with increased clinical response to ACT[28-31].

Metastatic melanoma is the most studied cancer type for ACT, and tumor-specific T cells can be recovered from 35-70% of patients depending on methodology and media used and the experience of the center. The response rate in patients reinfused with these TILs is 50-75%[32-34] when used in combination with lympho-depletion and high dose IL-2. Notably, 95% of the complete responders demonstrated a durable response of at least 5 years[34]. The use of ACT for patients with HNSCC has yet to be established. In HNSCC, tumor-specific T cells were able to be cultured from approximately 60% of the tumors, a number that is similar to melanoma[35, 36]. There has been very limited evidence regarding efficacy of treating HPV-negative HNSCC with ACT, the largest study is a Japanese group with 7 patients included in the trial, 5 with SCC, 1 melanoma and 1 spindle cell sarcoma[37]. The overall response rate was 43% with 1 complete responder (CR) who had SCC of the floor of the mouth and received ACT immediately after partial resection of the tumor and surrounding lymph nodes. Despite lacking larger and well-controlled studies with long-term follow-up, ACT represents a promising treatment strategy for the subset of

patients from whom tumor-specific TILs can be isolated and expanded *in vitro*.

A significant hurdle to the use of ACT is the ability to culture and expand tumor-specific T cells from patients' tumors. In renal, breast, and colon cancer, the cell recovery rate is extremely low (0-20%[38]). Strategies to increase the success of recovering tumor-specific T cells from tumor specimens are currently being studied and will be specifically discussed in Chapter 2.

Head and neck squamous cell cancer[#]

As a large portion of the work within this thesis is focused on HNSCC, a brief review of different immunotherapies for HNSCC is provided below. Head and neck squamous cell carcinoma (HNSCC) is the 6th leading cause of cancer worldwide. 45,000 new cases of HNSCC are expected in the United States 2015. Over the last three decades, new discoveries regarding the molecular basis underlying the neoplastic transformation of HNSCC have improved patient treatment and morbidity[39-42]. However, current treatments have failed to provide a significant mortality benefit, a failure potentially caused by an underlying inability of the immune system to contain and clear the malignancy[43-45]. The role of immune suppression has been described in HNSCC as early as the mid-1970s, with the recognition that tumor size and lymph node spread positively correlate with the depression of T cell response to exogenous stimulation[46]. More recent studies identified a hierarchical immunosuppression in lymph nodes of patients with HNSCC, with most immune dysfunction demonstrated in the lymph nodes

closest to the primary tumor[47]. Following the discovery of the role of human papilloma virus (HPV) in HNSCC[48-50], a series of studies have sculpted the distinction of HPV-related HNSCC as a separate disease compared to HPV-negative HNSCC[51-53]. Evidence suggests that this is potentially due to an immune response against viral antigens, leading to increased lymphocytic infiltrate, improved anti-tumor response, and a more favorable clinical outcome[54, 55].

For both HPV-positive and HPV-negative HNSCC, overcoming the immune-suppression through immunotherapies may provide significant long-term benefit in patient outcomes. Although many of these immunotherapy strategies have shown great promise in certain solid malignancies such as melanoma and non-small-cell lung cancer (NSCLC)[56-58], their utilization in HNSCC is still at an early stage. In this chapter, various strategies to increase anti-cancer immune response will be briefly discussed.

Checkpoint Blockade Therapy

Overview: The activation of $CD8^+$ cytotoxic T cells is a multistep process. The first step ("signal 1") is the engagement of the antigen to T cell receptor (TCR) via major histocompatibility complex I (MHCI)[59]. T cell activation is dependent on "signal 2", or the binding of CD80/CD86 from antigen-presenting cells (APCs) to the co-stimulatory receptor CD28[59]. After receiving both "signal 1" and "signal 2", the proliferation of T cell requires "signal 3", or the local cytokine milieu[60].

Cytokines such as IL-12 and IL-2 can strongly support T cell polarization and proliferation, leading to rapid expansion of these antigen-specific T cells that are the basis for an anti-tumor immune response[60, 61]. There are multiple immune "checkpoints", or receptors that serve to dampen an overactive immune response to restore proper homeostasis[19]. These checkpoints are critical in prevention of auto-immune diseases; however, in the case of tumor immunotherapy, they can be utilized by tumor cells to resist immune-mediated killing[19]. Checkpoint blockade antibodies are at the forefront of immunotherapy: blocking these immune checkpoints with antibodies results in restoration of T cell function and heightened anti-tumor response. The efficacy of these antibodies, especially in combination, against a variety of cancer types is ground breaking[56, 58, 62]. While most of the excitement has been focused on anti-CTLA-4, anti-PD-1, and anti-PD-L1, other novel checkpoint blockade inhibitors are also being tested in both preclinical and clinical settings.

CTLA-4: Cytotoxic T-lymphocyte-associated protein 4 (CTLA-4) is a CD28 homologue expressed on the surface of T lymphocytes[59]. CTLA-4 is expressed transiently on the surface of early activated CD8 T cells; however, its expression is constitutive on regulatory T cells (Tregs)[63]. The inhibition of CD8 T cells by CTLA-4 is two-fold: engagement of co-stimulatory molecules CD80 and CD86 to CTLA-4 on CD8 T cells results in the dephosphorylation of T cell receptor (TCR) signaling proteins such as CD3 and LAT, leading to T cell inhibition[64]. Additionally, CTLA-4 has higher affinity for CD80/CD86 than CD28[65]. This

effectively reduces the availability of “signal 2” required for the activation of CD8 T cells, a process that eventually leads to T cell anergy[65]. Blocking antibodies to CTLA-4 result in significant tumor shrinkage in some preclinical cancer models[66-68]. Ipilimumab (anti-CTLA-4, BMS) was approved for treatment of metastatic melanoma in 2011 based on a randomized phase III study demonstrating superior efficacy when compared to vaccine alone (gp100 peptide vaccine)[57]. The mechanism of action of anti-CTLA-4 is currently under investigation. Several groups have reported that anti-CTLA-4 can induce priming of new T cell responses to tumors and depletes Tregs within the tumor microenvironment in a macrophage dependent mechanism[69]. The efficacy of anti-CTLA-4 in head and neck cancer is current being tested in combination with radiation (NCT01935921).

PD-1: Programmed-death receptor 1 (PD-1) is another inhibitory receptor expressed upon T cell activation[70]. Similar to CTLA-4, binding of PD-1 to its ligand PD-L1 induces dephosphorylation of CD3 resulting in T cell anergy and exhaustion[71, 72]. The PD-1 blocking antibody restored CD8 T cell function and augmented anti-tumor activity in numerous pre-clinical models[73-77], and significantly improved survival in patients with melanoma, RCC, and NSCLC[58, 78-82]. For some patients, the response rate can be further increased when PD-1 blocking antibodies are used in combination with an anti-CTLA-4 agent[56, 83]. The FDA recently approved nivolumab (anti-PD-1, BMS) for the treatment of non-small-cell lung cancer based on a phase III study comparing its usage to

cytotoxic chemotherapy for late stage squamous NSCLC[58]. The adverse effects of anti-PD-1 are distinct compared to anti-CTLA-4, outlining their differential mechanism of influence on the immune system. The former is expressed on activated T lymphocytes and is thought to play less of a role in priming of new T cell responses[84]. Consequently, it is currently hypothesized that the efficacy of anti-PD-1 is limited to patients with a pre-existing tumor-specific immune response[22]. At the moment, there are multiple trials testing the efficacy of anti-PD-1 in head and neck cancer as a single agent, with the most recent data showing response rate of 18-23% for anti-PD-1 as a single agent in both HPV-positive and HPV-negative disease, doubling that of chemotherapy. Trials testing the efficacy of anti-PD-1 in combination with radiation and other immunotherapies such as anti-KiR, an inhibitory receptor present on surface of NK cells, are also currently underway. A list of clinical trials using PD-1 blockade is shown in Table 1.

Table 1.1: PD-1/PD-L1 axis for the treatment of HNSCC, adapted from ClinicalTrials.gov

Trial Name	Compound	Clinical Trial Number
Reirradiation With MK-3475 in Locoregional Inoperable Recurrence or Second Primary Squamous Cell CA of the Head and Neck	Pembrolizumab	NCT02289209
Study of MK-3475 (Pembrolizumab) in Recurrent or Metastatic Head and Neck Squamous Cell Carcinoma After Treatment With Platinum-based and Cetuximab Therapy (MK-3475-055/KEYNOTE-055)	Pembrolizumab	NCT02255097
A Combination Clinical Study of PLX3397 and Pembrolizumab To Treat Advanced Melanoma and Other Solid Tumors	PLX3397, Pembrolizumab	NCT02452424
Pembrolizumab (MK-3475) Versus Standard Treatment for Recurrent or Metastatic Head and Neck Cancer (MK-3475-040/KEYNOTE-040)	Pembrolizumab	NCT02252042
A Study of Pembrolizumab (MK-3475) for First Line Treatment of Recurrent or Metastatic Squamous Cell Cancer of the Head and Neck (MK-3475-048/KEYNOTE-048)	Pembrolizumab	NCT02358031
Trial of Nivolumab vs Therapy of Investigator's Choice in Recurrent or Metastatic Head and Neck Carcinoma (CheckMate 141)	Nivolumab	NCT02105636
A Phase I Study of an Anti-KIR Antibody in Combination With an Anti-PD1 Antibody in Patients With Advanced Solid Tumors	Lirilumab, Nivolumab	NCT01714739
A Study of the Safety, Tolerability, and Efficacy of INCB24360 Administered in Combination With Nivolumab in Select Advanced Cancers	Nivolumab, INCB24360	NCT02327078
A Study to Investigate the Safety and Efficacy of Nivolumab in Virus-associated Tumors (CheckMate358)	Nivolumab	NCT02488759
Phase II Study of MEDI4736 Monotherapy in Treatment of Recurrent or Metastatic Squamous Cell Carcinoma of the Head and Neck	MEDI4736	NCT02207530
Study of MEDI4736 Monotherapy and in Combination With Tremelimumab Versus	MEDI4736, Tremelimumab	NCT02369874

Standard of Care Therapy in Patients With Head and Neck Cancer		
Study to Assess Combination of MEDI4736 With Either AZD9150 or AZD5069 in Patients With Metastatic Squamous Cell Carcinoma of Head and Neck	MEDI4736, AZD9150, AZD5069	NCT02499328
A Phase 1 Study of MPDL3280A (an Engineered Anti-PDL1 Antibody) in Patients With Locally Advanced or Metastatic Solid Tumors	MPDL3280A	NCT01375842
A Phase I, Open-Label, Multicentre Study to Evaluate the Safety, Tolerability and Pharmacokinetics of MEDI4736 in Patients With Advanced Solid Tumours	MEDI4736	NCT01938612

PD-L1: Programmed-death receptor ligand-1 (PD-L1) is the ligand for PD-1, and ligation of PD-L1 to PD-1 leads to T cell inhibition[85]. PD-L1 is expressed in a multitude of tissues including muscles and nerves. Of relevance for cancer immunotherapy, PD-L1 can be expressed on the surface of tumor cells, tumor associated macrophages (TAMs), and T lymphocytes, and can subsequently inhibit PD-1 positive T cells[22, 85]. The expression of PD-L1 can be induced by cytokines such as interferons, or alternatively PD-L1 can be expressed autonomously through aberrations in the EGFR signaling pathway[86-89]. In clinical studies, antibodies blocking PD-L1 have demonstrated 6-21% objective response rate (ORR) in non-selected tumors[90, 91], 19% in triple-negative breast cancer[92], and 38% in patients with NSCLC demonstrating high PD-L1 expression[93]. The toxicity profile for anti-PD-L1, like anti-PD-1, is thought to be generally milder compared to the adverse events observed with anti-CTLA-4[91]. The mechanism of action of anti-PD-L1 is currently under investigation. Several studies have shown that clinical benefit is directly correlated with high expression of PD-L1[93]. The

multiple open clinical trials testing the efficacy of anti-PD-L1 in HNSCC are also summarized in Table 1.

Other checkpoint blockade agents: A large numbers of immune checkpoint inhibitors have been discovered and a significant portion of them are currently being tested in either a pre-clinical setting or in clinical trials for the treatment of cancer. Two examples that have moved into the clinical setting are anti-LAG-3, targeting an inhibitory receptor on the surface of T cells; and anti-KIR, to reverse the inhibited natural killer (NK) cells. Trials involving anti-LAG-3 and anti-KIR are underway for the treatment of hematologic and advanced solid malignancies.

Adoptive T cell Therapy with Autologous T cells

Regardless of HPV status, the presence of tumor-infiltrating lymphocytes is associated with more favorable outcomes in HNSCC[44, 45]. The use of adoptive T cell therapy in HNSCC was briefly discussed earlier in this chapter, limited studies have been performed in a few centers[36, 37, 94]. At our center, we have attempted to generate TILs from HNSCC tumors in over 100 patients and successfully generated tumor-specific TILs in about 50% of the samples. We have treated a single patient with aggressive HNSCC using ACT: although the patient progressed rapidly due to the bulk of the disease, there were a few nodules between 3cm and 10cm which showed rapid necrosis and regression, with one 3cm nodule completely disappearing only a week after T cell infusion. We believe that ACT represents a treatment strategy for HNSCC with some

promise, however, there is still a lot to be learned about dosing and timing with high dose IL-2 and potential combination therapies.

Cytokine based therapy

Cytokines are molecular signals that allow intercellular communication over some distance to generate rapid and robust immune responses in a controlled manner. The immune-mediated anti-tumor activities of a few cytokines have been well characterized in pre-clinical settings and led to many clinical trials testing the efficacy of interleukins including IL-2, IL-7, IL-12, IL-15, IL-21; interferons; and GM-CSF. Out of these, high-dose IL-2 was approved for treatment of metastatic melanoma and renal cell carcinoma[95], and IFNα for adjuvant therapy in patients with stage 3 melanoma[96].

IL-2: Interleukin-2 or IL-2, is a member of the IL-2-related family that functions to stimulate T cell growth through the IL-2 receptor. IL-2 exhibits a myriad of effects on the immune system: in addition to promoting CD4 and CD8 T cell proliferation, and differentiation into effector T cells and memory T cells. IL-2 also expands Tregs, which express high-affinity IL-2 receptors[97, 98]. This acts as a negative feedback mechanism to decrease CD8 T cell activity through both depletion of IL-2 and inhibition by Tregs. Systemic high-dose IL-2 plays a key role in the treatment of metastatic melanoma and renal cell carcinoma. Due to acute toxicities, use of high dose IL-2 is limited to patients who are in otherwise good health. It induces objective clinical response in 15-25% of patients with

metastatic melanoma and renal cell carcinoma, with complete response around 7-10%[33, 99-101]. Importantly, of the patients achieving complete response, 80-95% remain disease free for up to 20 years[100, 102].

The use of IL-2 in HNSCC has been used in local-regional or intralesional injection with mixed results. High-dose IL-2 injected local-regionally demonstrated induction of tumor-specific T cells in the draining lymph nodes of patients with HNSCC[103]. However, perilymphatic injection of low-dose, but not high-dose IL-2, demonstrated temporary regression of HNSCC and two complete responders in lip cancer[104-108]. The mechanism for resistance to IL-2 therapy in HNSCC is unclear. It has been suggested in melanoma that patients who fail to demonstrate significant Treg induction experienced an increased response to therapy[109]. One explanation for these observations is that the presence of abundant regulatory T cells unique to HNSCC could be rapidly expanded with IL-2 and thus limit the anti-tumor CD8 response. Combination therapy with systemic high-dose IL-2 and Treg depleting agents, such as cyclophosphamide, may be an avenue to overcome this pathway for the treatment of HNSCC.

IFNα: interferon-α is a type I interferon that is involved in the immune response to viral infections. In cancer immunotherapy, administration of IFNα can activate CD8 T cells, as well as the innate immune system, specifically, NK cells, DCs, and macrophages[110, 111]. This has led to a heightened anti-tumor immune response in pre-clinical models, especially when used in combination therapy

with checkpoint blockade[66]. The use of IFNα clinically has so far been limited to adjuvant setting in high risk melanoma, while it can significantly improve disease-free survival its overall survival benefit seems to be limited to a very small subset of patients[96]. Currently IFNα is being tested in solid tumors in combination with various targeted and immunotherapy agents.

Other cytokines: administration of cytokines such as IL-7, IL-12, IL-15, IL-21, GM-CSF, and inhibition of suppressive cytokines such as TGFβ are still being explored in the treatment of a variety of solid malignancies, including HNSCC. IL-12 has been reported to increase B cell distribution and activation when injected intratumorally in an adjuvant setting for treatment of HNSCC[112, 113], but the clinical benefit is currently unclear. It is possible that we may see increasing number of these agents used in combination therapy for the treatment of HNSCC, as pre-clinical evidence points to increased efficacy of these agents when used in combination with checkpoint blockade or T cell agonists.

Immune system agonists

Upon encountering an antigen, T cells can upregulate co-stimulatory receptors such as OX40 and 4-1BB[19]. Activation of these co-stimulatory receptors can significantly increase T cell proliferation, function, and survival, leading to a greater anti-tumor immune response. A few of these co-stimulatory receptors with clinical application potential are discussed below.

OX40: OX40 is a member of the tumor necrosis factor receptor (TNFR) superfamily and is present on surface of T cells, in particular CD4 T cells and Tregs[30]. Activation of OX40 through an agonist antibody, either directly or indirectly, increases CD4 and CD8 T cell priming, proliferation and function[30]. Interestingly, while OX40 activation in Tregs does not seem to affect their proliferation, their ability to inhibit the function of CD8 T cells appears to be hindered partly through the disruption of FoxP3 expression and inhibitory cytokine release[29, 114]. This tips the effector to inhibitor balance in the tumor microenvironment and results in significant anti-tumor efficacy in many immunogenic pre-clinical models[115]. In poorly immunogenic tumor models, combination with a vaccine appears to substantially improve therapeutic efficacy (Fox lab unpublished). Clinically, 9B12, an agonist antibody to OX40, has had safety demonstrated in a phase I trial[116]. The antibody is currently being tested as a single agent in neoadjuvant setting for the treatment of patients with HNSCC (NCT02274155). Based on pre-clinical evidence, OX40's antitumor activity could potentially be further improved by combining it with a vaccine or PD-1 blockade.

4-1BB: 4-1BB is another member of the TNFR superfamily expressed on activated T cells and NK cells[117]. Its engagement by 4-1BBL or by an agonist antibody on CD8 T cells results in increased proliferation, cytokine production, and survival[118]. 4-1BB activation also has profound impact on the humoral immune system and CD4 T cells[119]. Studies in pre-clinical models of lupus demonstrated suppressed B cell response and induction of CD4 T cell anergy

upon 4-1BB stimulation[120]. In pre-clinical tumor models, in vivo administration of 4-1BB agonist antibody demonstrated enhanced anti-tumor activity in a CD8 T cell dependent manner[121, 122], and currently these agents are being tested in clinical trials for treatment of solid and hematologic malignancies. 4-1BB agonists, either as a single agent or in combination with checkpoint blockade are currently being proposed for the treatment of HNSCC, and new trials could open in the near future.

CD40: CD40 is another member of the TNFR superfamily that is mainly expressed on the surface of APCs. CD40 plays an important role in licensing of APCs by T cells, its ligation by CD40L or an agonist antibody leads to increased expression of MHC complexes and co-stimulatory molecules; secretion of pro-inflammatory cytokines such as IL-12; and increased antigen-presentation. This in turn facilitates the priming of CD4 and CD8 T cells, leading to the activation of NK cells and to an enhanced anti-tumor immune response. CD40 agonist antibodies such as CP-870,893 (Pfizer) and dacetuzumab (Seattle Genetics, discontinued) demonstrated pre-clinical therapeutic efficacy in both solid and hematologic malignancies. Among solid tumors, CD40 agonist antibodies have been tested in the treatment of pancreatic cancer with objective response rate of around 20%. Preliminary study in melanoma with combination CP-870,893 and tremelimumab (anti-CTLA-4, Pfizer) was performed with an ORR at 27.3% and CR at 9.1%[123]. The utilization of anti-CD40 in HNSCC has not yet been extensively explored.

Vaccines

A coordinated anti-tumor immune response that induces both CD4 and CD8 T cell is critical to mediating therapeutic effect. To activate tumor-specific CD4 and CD8 T cells, tumor-associated antigens (TAAs) are processed and cross-presented by APCs. When the immune system is functioning optimally and in the presence of adequate co-stimulatory signals and cytokines, the T cells are activated and expanded in numbers that can recognize and eliminate tumor cells. It is currently hypothesized that a pre-existing anti-tumor T cell response is critical to the therapeutic effectiveness of checkpoint blockade, especially anti-PD-1. For patients lacking this pre-existing tumor-specific immune response, priming a new anti-tumor response through vaccines is expected to provide substantial benefit to therapy containing checkpoint blockade or immune system agonists. The many forms of vaccines will be briefly discussed below.

Peptide and whole protein vaccine: The utilization of peptide vaccine for the treatment of cancer has expanded since one of the first studies used a MAGE-1 peptide for the treatment of melanoma[124]. Delivery of peptide-based vaccine with an immune adjuvant or pulsed onto DCs has been shown to elicit peptide-specific CD8 T cell responses. Peptide cocktails have been used with various degrees of success in certain solid tumors, with one study using IDM-2101, a 10-peptide vaccine cocktail for treatment of patients with stage IIIB and IV NSCLC. The study reported no significant adverse effect with 17.3 month median overall

survival[125]. For vaccines containing single whole-protein, progression-free survival and median overall survival benefit has been observed[126, 127]. These results led to the first FDA-approved cancer vaccine, Sipuleucel-T, for the treatment of castration-resistant prostate cancer. However, very few durable responses were observed with single peptide vaccines, potentially because the protein antigen was down regulated by the tumor cells[128].

Whole cell vaccines: Whole cell vaccines are prepared using irradiated whole tumor cells and are frequently delivered with an adjuvant, such as GM-CSF. One advantage of whole cell vaccines, compared to a peptide vaccine, is that it contains a richer antigenic profile. By using the autologous tumor, multiple relevant antigens can potentially be targeted in a single vaccine, aimed to induce anti-tumor immune response when combined with a stimulatory adjuvant. Genetic modification of the tumor has also been accomplished, particularly with GM-CSF, which stimulates recruitment of DCs to the vaccine site and results in augmented antigen processing and presentation to both T and B cells[129]. Due to the cost and difficulty coordinating autologous vaccine preparation, allogeneic vaccine strategies now represent the bulk of whole tumor vaccine trials[130]. The assumption with allogeneic vaccines is that many antigens are shared between tumors so that vaccination with an allogeneic tumor can effectively prime an immune response towards antigens commonly overexpressed by a patient's autologous tumor. This approach demonstrated promise with one phase II study reporting median survival of 24.8 month in patients with pancreatic

adenocarcinoma vaccinated with GM-CSF secreting allogeneic tumor[131].

Autophagosome-based vaccines: Autophagy, the process by which cells recycle cellular components through autophagolysosomal fusion, is essential in the immune recognition of cancer[132-134]. Tumor autophagy is necessary for tumor-specific T cell priming through the induction of cross-presentation of tumor antigens by DCs[135, 136]. In addition, tumor-derived autophagosomes contain short-lived proteins and defective ribosomal products, which represent the major source of proteins for MHC class I-restricted self-peptides[137, 138]. These two types of proteins degrade rapidly and are not enriched in whole-cell vaccines but are captured and enriched in the autophagosome-based vaccines. Anti-tumor efficacy has been shown in several different pre-clinical models[135, 139, 140] and DRibbles (UbiVac), an autophagosome-based vaccine, is currently being tested in an ongoing multicenter phase II clinical trial in patients with non-small cell lung cancer (NCT01909752). A trial for the treatment of patients with HNSCC is being planned.

HPV vaccine: HPV-related HNSCC has been steadily on the rise for the last 3 decades in United States with a concurrent decrease in smoking related HNSCC[141]. It is estimated that by 2020, HPV-related HNSCC cases will be more frequent then HPV-negative cases[142]. HPV is a DNA virus that can inhibit the function of P53 and Rb through the E6 and E7 oncoproteins, respectively. A direct causal relationship has been established between high risk HPV and

HNSCC, and the E6 and E7 oncoproteins can be readily detected in many HPV-positive tumors. The therapeutic use of HPV vaccine is still being explored in HNSCC; studies in patients with cervical intraepithelial neoplasia grade 2/3 demonstrated that intramuscular vaccination with HPV E6/E7 vaccine induced CD8 T cell response that localized to the dysplastic mucosa. Currently, there are multiple trials opened for the treatment of HNSCC using HPV vaccines delivered using different platforms. These include ADXS 11-011 (Advaxis Inc.) study using Listeria as a vector for vaccine delivery (NCT 02002182), peripheral blood mononuclear cells pulsed with E6 and E7 peptide (NCT00019110), and intramuscular vaccination with VGX3100 and INO-9012 (Inovio Pharmaceuticals) followed by electroporation (NCT02163057). Additionally, a vaccine against high risk HPV subtypes has successfully reduced the incidence of cervical intraepithelial neoplasia (CIN) by 90-96%[143, 144] and is currently being implemented in the prevention of HPV induced HNSCC (NCT02382900).

Biomarkers

The final part of this chapter will briefly cover biomarkers, a rapidly advancing area for immunotherapy. With increasing numbers of immunotherapy strategies available for the treatment of solid malignancies, including HNSCC, identification of prognostic and predictive biomarkers is paramount to stratify patients and direct therapy. Understanding these biomarkers is an active area of research, with a majority of the attention focusing on the checkpoint blockades such as anti-PD-1. Recent studies have demonstrated that response to anti-PD-1 is

heavily dependent on the expression of PD-L1 in the tumor microenvironment, as well as the mutational burden of the tumor[20, 22, 145]. These findings suggest that the response to anti-PD-1 is hinged on a pre-existing anti-tumor immune response, and that anti-PD-1 acts to free the CD8 T cells from inhibition to exert their anti-tumor activities. A biomarker for anti-CTLA-4 clinical activity is also being researched; preliminary studies suggest that the response is dependent on FcgRIIIA (CD16)-expressing monocytes' mediated elimination of Tregs[69]. IHC is the most frequently used technique in the identification of these biomarkers. Studies using quantitative IHC have identified CD8 T cell infiltration as an important prognostic factor in predicting outcome for patients with HNSCC[44, 45]. More recently, multiplex immunohistochemistry has emerged as a more advanced tool for the analysis of the tumor microenvironment, offering a more efficient and comprehensive analysis of the tumor microenvironment for both diagnostic and mechanistic studies [23, 146]. This also allows us to explore the relationship between cell types in the peritumoral and intratumoral compartments, quantify the expression of specific biomarkers (Figure 1) and examine their impact on patient prognosis as well as response to therapy. As research on biomarkers advances we will hopefully be able to better direct patients' treatment, based on their tumor microenvironment and mutational status, to the immunotherapy that potentially offers the best response rate and ultimately, a cure for their disease.

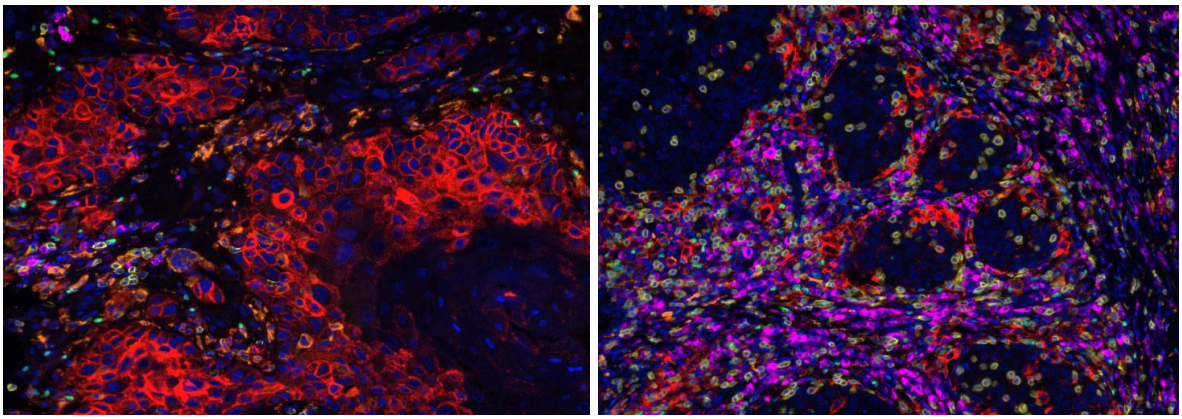

Figure 1.2: Distinct tumor microenvironment in HNSCC. Left: Tumor with low immune infiltrate and high PD-L1 expression. Right: Tumor with high immune infiltrate and low PD-L1 expression. Key – Red: PD-L1; Yellow: CD8; Green: FoxP3; Magenta: CD79A (B cells); Orange: CD163 (Macrophages); Blue: DAPI

Summary

The development of multiplex IHC highlights a gradual shift in the study of tumor microenvironment and biomarker development. By analyzing multiple parameters simultaneously, we seek to uncover important immune signatures in the tumor microenvironment in melanoma and HNSCC. Specifically, we hypothesize that the analysis of cell-cell relationship through multiplex IHC provides a more complete view of tumor microenvironment and results in 1) the development of better prognostic and predictive biomarkers; and 2) provides insight into the underlying biology and mechanism of action of different therapies. Both of these points will be discussed in detail in the subsequent chapters.

Originally published in Targeting Oral Cancer. ISBN 978-3319276458

Chapter 2: Multiplex analysis in melanoma predict generation of tumor-infiltrating lymphocytes[#]

Abstract

Background

Adoptive T cell therapy (ACT) has shown great promise in melanoma, with over 50% response rate in patients where autologous tumor-reactive tumor-infiltrating lymphocytes (TIL) can be cultured and expanded. A major limitation of ACT is the inability to generate or expand autologous tumor-reactive TIL in 25-45 percent of patients tested. Methods that successfully identify tumors that are not suitable for TIL generation by standard methods would help eliminate the costs of fruitless expansion and enable these patients to receive alternate therapy immediately.

Methods

Multispectral fluorescent immunohistochemistry with a panel including CD3, CD8, FoxP3, CD163, PD-L1 was used to analyze the tumor microenvironment in 17 patients with melanoma among our 36-patient cohort to predict successful TIL generation. Additionally, we compared tumor fragments and enzymatic digestion of tumor samples for efficiency in generating tumor-reactive TIL.

Results

Tumor-reactive TIL were generated from 21/36 (58%) of melanomas and for 12/13 (92%) tumors where both enzymatic and fragment methods were compared. TIL generation was successful in 10/13 enzymatic preparations and in 10/13 fragment cultures; combination of both methods resulted in successful generation of autologous tumor-reactive TIL in 12/13 patients. In 17 patients for

whom tissue blocks were available, IHC analysis identified that while the presence of $CD8^+$ T cells alone was insufficient to predict successful TIL generation, the $CD8^+$ to $FoxP3^+$ ratio was predictive with a positive-predictive value (PPV) of 91% and negative-predictive value (NPV) of 86%. Incorporation of CD163+ macrophage numbers and CD8:PD-L1 ratio did not improve the PPV. However, the NPV could be improved to 100% by including the ratio of $CD8^+$:PD-$L1^+$ expressing cells.

Conclusion

This is the first study to apply 7-color multispectral immunohistochemistry to analyze the immune environment of tumors from patients with melanoma. Assessment of the data using unsupervised hierarchical clustering identified tumors from which we were unable to generate TIL. If substantiated, this immune profile could be applied to select patients for TIL generation. Additionally, this biomarker profile may also indicate a pre-existing immune response, and serve as a predictive biomarker of patients who will respond to checkpoint blockade. We postulate that expanding the spectrum of inhibitory cells and molecules assessed using this technique could guide combination immunotherapy treatments and improve response rates.

Originally published in J Immunother Cancer. 2015 Oct 20;3:47

Introduction

ACT with autologous TIL has shown great promise against metastatic melanoma, with response rates of up to 50-70% and complete responses of up to 20%[32, 34, 147]. In patients with melanoma, 95% of the complete responders demonstrated a durable response for at least 5 years[34]. While the anti-tumor effect of ACT appears to be primarily mediated by $CD8^+$ effector T cells[147-149], $CD4^+$ T cells can also mediate tumor regression and may play a critical role in maintaining long-term immunity and cure of patients[150, 151]. T cells used for ACT are expanded from patients' autologous tumors by *in vitro* culture with high-dose interleukin 2. Cultured TIL that recognize autologous tumor and secrete γ-interferon are considered autologous tumor-reactive. These cells are then cultured using a rapid expansion protocol (REP) and adoptively transferred into patients[26, 27, 149, 152-156]. A major limitation of adoptive T cell therapy is the inability to generate or expand tumor-reactive lymphocytes from many tumors. Autologous tumor-reactive T cells can be produced from 50 - 75% of melanoma specimens, but success rates are much lower for other cancers (0-20% for renal, breast and colon cancers)[38]. Identifying the reasons for failure of TIL isolation and expansion is important if we are to make ACT available to more patients with melanoma and other tumor types. Additionally, recent reports suggest that the response to checkpoint blockade agents such as anti-PD-1 and anti-PD-L1 is limited to patients with pre-existing immune responses[20, 21]. Since the isolation of autologous tumor-reactive TIL is potentially the best indicator that a T cell response against a patient's tumor cells exists, we hypothesize that a

pretreatment immunohistochemical assessment that can predict the ability to generate autologous tumor-reactive T cells may also serve as a biomarker to predict response to checkpoint blockade or other immunotherapies.

Quantitative immunohistochemistry has been useful for predicting response rates, treatment selection and determining prognosis in many types of cancer[21, 157]. This is especially notable in colon cancer, where the type and amount of tumor-infiltrating lymphocytes is highly predictive of prognosis[17, 18]. Similar reports have been made in melanoma, in which patients with high $CD8^+$ T cells are associated with better prognosis [158-160]. Recently, multiplex immunohistochemistry (IHC) has emerged as an important tool for the analysis of the tumor microenvironment. Compared to traditional single color IHC methods, multiplex IHC methods are more efficient and contain richer information sets for both diagnostic and mechanistic studies [23, 146]. We utilized a multispectral quantitative fluorescent immunohistochemistry method, which allows simultaneous detection of 7 markers, to explore potential suppressive mechanisms in the tumor microenvironment that may prevent the generation of autologous tumor-reactive TIL. The results not only demonstrate for the first time the feasibility of this method in analyzing clinical tumor specimens, but also provide insight into possible reasons for the failure to isolate or expand autologous tumor-reactive TIL from patients with melanoma.

Materials and Methods

TIL Generation

Tumor procurement and processing: All tumors were resected as part of an IRB-approved protocol of the Providence Portland Medical Center and were numbered sequentially upon arrival in the Human Applications Laboratory (HAL) of the Earle A. Chiles Research Institute (EACRI). Appropriate consent was collected from patients from whom the tumors were collected for research use. At the beginning of these studies, all tumors were processed by triple enzyme digestion using a mixture of collagenase type IV (Cat# C-5138, SIGMA), hyaluronidase Type-V (Cat# H-6254, SIGMA) and deoxyribonuclease-1 (Cat# D-5025, SIGMA). Subsequently, tumors were processed using GMP manufactured enzymes that included Liberase MTF C/T, a combination of collagenase and thermolysin (Cat# 05339880529, Roche), Hylenex (Baxter) or Amphadase (Amphaster), and DNase-1 recombinant grade-1 (Cat# 04536282001, Roche). The freshly minced tumor suspension and enzyme mixture was subsequently mixed at room temperature for 4 to 18 hrs, using a magnetic stir bar and stir plate with rotations set at the lowest speed that would keep the tumor fragments suspended. The resulting tumor digest was filtered through a 200-micron nylon membrane and washed twice with HBSS, counted and resuspended in Human AB culture medium. Human AB culture medium (CM) is comprised of RPMI 1640 (Lonza, Walkersville, MD), 25mmol/L HEPES pH 7.2 (Lonza), L-Glutamine (200 mM) (Lonza), penicillin/streptomycin 10,000 units/ml (Lonza), gentamicin 50mg/mL (Cambrex), 5.5×10−5M β-mercaptoethanol (Life Technologies, Eugene, OR), supplemented with 10% heat-inactivated human AB serum (Valley Biomedical, Inc, Winchester, VA; Cat #HP1022; Lot numbers K-61552, G-81460

and B-90211). These lots of human AB serum were screened by the Surgery Branch, NCI, NIH and shown to support generation of human TIL (Screening information supplied by Dr. Maria Parhkurst and Linda Parker).

For the head-to-head comparison of TIL generation from tumor fragments and enzymatic digests, the same tumor specimen was minced into 1-2 mm^2 fragments and representative fragments were taken to set up fragment TIL cultures. The remainder of the minced tumor was processed for isolation of cells by enzymatic digestion.

Briefly, TIL generation was performed similarly to that outlined by Surgery Branch, NCI, NIH, tiltum protocol 9-6-05 (provided by DR. John Wunderlich). Typically, at least 6 wells of tumor fragments and 6 wells enzymatically digested tumor were plated for culture. For tumor fragment cultures, typically 4 to 10 fragments were plated into each well of a 24 well plate containing 2 mL human AB CM supplemented with 1000 cU/mL. Enzyme digested tumor suspensions were adjusted to 5.0 x 10^5/mL in human AB CM supplemented with 1000 cU/ml IL-2 and 2mls were plated per well of a 24 well plate. The 24 well plates were placed in a humidified 37°C incubator with 5% CO2 and cultured until lymphocyte growth was evident. Each well of the plate was inspected on alternate days using a low-power inverted microscope to monitor the extrusion and proliferation of lymphocytes. Whether or not lymphocyte growth was visible, half of the medium was replaced in all wells no later than 1 week after culture initiation. Typically, about 1 to 2 weeks after culture initiation, a dense lymphocytic carpet would cover a portion of the plate surrounding each fragment. When any well

became almost confluent, all the growing lymphocytes were mixed vigorously, split into two daughter wells and filled to 2 mL per well with CM plus 1000 cU/mL IL-2. Subsequently, the cultures were split to maintain a cell density of 0.5 to 1.0 × 10^6 cells/mL, or half of the media was replaced at least twice weekly or (as needed). The age of TIL cultures used in these studies varied from 12 to 67 days. Each culture originating from each of the initial 6 wells plated for each condition were considered to be an independent TIL culture or "cloid" and maintained in a separate plate with separate pipettes used to maintain integrity of each cloid during expansion.

Cytokine release assays (IFNγ Release):

Tumor specificity or reactivity assays were initiated the same day cells were harvested and frozen for future use. TIL activity and specificity were determined by analysis of IFNγ secretion following stimulation with autologous tumor cells. TIL (1×10^6 cells/well) were plated in a 24-well plate with 2.5×10^5 autologous stimulator tumor cells/well. Autologous tumor cells were either cryopreserved enzymatic tumor digests or autologous melanoma cell lines. Control wells contained either TIL alone or tumor cells alone. Supernatants were harvested after 18-20 hours and IFNγ secretion was measured by enzymes linked-immunosorbent assay (ELISA) technique according to manufacturer's guidelines (eBioscience). TIL. were considered autologous tumor-reactive if at least one of the TIL cloids released >100 pg/ml of IFNγ and this value was > twice the background values (IFNγ release from TIL alone).

Immunohistochemistry

Slides were placed onto staining rack in the Leica autostainer and deparaffinization protocol (70% ethanol 30min, 95% ethanol 30min x 2, 100% ethanol 30min x 3, xylene 40min x 2, paraffin 35min x 4) was run. Samples were marked with ImmEdge hydrophobic pen (Vector) and let dry. Slides were subjected to antigen retrieval with Citra buffer (Biogenex) and rinsed once with 1x TBST (10x solution: 88g Trizma base, 24g of NaCl in 1L ddH_2O, pH to 7.60). and blocked with Ventana antibody diluent for 10 minutes. Primary antibody was diluted in Ventana antibody diluent: the dilutions are 1:50 for CD3 (SP7, Spring Bioscience, M3074), 1:50 for CD8 (SP239, Spring Biosciences), 1:100 for FoxP3 (236A/E7, Abcam), 1:200 for PD-L1 (E1L3N, Cell Signaling), 1:25 for melanoma cocktail (ab732, Abcam); and pre-dilute for CD163 (MRQ26, Ventana). Primary antibodies were incubated for 45' on an orbital shaker (Thermo Scientific, SHKA2000) at room temperature. Antibodies were subsequently removed by vacuum and slides were washed 3x for 30s in TBST.

Anti-rabbit or anti-mouse secondary antibody (Life Technologies) was added to slides drop wise to cover the tissue area, slides were incubated for 10 minutes at RT and subsequently washed 3x for 30s in 1x TBST.

Tyramide-conjugated fluorophore (TSA-fluorophore) (PerkinElmer, NEL791001KT; Life Technologies, T20950) was added to slides at 1:100 dilutions in Amplification plus buffer (PerkinElmer, NEL791001KT) and incubated for 10 minutes at RT; TSA was vacuumed off and slides were washed 3x for 30s in 1X TBST

For multiplex imaging, heat based antigen-stripping method with Citra buffer was

used between each sequential staining step. On the final step, DAPI (Life Technologies, D1306, 1mg/mL stock) was diluted 1:500 in TBST and added to slides. Slides were incubated for 5 minutes at RT and washed 2x for 30s in TBST Slides were rinsed with ddH2O and coverslipped with VectaShield Hard Mount (Vector). Slides were painted with nail polish (L.A. Colors) and stored at 4°C in a covered slide box. Slides were imaged at both 4x and 20x using Vectra imaging software (PerkinElmer) and the number of cells were enumerated from 20x fields using inForm analysis software (PerkinElmer).

Results

Patients

Between 2001 and 2009, melanoma samples from 39 patients with melanoma enrolled in a cancer immunotherapy research study approved by the Providence Portland Medical Center's (PPMC) Institutional Review Board, were used to generate TIL. Signed informed consent was obtained from all patients. Tumor specimen from 3 patients were excluded from our study, 2 of them are contaminated due to the site from which they were resected, and 1 was not able to be tested for tumor-reactivity because autologous tumor was unavailable. Surgical specimens for immunohistochemistry studies were obtained from the PPMC Pathology Department. Formalin-fixed-paraffin-embedded (FFPE) specimens and frozen section controls frozen section controls (FSC) samples from the same date were retrieved from Pathology for a subset of the patients whose tumors were resected at PPMC. FSC samples were prepared by thawing the frozen samples in OCT medium, fixing in 10% formalin, and subsequently processed and embedded at PPMC pathology. In some cases, these reprocessed cryopreserved tumors were not useful for multispectral imaging and were excluded from our multispectral studies. Patient demographics are shown in Table 2.1. The median age was 56, with a range between 23 and 79; 65% of the patients were male.

Mel number	Sex	Successful expansion (N = 29)	Tumor-reactive (N = 21)	FFPE (N = 17)	Site	Time to growth (days)
Mel-119	M	No			Right Groin	
Mel-120	F	No				
Mel-131	M	Yes	Yes		Right Back	29
Mel-133	M	Yes	Yes	FFPE	Liver	30
Mel-134	M	Yes	Yes			38
Mel-135	F	No		FFPE	Right supraclavicular mass	
Mel-140	F	Yes	No			37
Mel-144	M	No		FFPE	Intraperitoneal mass	
Mel-145	M	Yes	Yes			27
Mel-150	F	No			Right back mass	
Mel-160	F	Yes	Yes	FFPE	Right Thigh	26
Mel-163 A	F	Yes	Yes	FFPE	Illiac LN	55
Mel-173-C	5 F	Yes	Yes	FSC		40
Mel-176	M	Yes	Yes	FFPE	lower left lobe	34
Mel-177A	F	Yes	Yes	FSC	Right Leg mass	25
Mel-179	F	Yes	No	FSC	Right axillary mass	56
Mel-180A	M	Yes	Yes		Axillary tumor mass	40

Mel number	Sex	Successful expansion (N = 29)	Tumor-reactive (N = 21)	FFPE (N = 17)	Site	Time to growth (days)
Mel-181	F	Yes	Yes			12
Mel-182	M	No		FFPE	Left pelvic mass	
Mel-185	M	Yes	Yes	FSC	Superior medistinal mass	33
Mel-186	M	No		FSC	Right lower lobe mass	
Mel-187	M	Yes	No		Paracenthesis fluid	67
Mel-188	M	Yes	No	FFPE	Right Axillary LN	41
Mel-189	M	No			Left Chest wall	
Mel-189A	M	Yes	Yes			32
Mel-190	M	No		FFPE	Small Bowl	
Mel-191	M	Yes	No		LN	28
Mel-192	F	No			Thigh	
Mel-193	F	No			Left Lung Upper Lobe	
Mel-199	M	Yes	Yes	FSC		48
Mel-200	M	Yes	Yes	FSC	Left lower tumor	37
Mel-201	M	Yes	Yes			26
Mel-206	M	Yes	Yes			56
Mel-207	M	Yes	Yes			35
Mel-	M	Yes	Yes		Left lower lobe	33

Mel number	Sex	Successful expansion (N = 29)	Tumor-reactive (N = 21)	FFPE (N = 17)	Site	Time to growth (days)
208					LN	
Mel-209	M	Yes	Yes	FFPE	Liver mass	29
Mel-211	F	Yes	Yes		Liver mass	26

Table 2.1: Sample descriptions. Tumor specificity is determined by IFN-γ release when stimulated with the autologous tumor cell line or tumor digest (defined as IFN-γ release greater than 100 pg/ml and double the background (T cells alone). FFPE or FSC (frozen section control) samples are available where indicated. The letters (A, B, C) after Mel-# designate tumors from different sites

Comparison of methods to isolate and culture tumor-infiltrating lymphocytes

The recent regulatory concerns regarding the source of enzymes used for enzymatic digestion of tumors may have led to an increased reliance on fragment cultures of tumor samples at cancer centers investigating TIL therapy. Fragment culture methods are faster and more cost effective and studies have reviewed the efficiency of fragment culture and enzymatic digest on different tumors [26]. However, we are unaware of any head-to-head comparison of TIL generation from fragments and enzymatic digests of the same tumor. In this report, we compared the efficiency of fragment culture and enzymatic digestion in the generation of autologous tumor-reactive TIL cultures in 13 patients. A summary of results from this comparison is shown in Figure 1. To generate TIL a minimum of 12 wells of a 24 well culture plate was initiated; 6 wells contained enzymatically digested tumor cell suspensions and 6 wells contained tumor fragments. Culture efficiency was evaluated in two ways. First, we determined the percentage of wells where it was possible to grow cultures of lymphocytes.

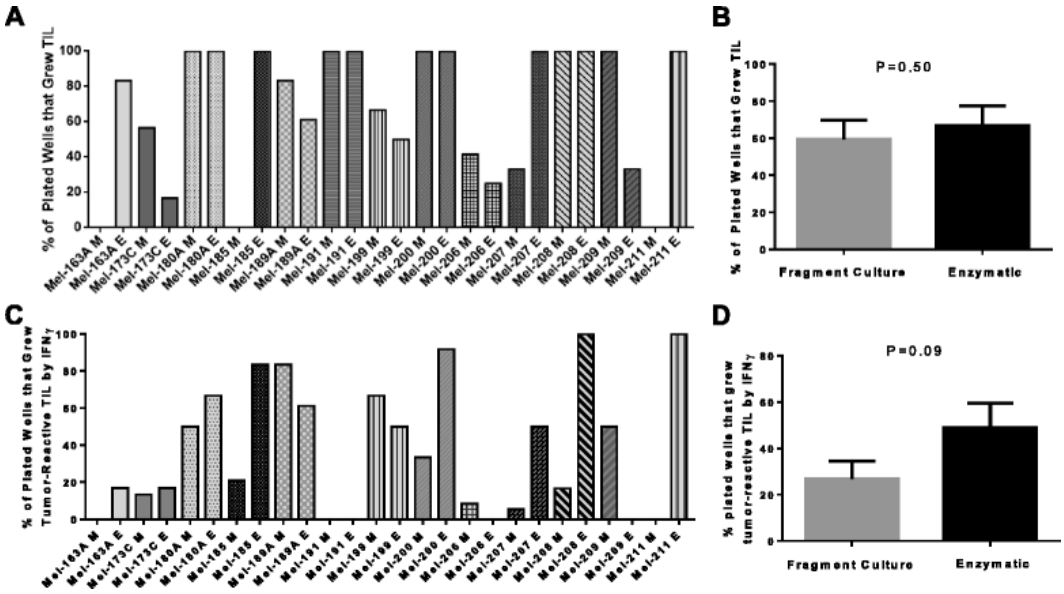

Fig. 2.1: Efficiency of TIL Generation using tumor fragment and enzymatic digest. **a-b** Percentage of plated wells that grew TILs for (**a**) each patient and (**b**) average for all 13 patients. **c-d** Percentage of plated wells that grew tumor-reactive TILs for (**c**) each patient and (**d**) average of all 13 patients. Statistics are established using paired parametric analysis. M: tumor fragments; E: Enzymatic digest

Second, we evaluated whether the lymphocytes that grew out exhibited autologous tumor-reactive function, as defined by >100pg/mL IFNγ release when stimulated with autologous tumor and at least two times the background of T cells cultured alone. While the ability to expand lymphocytes from tumors appeared equivalent between fragment culture and enzymatic digest isolation methods, there was a trend towards superiority for growth of autologous tumor-reactive lymphocytes with enzymatic digestion (P=0.09). Importantly, we failed to generate autologous tumor-reactive TIL from 3 patients (23%) using tumor fragment culture, and from 3 patients (23%) when enzymatic digestion was used (Figure 2.1C). If both methods were used to generate TIL, the success rate of generating an autologous tumor-reactive TIL culture improved to 92% (12/13).

While the numbers are small, this suggests that including both fragment culture and enzymatic digestion may enhance the success of tumor-reactive TIL isolation.

Predicting the ability to generate autologous tumor-reactive TIL

We were able to culture autologous tumor-reactive TIL from 21/36 (58%) of patients. This number is similar but a bit lower than the percentage of autologous tumor-reactive T cells generated from a large ACT clinical trial for treatment of melanoma (57/82, 70%)[35]. The schematic for our culturing conditions is shown in Figure S2.1. The patients from whose tumor we could not culture TIL were retested using cryopreserved tumor digest and the failure to grow TIL was confirmed. The first question we asked about the tumors from which TIL could not be grown was whether they were infiltrated by low numbers of $CD8^+$ T cells. To address this question, we were able to retrieve 11 FFPE and 6 FSC blocks from our 36-patient cohort. Two blocks (Mel-179, Mel-188) represent cases which TIL could be successfully cultured but were not tumor-reactive; we included these in our study and they are highlighted in the figures for distinction. H&E sections from selected patients were blindly reviewed by a board-certified hematopathologist (C.B.B.) at our institute. Lymphocytic infiltrate within the tumor was classified as low (1+), intermediate (2+), or high (3+). No correlation was noticed between extent of lymphocytic infiltrate and the ability to generate TIL from the tumors (Figure 2.2).

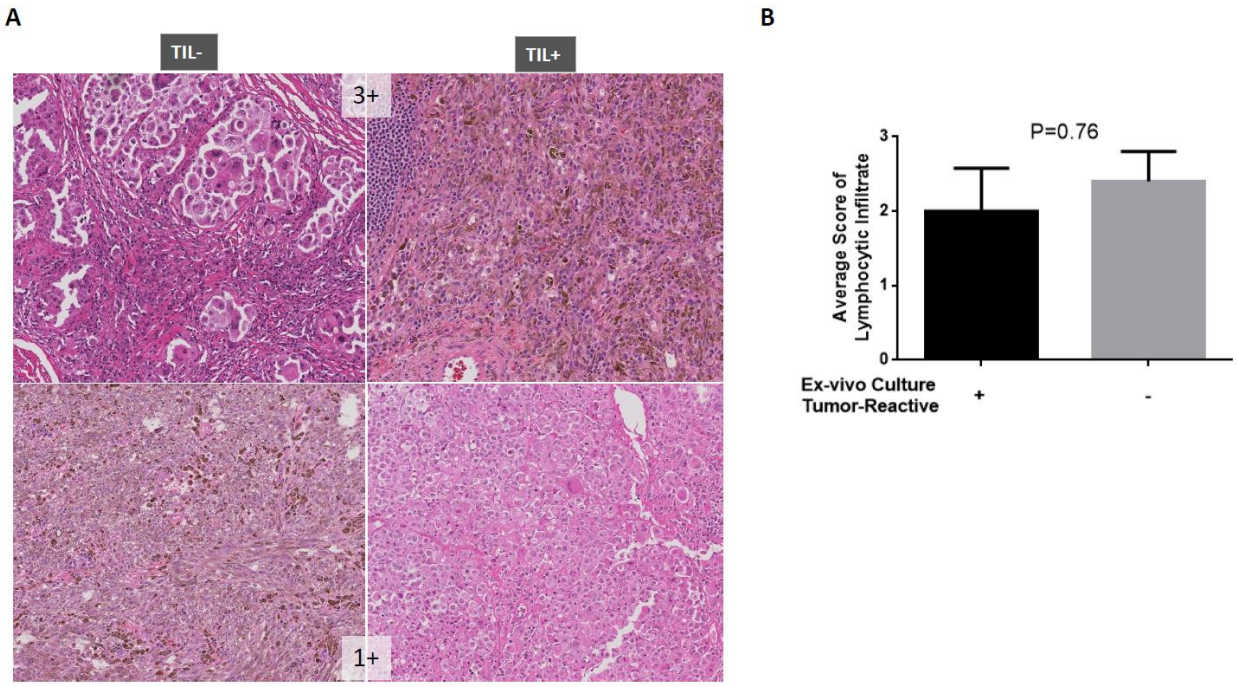

Figure 2.2: Lymphocytic immune infiltrate is insufficient to predict TIL culture success. A) Representative H&E stain from 4 patients, two are classified as 3+ (Top) and two are classified as 1+ (Bottom), TIL culture status is indicated above images. A summary of our observations is shown in B, which compares the average pathology score of lymphocytic infiltrate between tumors that grew tumor-reactive TILs and those that did not.

From this we hypothesized that the tumor microenvironment in some patients is immunosuppressive such that the ability to culture TIL is limited. To address this question and further confirm our initial finding, we utilized a multispectral quantitative immunohistochemistry platform (Vectra, PerkinElmer, Hopkinton, MA) to quantitatively and qualitatively assess the immune infiltrates within tumors. Four representative images are shown in Figure 2; there were two distinct patterns of immune infiltrate observed in our cohort: the patients with extensive immune infiltrates (Figure 2.3A, B) and those with limited immune infiltrate (Figure 2.3C, D).

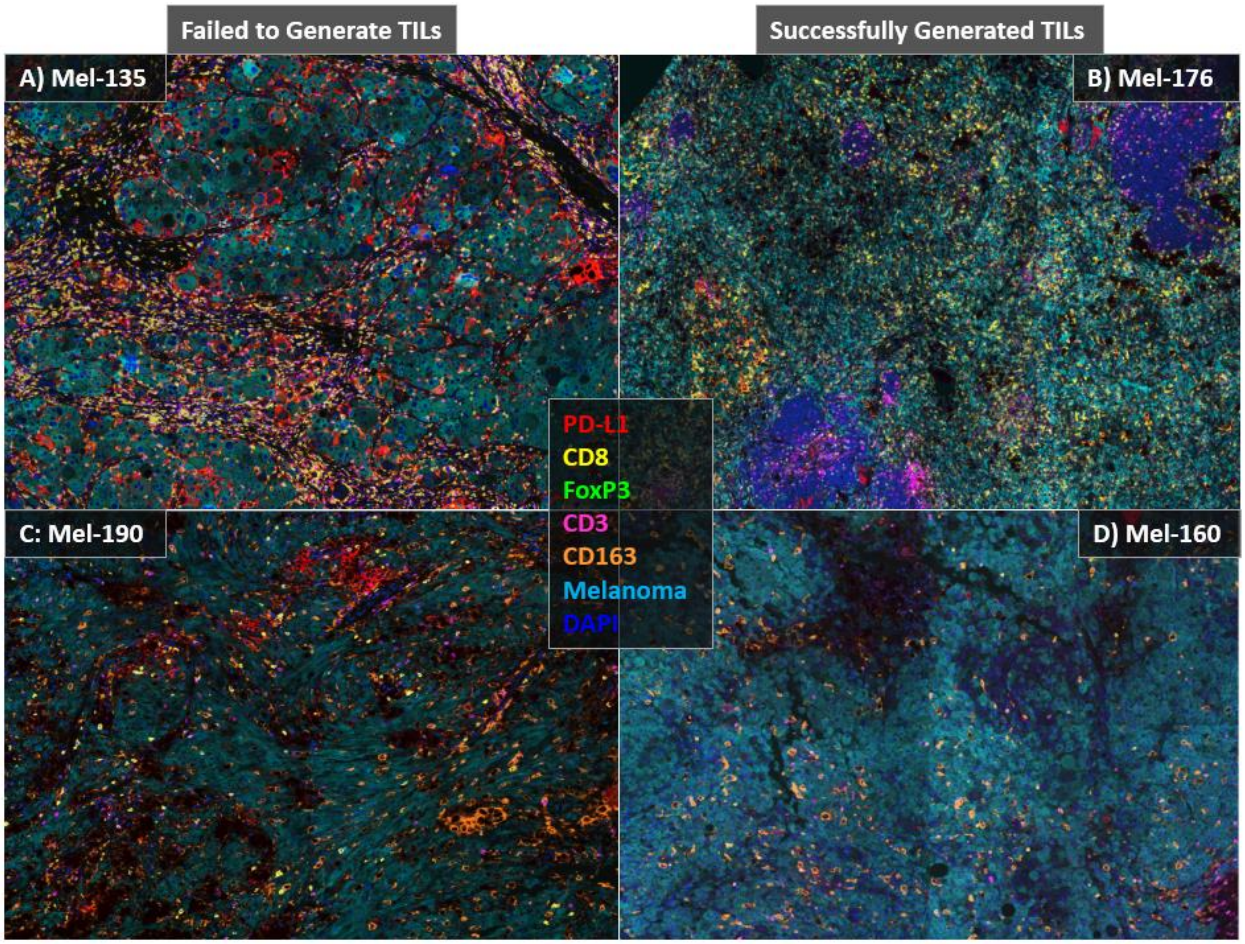

Fig. 2.3: Sample 7-plex Images. Patients with high (Top) and low (Bottom) immune infiltrate from whom TIL did not (Left) or did (Right) grow. Images are 9 (Top) or 4 (Bottom) 200x fields stitched together for the specified melanoma specimens (**A-D**)

Supporting our initial observation with in Figure S2, the extent of immune infiltrate alone was insufficient in predicting the ability to generate TIL (Figure 2.4). We next examined specific immune markers for their ability to predict generation of TIL. We found that enumeration of the $CD3^+$ and $CD8^+$ T cell infiltrates alone is insufficient to predict successful generation of TIL. Representative images of tumors from two patients are shown in Figure 2.4; although both tumors have high $CD3^+$ (magenta) and $CD8^+$ (yellow) T cell

infiltrate, we were unable to culture TIL from the tumor on the left, while we were able to generate TIL from the tumor on the right.

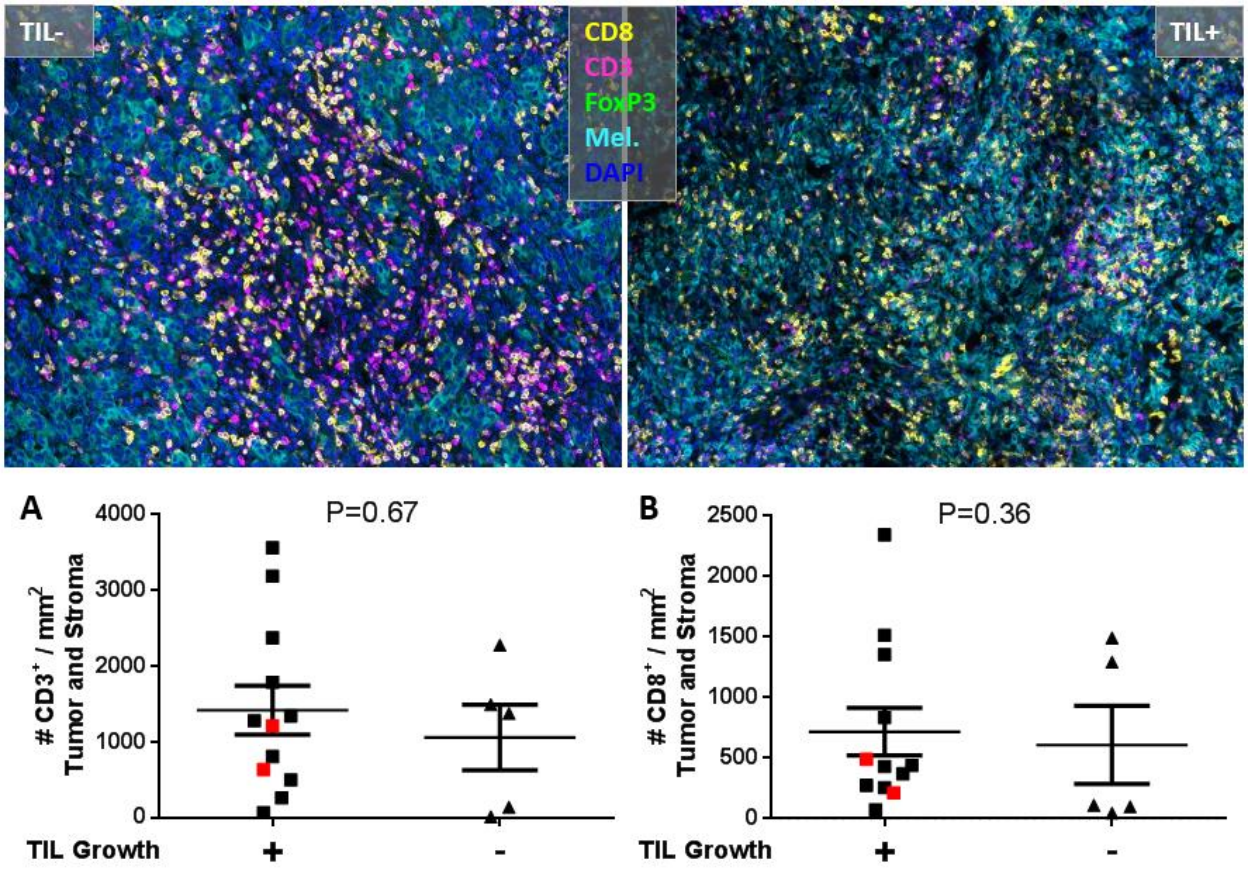

Fig. 2.4: CD3 and CD8 are insufficient in predicting ability to generate TILs. Top: Pseudocolor H&E image of two example patients with similar CD3+ and CD8+ T cell infiltrate. Bottom: **a-b**) Quantification of the total percent of CD3+ and CD8+ T cells. Red colored dots indicated tumor sample that grew TIL but did not react to autologous tumor

Considering the failure to generate TIL may be a consequence of an immune-suppressive environment, we evaluated tumors for the number of $CD3^+FoxP3^+$ regulatory T cells, and $CD163^+$ alternatively activated (M2) macrophages; and also quantified the number of cells expressing PD-L1. As PD-L1 can also be expressed on melanoma cells (Figure 2.5A), we used a cocktail consisting of HMB45, Mart-1 and Tyrosinase to identify tumor cells. The cocktail was positive

in 70% of the patients in our cohort. Since PD-L1 can also be expressed on $CD163^+$ macrophages, and $CD3^+CD8^+$ T cells (Figure 2.5B-C), we included their expression in our evaluation as well.

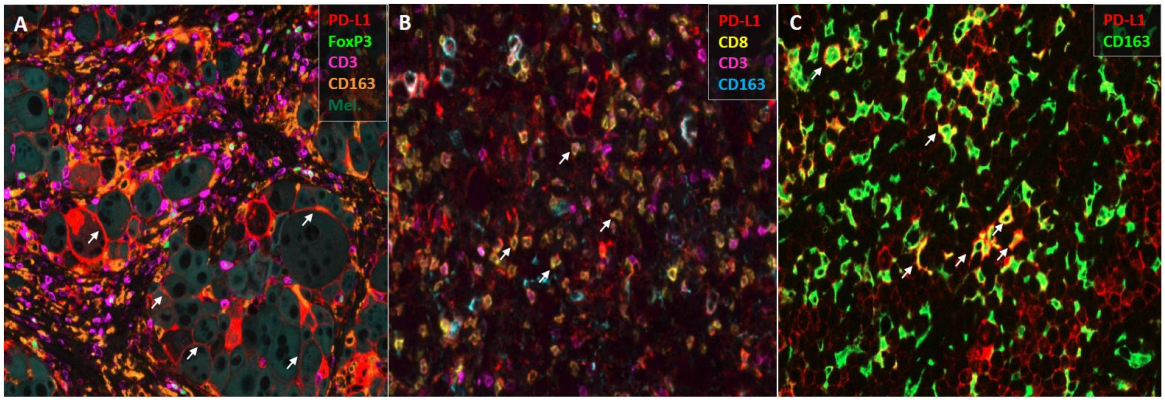

Figure 2.5: PD-L1 Localization. A) On tumor cells B) on CD8+ T cells and C) on CD163+ macrophages.

We analyzed the percent of $CD3^+FoxP3^+$ regulatory T cells, percent of $CD163^+$ macrophages, and PD-L1 expression using H-Score, a value based both on the intensity of the PD-L1 expression on a 0-3+ scale, and the number of cells that are positive for PD-L1. We did not find any significant correlation between the amount of $CD3^+FoxP3^+$ regulatory T cells and the ability to generate TIL. However, when we evaluated the relative proportion of $CD8^+$ and $CD3^+FoxP3^+$ regulatory T cells, we found that the ratio was highly significant (P=0.006, PPV=91%) in predicting TIL culture success (Figure 2.6B). This suggests that the percent of regulatory T cells present in the tumor may be a determining factor in limiting the proliferation of T cells *in vitro.* PD-L1 expression by itself did not correlate with the ability to culture TIL, however, when we took the ratio of $CD8^+$ T cells to PD-$L1^+$ cells, there was an increased trend(P=0.09) (Figure 2.6C-D), suggesting a potential contributory immunosuppressive role for PD-L1 in

preventing the generation of TIL *in vitro*. We also found an inverse correlation between the number of $CD163^+$ macrophages and the ability to culture TIL (P=0.03). This correlation, was however not further improved when the number of $CD8^+$ T cells was taken into account (Figure 2.6E-F).

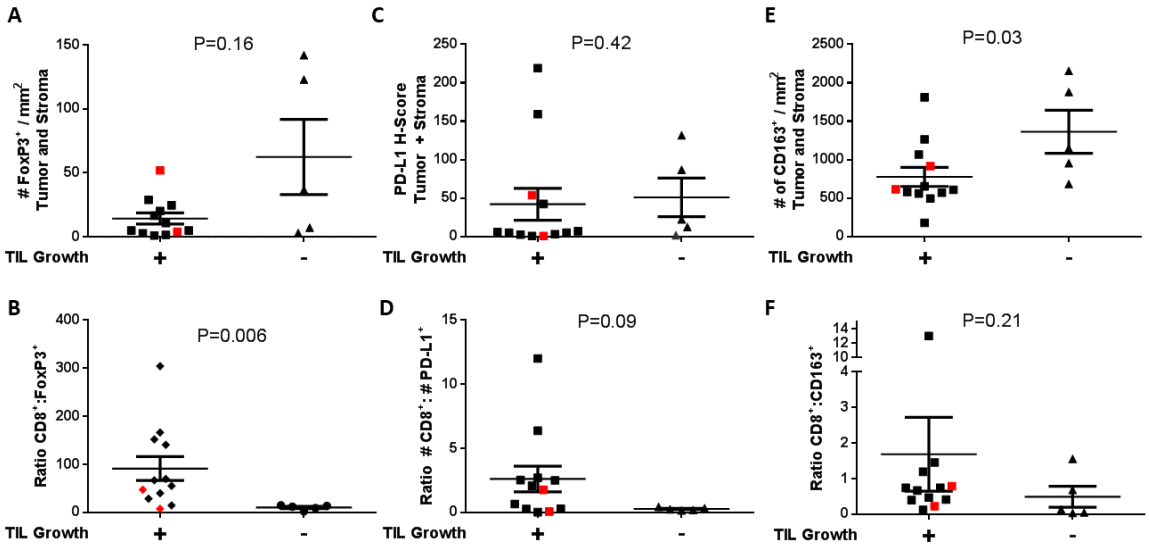

Figure 2.6: CD8 to FoxP3 ratio is predictive of ability to culture autologous TILs. A-B) FoxP3 alone and CD8:FoxP3 ratio. C-D) PD-L1 alone and CD8: PD-L1 ratio. E-F) CD163 alone and CD8:CD163 ratio. Statistics are done with unpaired nonparametric T test (Mann-Whitney Ranked Comparison). Significance is established at P<0.05. Red colored dots indicated tumor sample that grew TIL but did not react to autologous tumor

We then constructed a heat map using all available data sets and performed an unsupervised hierarchical analysis on all samples (Figure 2.7). We found that the $CD8^+$ to $PD\text{-}L1^+$ ratio was able to further enhance the NPV of $CD8^+$ to $FoxP3^+$ ratio from 86% to 100%. Neither positive nor negative predictive values were further improved by the amount of $CD163^+$ infiltrate.

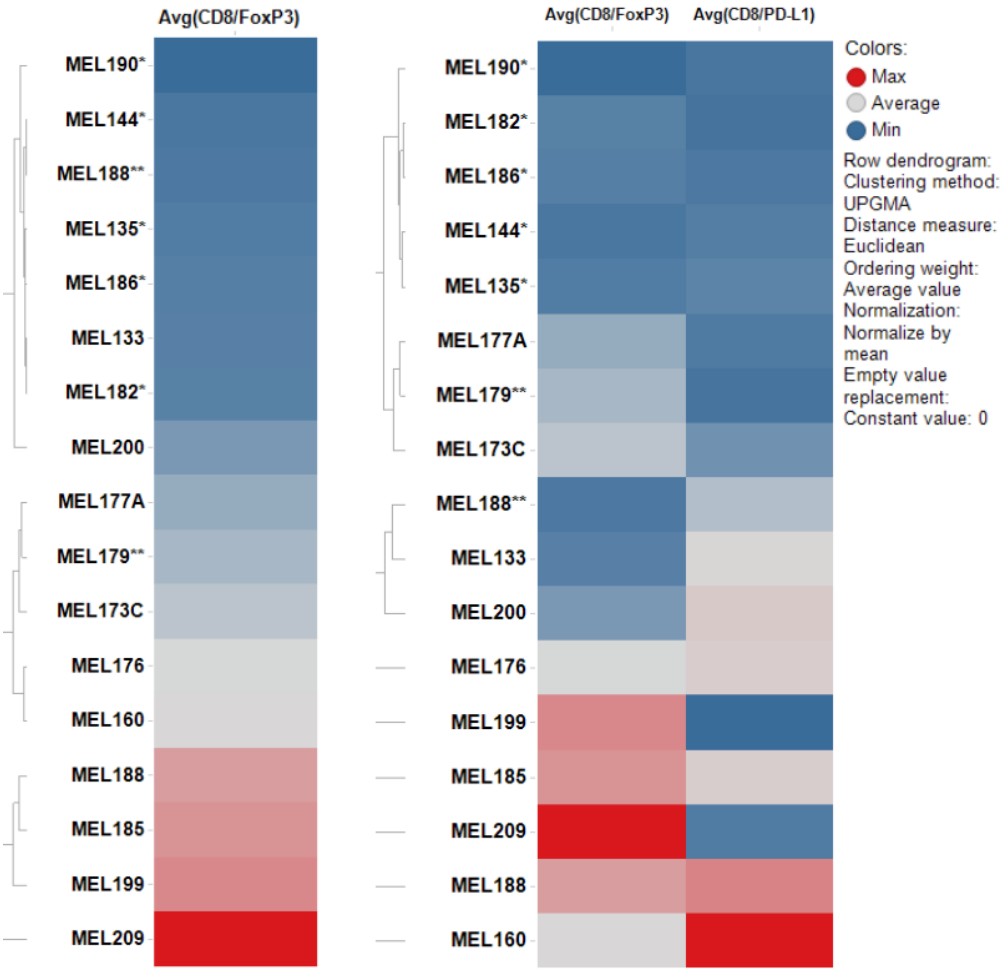

Figure 2.7: Unsupervised hierarchical clustering of CD8+:FoxP3+ and CD8+:PD-L1+ ratios. The color is a continuing spectrum with dark red indicating max expression and dark blue indicating minimum expression. *indicates patients from whom we failed to culture tumor-specific TIL. **indicates tumor sample that grew TIL but did not react to autologous tumor

Discussion

Adoptive T cell therapy using autologous T cells has been shown to be an effective way to treat patients with melanoma. The infrastructure and laboratory support required is quite substantial and has limited TIL therapy to a small number of academic sites. A further limitation is that the success rate for production of tumor-reactive TIL in melanoma has been between 50 and 70%. Thus this therapy is currently limited to a subset of patients with melanoma from

whom tumor-reactive TIL can be isolated and expanded. Methods that improve the success rate of culturing tumor-reactive TIL might increase the availability of ACT to more patients with melanoma, and perhaps other malignancies. The two standard methods of processing tumor for TIL generation are culture of tumor fragments and enzymatic digestion of tumor fragments with culture of the isolated tumor cell suspension. We have compared both methods for their efficiency in generating tumor-reactive TIL using fragment culture and enzymatic digestion and found a trend favoring increased efficiency using enzymatic digest. Importantly, we found that regardless of the method there was a failure to produce clinically useful T cells for adoptive immunotherapy in one of every three patients. Our data suggest that employing both methods increased the chances for success and could maximize the number of patients from whom TIL can be grown. In addition, time in culture seemed to play an important role, as previously reported[161]. We found an inverse correlation between the autologous tumor-reactivity of TIL and the amount time they had spent in culture (Figure 2.8).

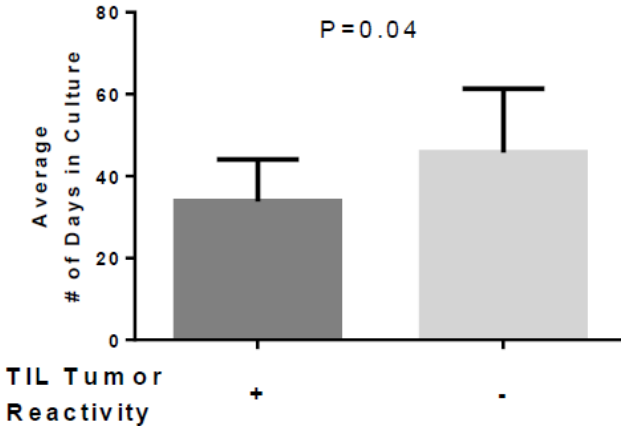

Figure 2.8: Number of days it takes for TIL to grow in culture is predictive of tumor reactivity. Statistics is done using unpaired non-parametric T test. Significance is established at P<0.05.

The second main aim of our study was to analyze the tumor microenvironment for factors that may limit the generation of tumor-reactive TIL. We utilized a novel multispectral immunohistochemistry method employing the PerkinElmer Vectra platform to examine the microenvironment of melanoma. Part of our aim was to test the feasibility of this method to analyze multiple markers on a single 4-micron section of a FFPE tumor sample. Overall, we found that the method was reproducible and permitted the simultaneous detection of up to 7 markers (Figure 2.3, Figure 2.9).

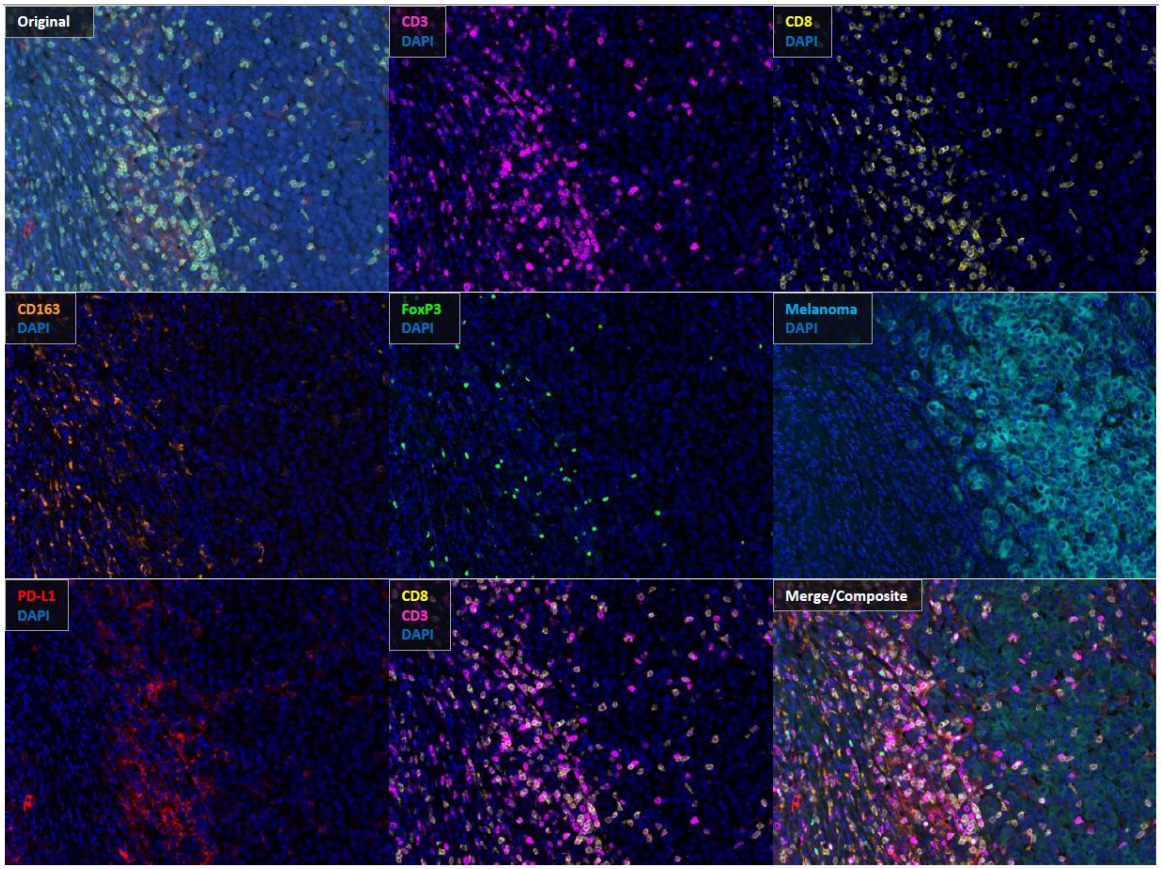

Figure 2.9: Sample multispectral image with individual channels. Original is the raw image with all channels taken using the Vectra imaging software. The spectrum for each fluorophore is subsequently measured with control slides, and subtracted from the original image to establish each individual channels and the composite.

We have compared two different methods for image analysis and found no significant difference between using the percentage of immune infiltrate or the number of immune infiltrating cells per mm^2 (Figure S2.3A). We also found no significant difference in the results of the immune infiltrate analysis whether we used the PerkinElmer inform software or the Definiens Tissue Studio (Figure S2.3B). The method works best with FFPE samples, which we could retrieve from 11 patients. For frozen sections that are subsequently fixed with formalin, certain markers such as CD8 can demonstrate an artifactual punctate pattern of positivity (Figure 2.10F, black arrows), which increased the difficulty of the digital morphometric analysis. We also found that FoxP3 staining in frozen sections had a higher background and can lead to over-estimation of the number of $FoxP3^+$ cells due to artifacts (Figure 2.10I, black arrows). Since the artifacts are not $CD3^+$, this problem was circumvented in our study by using both CD3 and FoxP3 to determine the number of regulatory T cells and including only the cells that were positive for both CD3 and FoxP3 (Figure 2.10I, red arrows). Detection of CD163, CD3 and PD-L1 did not seem to be affected to the same degree by artifactual changes induced by freezing (Figure 2.10B, C, E). Detection of melanoma cells by the melanoma cocktail was only positive in 70% of specimens. An alternative approach to improve detection may be the use of an antibody against SOX10, which has shown superior sensitivity and specificity over the melanoma cocktail[162].

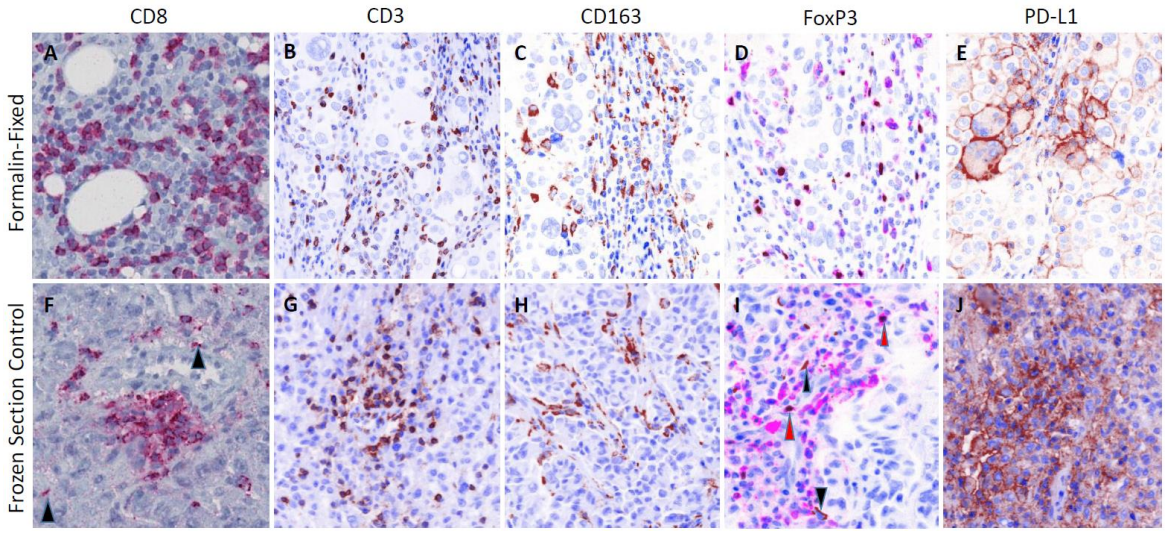

Figure 2.10: Comparison between FFPE (Top) and frozen (Bottom) sections. A,F) CD8; B,G) CD3; C,H) CD163; D,I) FoxP3; E,J) PD-L1

From our multispectral analysis, we found that the presence of $CD8^+$ T cells alone was insufficient in predicting the success of generating a TIL culture, while the ratio of $CD8^+$ T cells to $CD3^+FoxP3^+$ regulatory T cells was a significant predictor (P=0.006). This is consistent with previous reports in preclinical models showing that depletion of $FoxP3^+$ regulatory T cells, or inhibiting regulatory T cell function through OX40 or GITR activation, can lead to an increased CD8: $FoxP3^+$ T cell ratios that correlated with improved $CD8^+$ T cell function and therapeutic efficacy[28-30]. In other studies, regulatory T cells isolated from tumor were shown to directly inhibit T cell function in non-small cell lung cancer[31], and may negatively influence the response rate of patients receiving ACT[163, 164]. We also found that the number of $CD163^+$ macrophages inversely correlated with the ability to culture TIL (Figure 2.6E); consistent with reports suggesting depletion of macrophages through inhibition of CSF1R signaling inhibition can enhance $CD8^+$ T cell function in preclinical models[11, 12, 165]. This has led to a phase I clinical trial evaluating anti-CSF-1R administration, which identified partial clinical responses

in 5/7 patients with diffuse-type giant cell tumor[166]. We evaluated the effect of arginase I and iNOS inhibition during the generation of TIL cultures but found no significant increase in recovery success (Puri et al. manuscript in preparation). Recently, other have shown that by using an agonist 4-1BB antibody during the initialing of culture increased the numbers of memory $CD8^+$ TIL that were specific for autologous tumor and represents a promising approach to increase the number of patients eligible to receive adoptive immunotherapy with TIL[167].

While PD-L1 expression by itself is not an indicator of TIL culture success, the ratio of $CD8^+$ T cells to PD-$L1^+$ cells is trending towards a significant separation, suggesting this important negative feedback loop may limit the ability to grow tumor-reactive TIL *ex vivo.* We subsequently performed unsupervised clustering of the data, which allowed us to further analyze the large amount of information generated with multispectral imaging. From this analysis, we were able to incorporate 2 out of 3 suppressive markers from our panel and identify a cluster of patients whose tumor demonstrated both low $CD8^+$:$FoxP3^+$ and low $CD8^+$:PD-$L1^+$ ratios (Figure 2.7); and we failed to generate TIL from these tumors. Our observations raised the question whether $CD8^+$ T cell proliferation was suppressed during culture, or whether they were already anergic and unable to proliferate at the time they were placed in culture due to pre-existing suppressive mechanisms. Evidence from murine and human studies suggests that expression of PD-L1 and the presence $FoxP3^+$ regulatory T cells can reduce the anti-tumor effect of ACT[163, 164, 168, 169]. These studies imply that regulatory T cell depletion and use of anti-PD-L1 antibody before culture may increase the success rate in

growing tumor-reactive TIL, and potentially expand the use of ACT to greater number of patients with melanoma and potentially other malignancies.

Checkpoint blockade therapy is one of the most promising treatments for patients with solid tumors. Recent studies suggest that the response to agents such as anti-PD-1 and anti-PD-L1 is limited to patients with pre-existing immune response[20, 21]. We consider the ability to culture tumor-reactive lymphocytes from tumors of patients to be a very specific indicator of a pre-existing anti-cancer immune response. The density of $CD8^+$ T cells has shown to be a powerful marker in predicting response to anti-PD-1 therapy in a small cohort of patients, correctly predicting 13/15 patients who are treated with anti-PD-1 therapy[20]. It is possible that including $FoxP3^+$ regulatory T cells may further increase the prediction for anti-PD-1 response. We plan to apply our multispectral immunohistochemical analysis to patients receiving T cell checkpoint antibodies to assess their impact on the tumor microenvironment and correlate it with functional and clinical outcome.

Conclusion

In summary, this is the first study to apply 7-color multispectral immunohistochemistry to analyze the immune environment of tumors from patients with melanoma. Enumeration of staining with objective assessment software and analysis of the data using unsupervised hierarchical clustering identified tumors where we were unable to generate TIL. These results could be evaluated with a prospective study to determine if this immune profile could

select patients for successful TIL generation. Additionally, since this biomarker profile appears to identify presence of tumor-reactive T cells, it may represent a predictive biomarker of patients who will respond to checkpoint blockade. While application of this methodology is at an early stage, we consider that its greatest promise will be as a means to identify resistance mechanisms operational at the tumor site. In this era of combination immunotherapy, this information will be a useful guide to tailor specific therapies to patients with cancer.

Respective contributions:

I have designed and performed the multiplex experiments, analyzed the TIL culturing data, and wrote the manuscript. SP has performed the TIL cultures and analyzed the culturing data and revised the manuscript. TM performed and analyzed experiments and helped revise the manuscript. WW provided surgical specimens and scientific input into the design of experiments and helped revise the manuscript. CCH provided reagents, software and guidance in analyzing results and helped revise the manuscript. CW provided expertise and training in the methodology and provided scientific input into the experimental design and helped revise the manuscript. WJU and BDC provided scientific input into the experimental design and interpretation of the data and helped revise the manuscript. CBB validated the histological images, provided scientific input into the design, performance and analysis of the experiments and helped revise the manuscript. BAF designed and analyzed the experiments and wrote the manuscript. All authors read and approved the manuscript.

Chapter 3 – A novel tool to evaluate T and B cells populations by IHC in murine tissue[#]

Abstract

Recent advances in multiplex immunohistochemistry techniques allow for quantitative, spatial identification of multiple immune parameters for enhanced diagnostic and prognostic insight. However, applying such techniques to murine fixed-tissues, particularly sensitive epitopes such as CD4, CD8α, and CD19, have been difficult. We compared different fixation protocols and antigen retrieval techniques, and validated the use of multiplex immunohistochemistry for detection of $CD3^+CD4^+$ and $CD3^+CD8^+$ T cell subsets in both murine spleen and tumor. This allows for enumeration of these T cell subsets within immune environments as well as the study of their spatial distribution.

Keywords: T cells, B cells, tumor immunity, imaging

Originally published in J Immunol. 2016 May 1;196(9):3943-50

Introduction

Assessment of patterns of immune infiltrates has been shown to be highly prognostic and diagnostic in many types of cancers[21, 157]. The clinical impact of such analysis is most notably shown in colon cancer, where objective quantification of $CD3^+$ and $CD8^+$ T cells densities in the primary tumor has a highly significant impact on patient prognosis[18]. More recently, multiplex immunohistochemistry (IHC) has emerged as a powerful technique for the study of multiple immune parameters on a single slide. This not only increases efficiency, but more importantly, allows for the study of relationships between cell populations, offering greater insight into the mechanisms underlying various disease processes[13].

Currently, multiplex IHC platforms have been applied for use in human tissues, but its use in murine fixed-tissues is still being optimized. Many antibodies against human antigens are successfully used with paraffin sections for human IHC, but considerably less are available for mouse antigens. Notably, there has been a dilemma in the field about performing IHC staining on certain immune epitopes such as CD4, CD8α, and CD19 which stain functionally distinct T and B cell populations. These fixation sensitive epitopes are not easily detected in formalin-fixed paraffin embedded tissues, but have historically relied on frozen tissue for detection; however, this comes with sacrifices of the integrity of tissue architecture making it difficult to study tissue morphology[170-173]. While it has been suggested that Zinc-based fixation buffers are superior in preserving these

epitopes compared to formalin fixation[174, 175], the specificity of the antibodies and the ability to multiplex under these conditions have not been tested. Being able to perform CD4 and CD8 staining reliably in paraffin-embedded murine tissues is critical to our understanding of their function in various physiological and disease processes. Especially given certain immune cell subtypes, such as tissue resident memory T cells, have been reported to be underestimated using standard flow cytometry techniques[176]. In our study, we compared multiple fixation protocols as well as antigen retrieval methods to validate the use of multiplex IHC in murine tissues with sensitive epitopes such as CD4, CD8α and CD19. Our approach allows for successful detection and quantification of 5 or more markers on murine tissues.

Material and methods

Mice

Female C57BL/6 mice, Rag1$^{-/-}$ mice (B6.129S7-Rag1^{tm1Mom}/J)**,** pmel-1 TCR transgenic mice (B6.Cg-*Thy1^{a}*/Cy Tg(TcraTcrb)8Rest/J), and TRP1 TCR/Rag1$^{-/-}$ transgenic mice (B6.Cg-*Rag1^{tm1Mom} Tyrp1^{B-w} Tg(Tcra,Tcrb)9Rest/J*) were purchased from the Jackson Laboratory (Bar Harbor, ME). pmel-1 TCR transgenic mice were bred Rag1$^{-/-}$ mice to generate pmel TCR/Rag1$^{-/-}$ mice. pmel TCR/Rag1$^{-/-}$ mice have CD8^{+} T cells expressing a transgenic TCR specific for mgp100$_{(25\text{-}33)}$ peptide. TRP1 TCR/Rag1$^{-/-}$ transgenic mice have CD4^{+} T cells expressing a transgenic TCR specific for mtyrp1$_{(113\text{-}127)}$ peptide. All mice were maintained in a specific pathogen-free environment. Recognized principles of

laboratory animal care were followed (Guide for the Care and Use of Laboratory Animals, National Research Council, 2011), and all animal protocols were approved by the Earle A. Chiles Research Institute Animal Care and Use Committee.

Tumor cell lines

The sarcoma cell line, MCA-310[177], and squamous cell carcinoma cell line, SCCVII[178], were maintained in complete media. For MCA-310, 20,000 cells were injected subcutaneously on the flank of C57Bl/6 mice; and for SCCVII, 1 million cells were injected subcutaneously on the back of the neck of C3H/HeJ mice. Mice were sacrificed and the established tumors were resected, fixed in zinc fixation buffer and processed with a Tissue-Tek automated tissue processor.

Immunohistochemistry

Tissue Fixation and Processing

One liter of Zinc-Fixation Buffer was prepared by mixing 0.5g calcium acetate (Sigma 402850), 5g zinc acetate (Sigma, Z0625) and 5g zinc chloride (Sigma, 208086) to 0.1M Tris (Sigma, 251-018) pH 7.4. Final pH 6.5-7.0. PLP was prepared by mixing Lysine HCl (Sigma, L5626) solution (13.9g Lysine HCl in 375 ml dd$H_2$0 and pH to 7.4 with Na_2HPO_4 (Sigma, W239901) with 15.6 ml of 16 % paraformaldehyde (Electron microscopy sciences, 15712). 2.14g of Sodium Periodate (Sigma, 311448) was added and the solution was brought up to 1L with 0.1M phosphate buffer (Sigma, W2399D1).

Spleens and tumors were harvested and fixed for 24 hours at room temperature. Spleens and tumors were processed using Tissue-Tek automated tissue processor (Sakura) on Zinc setting for zinc and PLP-fixed samples (start on 70% ethanol, skip formalin fixation) and embedded with Leica tissue embedder. 4µm thick sections were cut and floated onto plus-slides (Cardinal ColorFrost) in a tissue floatation bath set at 40ºC (Fisher Healthcare). Slides were allowed to dry at room temperature overnight and stored in 4°C until use.

Deparaffinization, Staining, Imaging and Analysis

Slides were placed onto staining rack in the Leica autostainer and deparaffinization protocol (70% ethanol 30min, 95% ethanol 30min x 2, 100% ethanol 30min x 3, xylene 40min x 2, paraffin 35min x 4) was run. Samples were marked with ImmEdge hydrophobic pen (Vector) and let dry. Slides were rinsed once with 1x TBST (10x solution: 88g Trizma base, 24g of NaCl in 1L ddH_2O, pH to 7.60) and blocked with Renaissance antibody diluent (Biocare Medical, PD905) for 10 minutes.

Primary antibody was diluted in Renaissance antibody diluent (Biocare Medical, PD905). The dilutions are 1:50 for CD3 (SP7, Spring Bioscience, M3074), CD4 (RM4-5, BD Biosciences, 550280; GK1.5, eBioscience 14-0041-85), CD8 (53-6.7, BD Biosciences, 550281), CD19 (1D3, BD Biosciences, 553783), and granzyme B (polyclonal rAB, Abcam ab4059); 1:100 for FoxP3 (FJK-16s, eBioscience, 14-5773), PD-L1 (Abcam, ab58810); 1:250 for F4/80 (CI:A3-1, AbD Serotec, MCA497GA). Primary antibodies were incubated for 45’ on an orbital shaker

(Thermo Scientific, SHKA2000) at room temperature. Antibodies were subsequently removed by vacuum and slides were washed 3x for 30s in TBST. Anti-rabbit secondary antibody (Life Technologies, 87-9623), or anti-rat (Vector Labs, MP-7444-15) was added to slides drop wise to cover the tissue area, slides were incubated for 10 minutes at RT and subsequently washed 3x for 30s in 1x TBST.

Tyramide-conjugated fluorophore (TSA-fluorophore) (PerkinElmer, NEL791001KT; Life Technologies, T20950) was added to slides at 1:100 dilution in Amplification plus buffer (PerkinElmer, NEL791001KT) and incubated for 10 minutes at RT; TSA was vacuumed off and slides were washed 3x for 30s in 1X TBST

For multiplex imaging, antigen-stripping buffer (0.1M glycine (Sigma, G2879), pH10 using NaOH (Fisher chemical, SS267), 0.5% Tween) was added to slides and incubated at room temperature for 10 minutes, slides were rinsed in TBST, blocked briefly and incubated with subsequent primary antibody at desired dilution and time. DAPI (Life Technologies, D1306, 1mg/mL stock) was diluted 1:500 in TBST and added to slides. Slides were incubate for 5 minutes at RT and washed 2x for 30s in TBST Slides were rinsed with ddH2O and coverslipped with VectaShield Hard Mount (Vector). Slides were painted with nail polish (L.A. Colors) and stored at 4°C in a covered slide box. Slides were imaged at both 4x and 20x using Vectra imaging software (PerkinElmer) and the number of cells were enumerated from 20x fields using inForm analysis software (PerkinElmer).

Results

Murine CD3, CD4, CD8 fluorescent immunohistochemistry

Neutral buffered 10% formalin (NBF) has been the standard in fixation for human tissues; it is superior in preserving tissue architecture and is able to withstand repeated heat-mediated antigen retrieval for use of multiplex immunohistochemistry[170, 179]. For murine tissues, 10% NBF, when combined with standard heat-mediated antigen retrieval, is excellent in detecting immune markers such as CD3 (Figure 3.1).

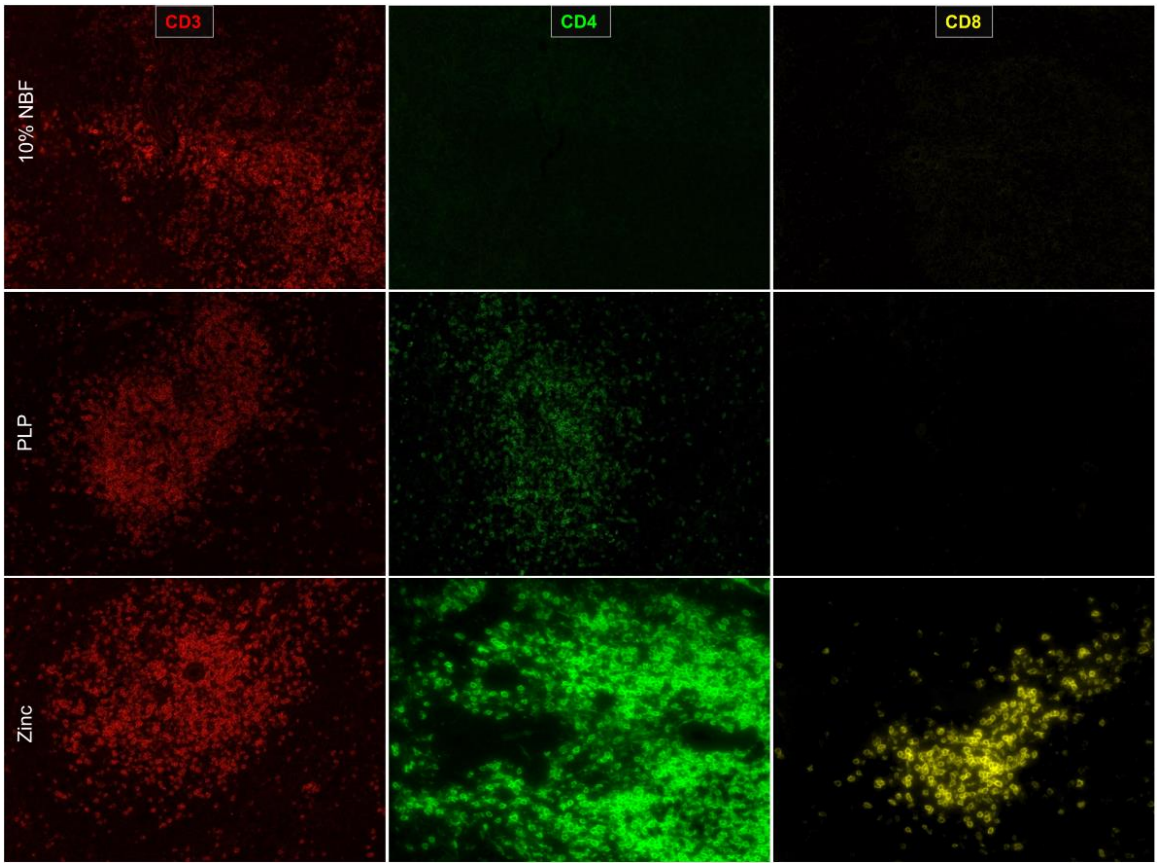

Figure 3.1: Zinc-based buffer is superior in detection of CD4 and CD8α. Spleen sections are fixed for 24 hours in each condition and 4µm sections are cut and prepared. Antigen retrieval is performed on formalin-fixed tissues but not on either PLP or zinc-fixed tissues. Tissue sections are imaged at 20x with PerkinElmer Vectra platform.

However, the use of NBF to fix mouse spleens resulted in the inability to detect either CD4 or CD8α epitopes (Figure 3.1). To address this problem, we examined two alternative fixation methods. PLP, or periodate-lysine-paraformaldehyde, is a fixative that acts by crosslinking lysine residues and has been shown to be compatible with many different epitopes for the use of IHC[180, 181]. In murine spleen sections fixed with PLP, we were able to detect both CD3 and CD4 epitopes. However, the intensity of CD4 staining was weak and we were not able to detect CD8α (Figure 3.1).

Zinc-based fixation has traditionally been an additive to NBF for improved antigen preservation. However, reports have suggested that zinc-based fixative devoid of NBF could maintain antigen integrity without sacrificing much of the architecture[174, 175, 182]. We did not notice a significant difference in tissue architecture between NBF and the zinc-based fixative (Figure 3.2a-b).

Importantly, we found that spleen tissue fixed in the zinc-based fixation buffer was superior to both formalin-fixed and PLP-fixed tissue in detection of CD4, and CD8α epitopes (Figure 3.1).

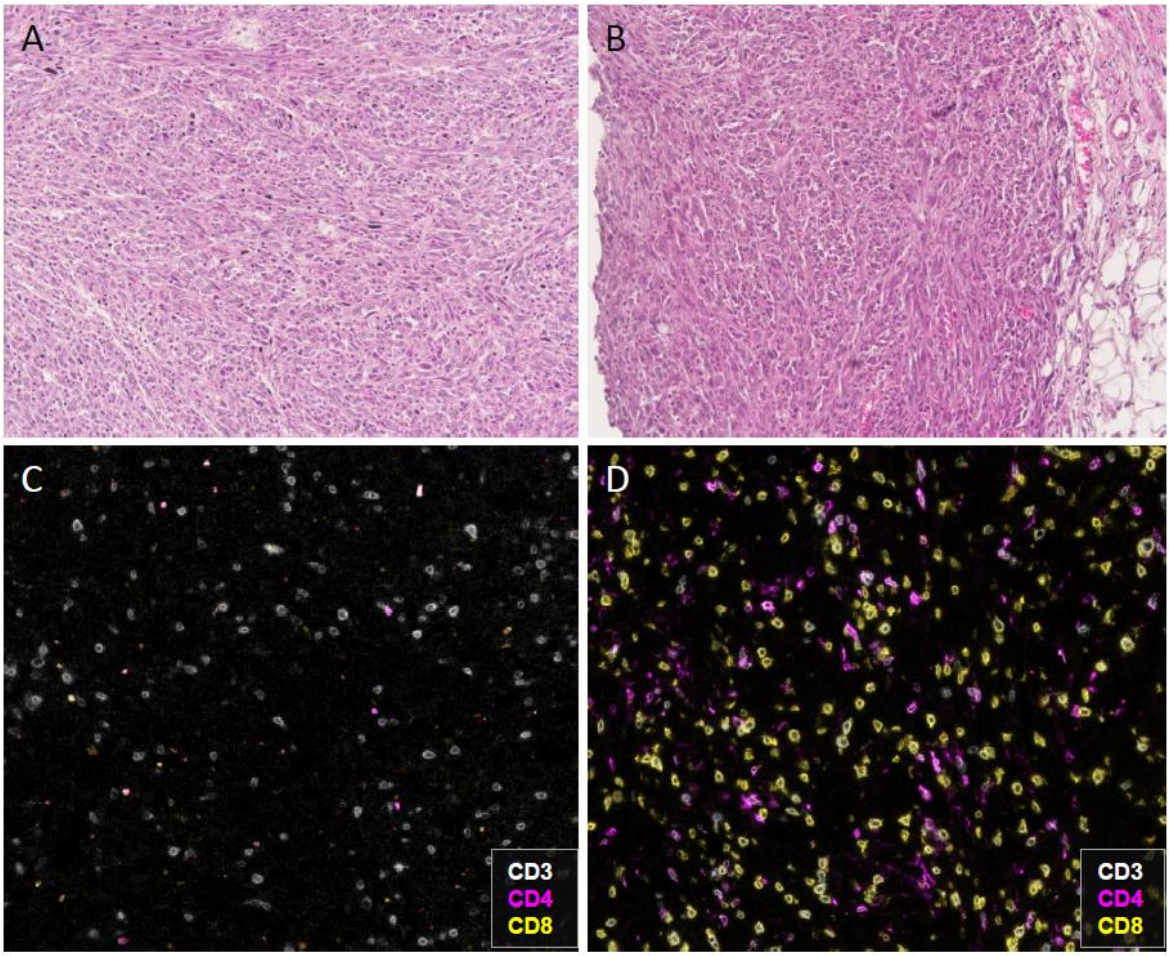

Figure 3.2: Comparison between NBF fixation and Zinc-based fixation. A) H&E staining for SCCVII squamous cell tumor fixed with NBF. B) H&E staining for SCCVII squamous cell tumor fixed with zinc-based buffer. C) Immunostaining of CD3 (white), CD4 (magenta), and CD8 (yellow) in SCCVII tumor fixed with formalin. D) Same staining done in the same tumor fixed with zinc-based buffer.

To validate the CD4 and CD8α staining, we obtained spleens from $Rag1^{-/-}$ transgenic mice which lack both T cells and B cells; or spleens from either a transgenic $CD8^{+}$ T cell receptor mouse that recognizes gp100 (pmel) or a transgenic $CD4^{+}$ T cell receptor mouse that recognizes tyrp1 (TRP1). Both of the T cell receptor transgenic mice were crossed to $Rag1^{-/-}$ mice to ensure only transgenic T cells were present. Spleen sections were cut and stained with CD3, CD4, and CD8α antibodies. As expected, we observed the absence of CD3

staining in the Rag1$^{-/-}$ spleens but the presence of CD3^{+} cells in both pmel and TRP1 spleens (Figure 3.3A-C, M). Interestingly, we observed the presence of a small population of cells that stained with CD8α in Rag1$^{-/-}$ mice; however, these CD8^{+} cells did not stain with CD3 (Figure 3.3A, E) and based on their morphology and location within the spleen, they are most likely CD3^{-}CD8α^{+} dendritic cells [183]. In pmel transgenic animals, we saw an increase in CD3^{+}CD8α^{+} cells (Figure 3.3B, F, M), confirming the recognition of the antibody to CD8^{+} T cells. We observed CD3^{-}CD4^{+} cells in the spleens from Rag1$^{-/-}$ and Rag1$^{-/-}$ pmel TCR transgenic mice (Figure 3.3A, B, I, J). Examination of spleens from Rag1$^{-/-}$ TRP1 TCR transgenic mice showed a small population of CD3 expressing cells in the T cell areas of the spleen (Figure 3.3C), but interestingly this did not correlate with an increased expression of CD4 in these spleens compared to Rag1$^{-/-}$ or Rag1$^{-/-}$ pmel TCR (Figure 3.3I, J, K, M). Although CD4, like CD8α, can also be expressed in non T cells such as macrophages and DCs[184-186], we wanted to validate the specificity of the CD4 staining. To do this, we stained a spleen from a CD4$^{-/-}$ mouse. We did not observe any CD4 staining in the CD4$^{-/-}$ spleen, confirming the specificity of the antibody (Figure 3.3D, H, L). The existence of these CD3^{-}CD4^{+} cells highlights the importance of multiplex immunohistochemistry, which allows us to separate the CD3^{+}CD4^{+} T cells from the CD4^{+} myeloid cells to accurately identify and study these distinct populations.

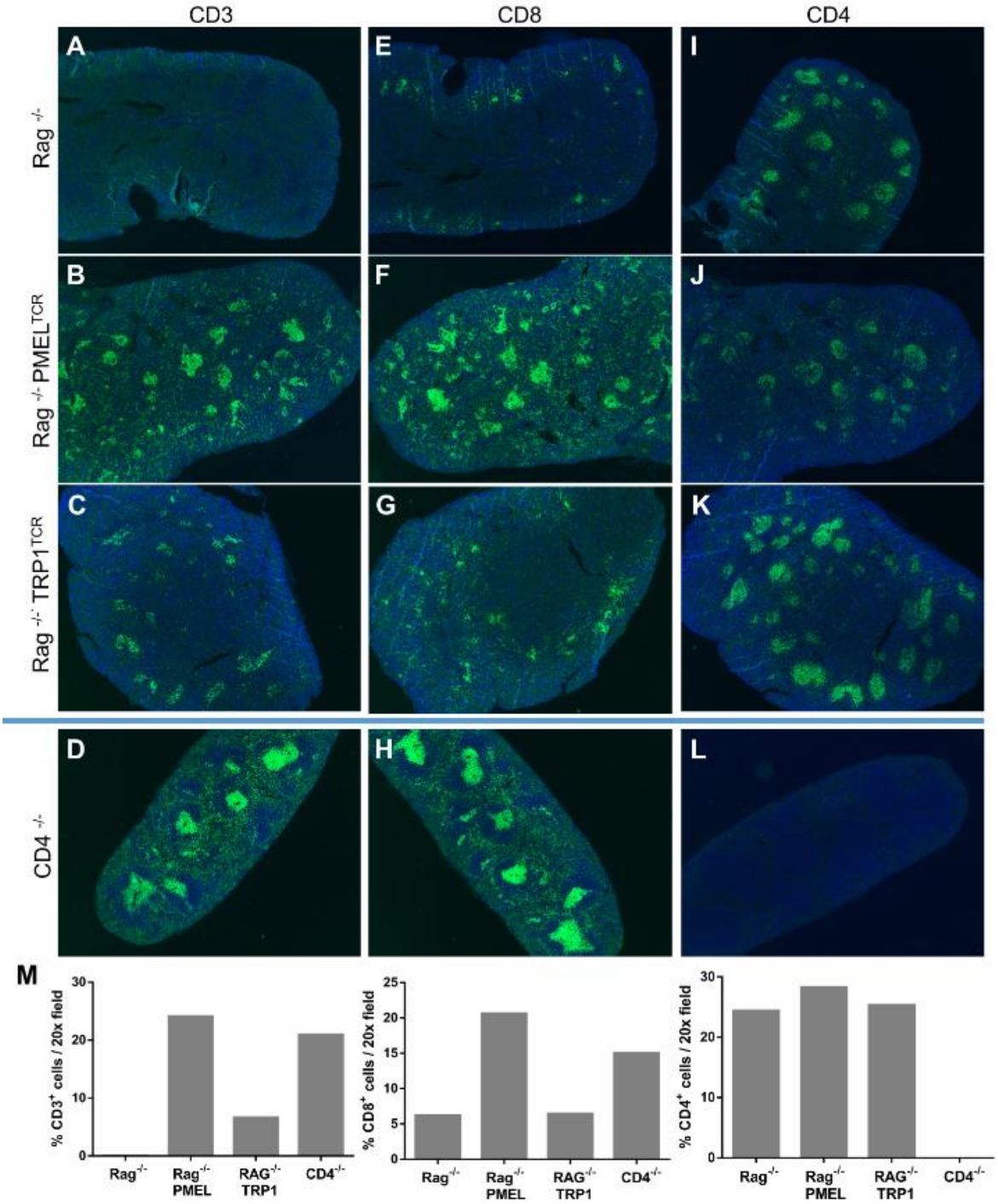

Figure 3.3: CD4 and CD8 staining in spleen sections. Spleens are fixed for 24 hours in each condition. Single stains with CD3, CD4, and CD8 antibody are performed and tissue sections are imaged at 4x with PerkinElmer Vectra platform. Spleens from RAG1 knockout were stained with CD3 (A), CD8 (B), CD4 (C). Stains were also performed on spleens from RAG1 knockout with transgenic PMEL TCR (B, F, J), RAG1 knockout with transgenic TRP1 TCR (C, G, K), and CD4 knockout (D, H, L). Cells were enumeration as % of positive cells in a 20x

field (M).

Murine multiplex fluorescent immunohistochemistry

Our previous work has shown that a tyramide-based multiplex fluorescent imaging platform can be used to predict the success of culturing tumor-infiltrating lymphocytes from human melanoma samples[24]. A simple diagram of this protocol is shown in Figure S2. Briefly, tissue sections were antigen-retrieved, stained with primary, secondary antibodies, and then stained with tyramide (TSA) conjugated to a fluorochrome label. This was followed by heat-mediated antigen stripping to remove the primary antibody in order to label with new primary antibody. To establish a multiplex protocol in murine samples, we tried heat-mediated antigen stripping on murine zinc-fixed tissues. We found that after antigen retrieval, we were able to stain for CD3 (Figure 3.4A-B), but we lost the ability to stain for CD4 (Figure 3.4C-D) and CD19 (Figure 3.4E-F). Although we saw CD8α staining on the tissue following antigen retrieval (Figure 3.4G-H), these were not T cells as none of the $CD8\alpha^+$ cells co-stained with anti-CD3 (Figure 3.4I).

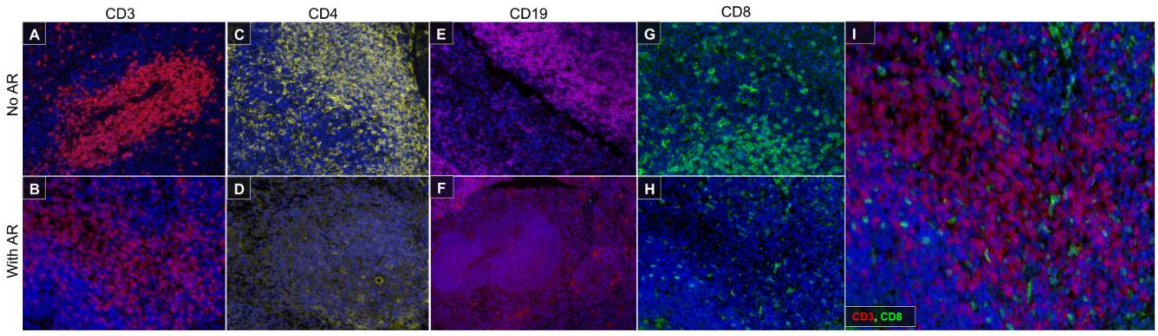

Figure 3.4: Heat-mediated antigen retrieval diminishes CD4, CD19 and CD8 staining. Heat-mediated antigen retrieval with Biogenex Citra buffer was performed using microwave. Slides were microwaved for 25 seconds to bring to a boil on high power and maintained for 10 minutes on 10% power. Antibody

staining were performed with (B,D,F,H) or without (A,C,E,G) antigen retrieval. I) Merge of CD3 and CD8 after antigen retrieval.

To circumvent this issue, we prepared and compared two non-heat-mediated glycine-based stripping buffers that are either basic (pH 10) or acidic (pH 2). Spleen tissue sections were sequentially stained with CD8α, CD4, and CD19 in that order and antigen stripping buffer was applied between antibodies. We found that the basic antigen stripping buffer (pH 10) was superior in maintaining subsequent CD4 and CD19 staining intensity (Figure 3.5A) compared to the acidic stripping buffer (Figure 3.5B). We subsequently tested the stripping efficiency using the basic stripping buffer. We found that the pH 10 buffer was able to sufficiently strip the previous antibody, allowing for subsequent staining with no cross epitope staining (Figure 3.5C-F). This demonstrates that the basic stripping buffer is suitable for multiplex fluorescent immunohistochemistry detection of sensitive T and B cells markers in murine tissues. We were able to use the basic stripping buffer to successfully identify CD3, CD4, CD8 populations in the spleen (Figure 3.6A-G).

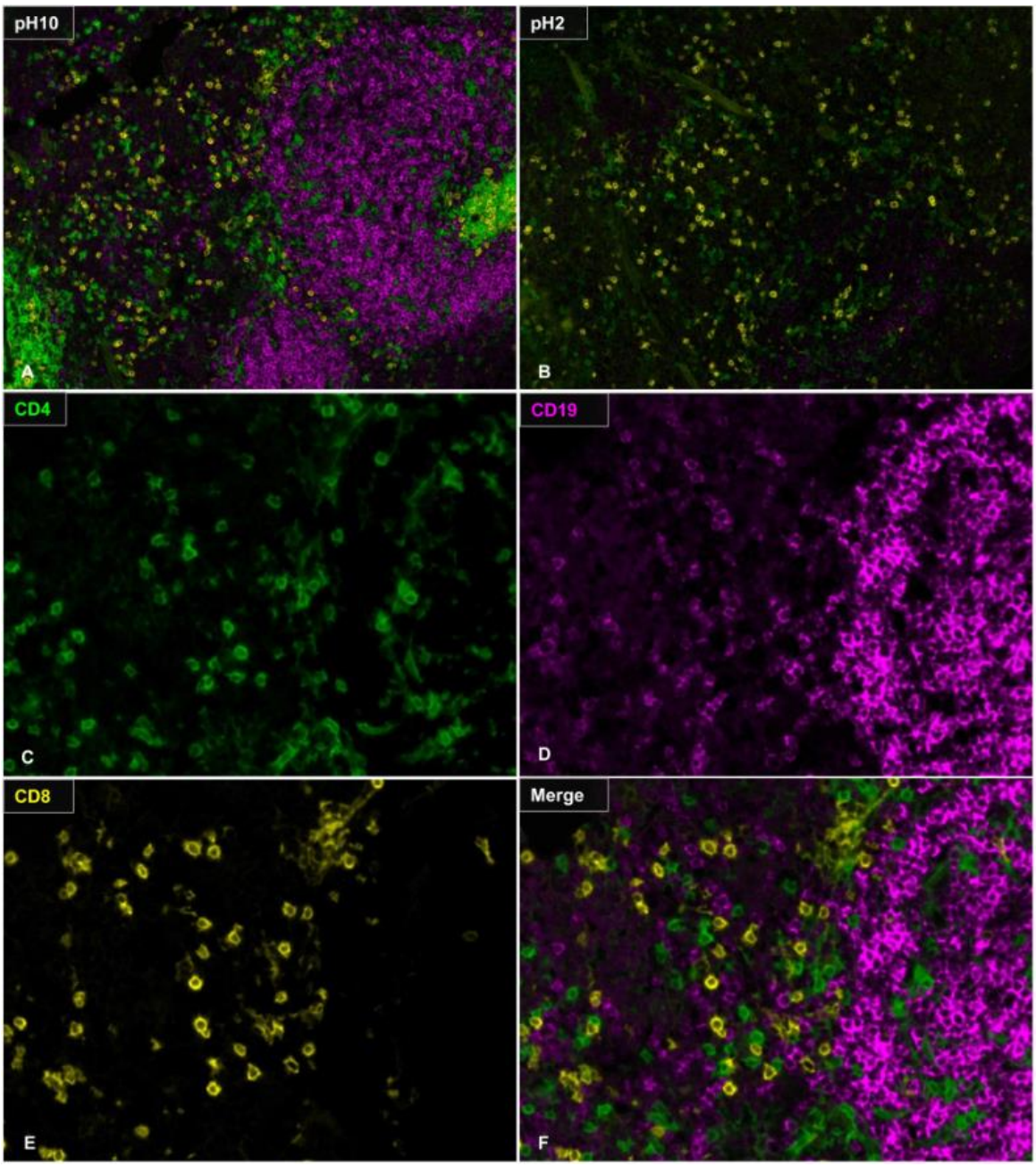

Figure 3.5: Multiplex Immunohistochemistry with CD4, CD8 and CD19. Slides were first stained with CD8 (yellow), and exposed to antigen stripping buffer (100mM glycine, 0.5% Tween, pH10(A) or pH2(B)). Slides were stained for CD4 (green), followed by antigen stripping and CD19 staining (magenta). C-F) Higher magnification of the slides stripped with pH10 buffer.

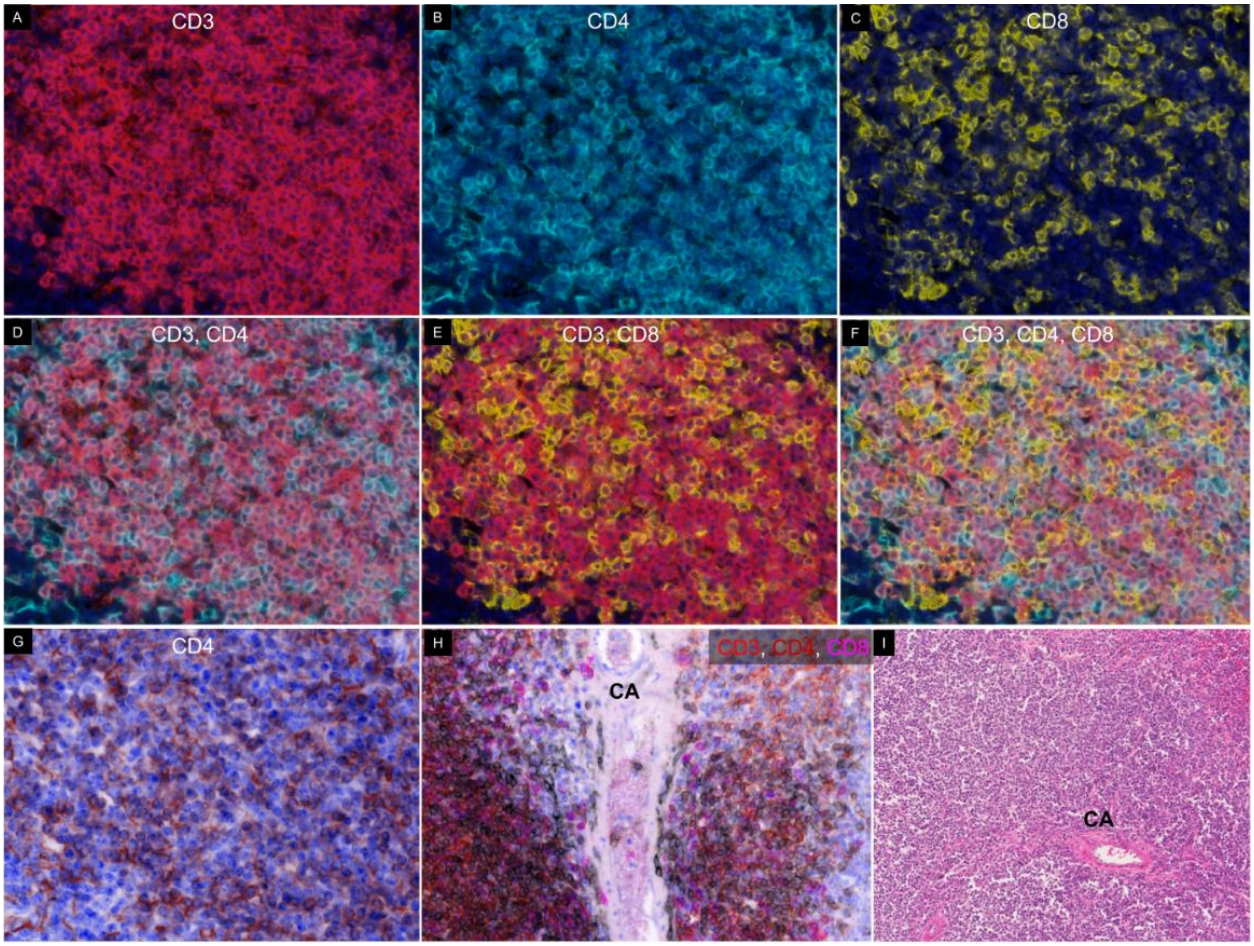

Figure 3.6: Staining of CD4 and CD8 T cells in spleen. Slides were stained with CD3 (A), CD4 (B) and CD8 (C) in that order with antigen stripping in between. D) Merge of CD3 and CD4; E) Merge of CD3 and CD8; and F) Merge of CD3, CD4, and CD8 G) Pseudo H&E image of CD4 staining with DAPI H) Pseudo H&E image of CD3 (Red), CD4 (Brown) and CD8 (Magenta) on cells adjacent to a central artery (CA). I) H&E image of spleen sections outlining lymphocyte distribution around a central artery (CA).

The observation of follicular CD4 staining in Rag1$^{-/-}$ is interesting, reports have established the presence of CD3^{-}CD4^{+} DCs in murine tissues[184, 186]. To determining whether these CD3^{-}CD4^{+} cells are DCs, we stained for DC marker CD11c using our multiplex protocol and found a significant portion of the CD4^{+} cells expressing CD11c (Figure 3.7A-D). Using flow cytometry, we also determined that these CD3^{-}CD4^{+} cells can also express CD11b, consistent with previous reports that macrophages can express CD4[187] (Figure 3.7E).

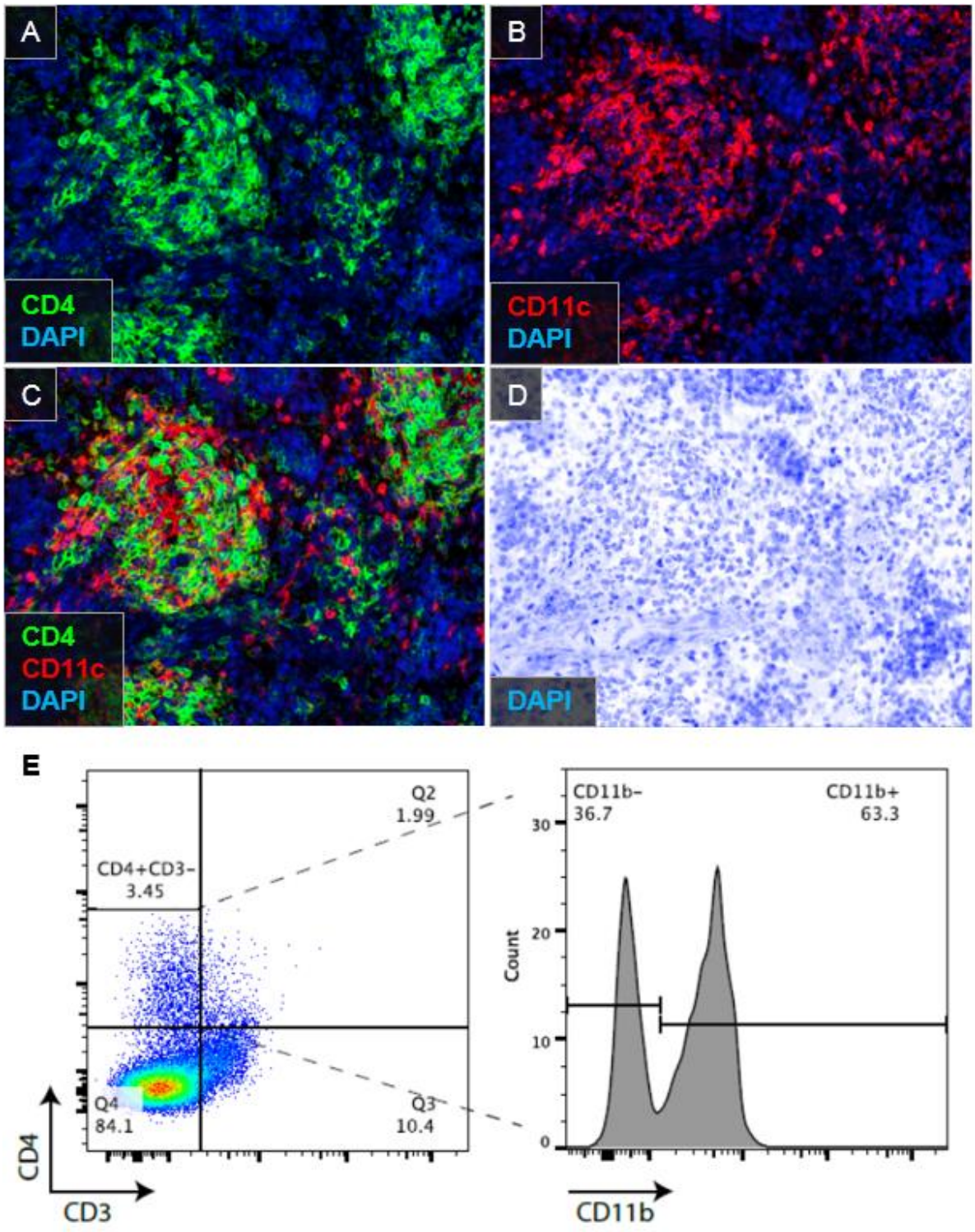

Figure 3.7: CD3-CD4+ cells co-express CD11b and CD11c. Spleen sections from Rag1$^{-/-}$ animal were stained with CD4 and CD11c by IHC (A-C). D) Pseudo H&E of the section demonstrating spleen architecture. E) Spleen sections from Rag1$^{-/-}$ were collected and stained for CD3, CD4, and CD11b by flow cytometry.

We next wanted to address if their residence in the follicles of the spleen of Rag1$^{-/-}$ mice would be displaced if CD3^{+}CD4^{+}, CD3^{+}CD8^{+} and CD19^{+} B cells were adoptively transferred into these mice. To do this, we adoptively transferred splenocytes from wild-type C57BL/6 to syngeneic Rag1$^{-/-}$ transgenic mice. Spleens from the receiving animal were harvested 14 days post adoptive transfer and assessed for the presence of T and B cells. We found that following the adoptive transfer, there is a significant increase in CD19^{+} B cells and CD3^{+} T cells (Figure 3.8F, I, L, N) with a concurrent decrease of CD3^{-}CD4^{+} cells (Figure 3.8K). Furthermore, the location of the majority of CD19^{+} B cells and CD3^{+} T cells, as indicated by IHC, are inside the follicles, surrounded by CD3^{-}CD4^{+} cells (Figure 3.8F-J).

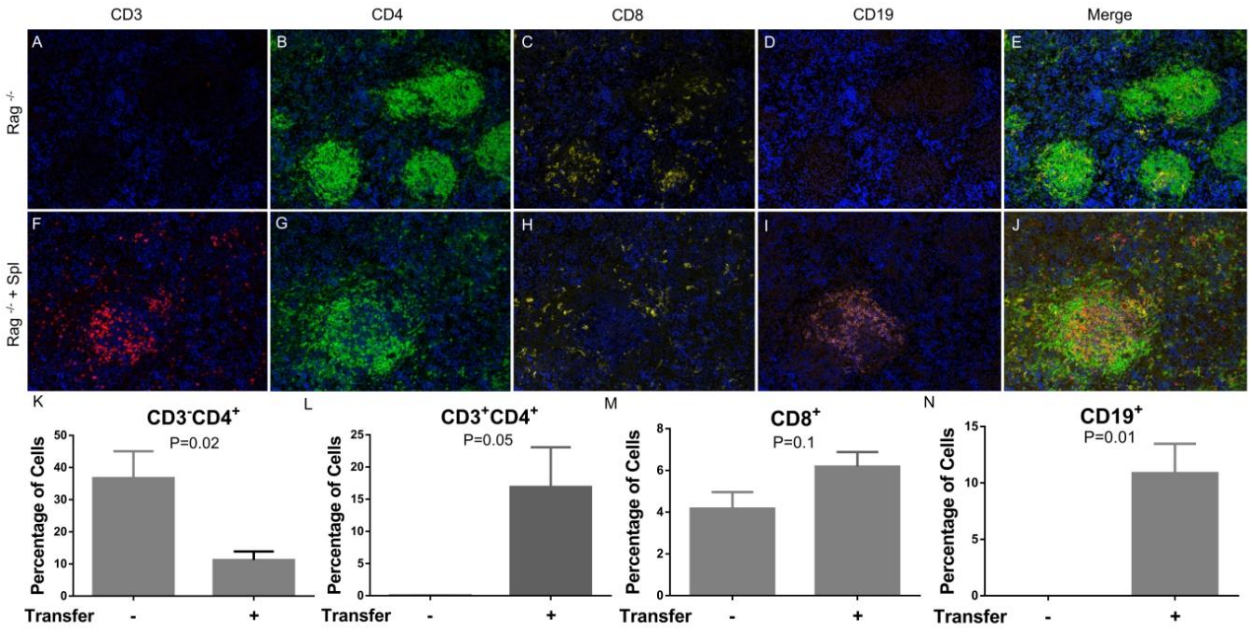

Figure 3.8: Adoptive transfer of splenocytes into Rag-/- mice. 10 million splenocytes from WT C57Bl/6 were transferred to Rag1$^{-/-}$ mice. Spleens were

harvested 14 days later. Multiplex fluorescent IHC was performed on both Rag$^{-/-}$ (A-E), and adoptively transferred animals (F-J). Statistics (K-N) were performed using unpaired T test. N=3-4. The % positive cells enumerated are based on total DAPI^{+} cells in the area imaged.

The simultaneous increase in T and B cells and decrease in CD3^{-}CD4^{+} cells could suggest that there may be signals exist in these follicles that drives the survival of these CD3^{-}CD4^{+} cells, and similar signals may exist to facilitate the migration of adoptively transferred T and B cells.

Finally, we wanted to evaluate whether this multiplex technique could be used to stain immune cells in a tumor setting. We subcutaneously injected C57BL/6 mice with a methylcholanthrene-induced sarcoma cell line. Tumors were harvested and stained for CD3, CD4, CD8, FoxP3, and F4/80 using our multiplex IHC protocol. We were able to identify distinct T cell populations in the tumor (Figure 3.9A-G), and separate them into CD3^{+}CD4^{-}CD8^{-} T cells, CD3^{+}CD8^{+} T cells, CD3^{+}CD4^{+}FoxP3^{-} T cells, and CD3^{+}CD4^{+}FoxP3^{+} regulatory T cells. This multiplex IHC protocol was verified in a second murine tumor model with a spontaneously squamous cell carcinoma cell line, SCCVII.

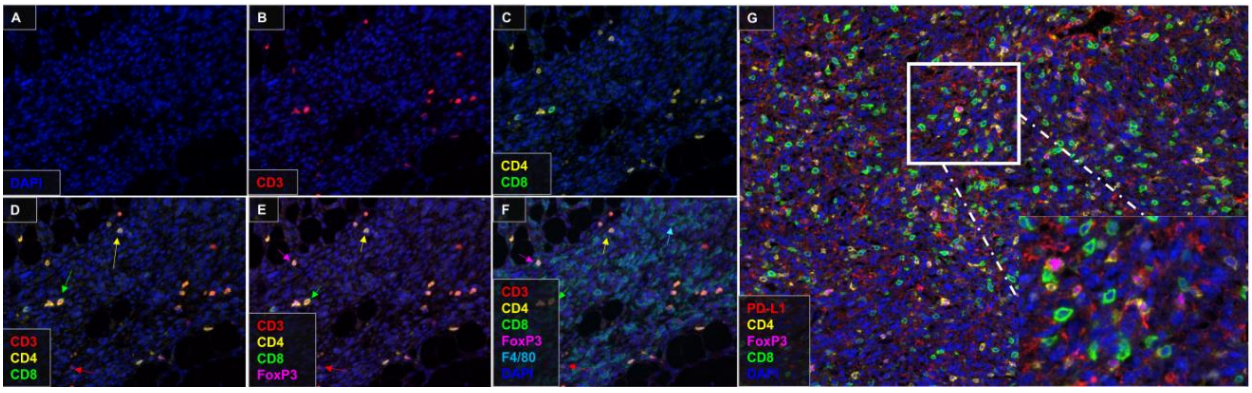

Figure 3.9: Multiplex fluorescent IHC on tumor samples. A-F) MCA310 sarcoma tumor was stained with CD3, CD4, CD8, FoxP3, F4/80 and DAPI. Red arrows indicating CD3^{+}CD4^{-}CD8^{-} T cells, green arrows showing CD3^{+}CD8^{+} T cells,

yellow arrows indicating $CD3^+CD4^+FoxP3^-$ T cells, and magenta arrows indicate $CD3^+CD4^+FoxP3^+$ T cells G) SCCVII squamous cell carcinoma tumor was stained with PD-L1, CD4, CD8, FoxP3, and DAPI. Inlay: higher magnification of a section of tumor demonstrating CD4, CD8, FoxP3 and PD-L1 staining.

Discussion

Immunohistochemistry approaches on formalin-fixed-paraffin-embedded tissues have long been the standard for morphological analysis. More recently, quantitative IHC methods have shown promise in development of cancer diagnostics and prognostic biomarkers for tailored therapy[188, 189]. This is especially useful in the era of immunotherapy as many immunotherapies can benefit from biomarkers allowing for directed treatment. Methods such as multiplex immunohistochemistry have been in the forefront of development as they significantly enrich the data extracted from the tissue microenvironment, and allow for relationship analysis between cell subsets for added information. Much of the work has been performed on human tissues as the staining of various epitopes on FFPE tissues has been optimized[13, 24]. For murine studies, characterizing tissue immune-environment by IHC are lacking due to many epitopes, notably CD4 and CD8, being sensitive to cross-linking and unable to be detected in FFPE samples. Frozen sections are sometimes used for these sensitive antibodies[190], but results in distorted tissue architecture and artifacts that are poor for morphological studies. For these reasons, flow cytometry has long been the gold standard for analysis of immune infiltrate in the tumor microenvironment[191]. However, flow cytometry does not provide sufficient contextual information, which has been shown in both murine and human studies to be important in understanding the biological basis of diseases, and predicting outcome in various types of cancer[18, 157]. It has been suggested that alternative fixation methods, such as PLP and zinc-based fixation are superior to formalin in

preserving certain epitopes, but the specificity of the antibodies under these conditions are not characterized and their application in a multiplex platform is unknown. Our study showed that zinc-based fixation is superior to PLP and formalin in the detection of sensitive epitopes such as CD4 and CD8 (Figure 3.1), and may be applied to a boarder selection of antibodies traditionally reserved for flow cytometry and frozen-section such as CD19. These results were not unique to the chosen clones of monoclonal antibodies as we also observed staining with a different clone targeting CD4 (RM4-5 - Fig 3.1; GK1.5 – Fig 3.2c-d). In addition we have had success with polyclonal antibodies targeting PD-L1 (Figure 3.9G) and granzyme B (Figure 3.10).

While validating the specificity of CD4 staining (Figure 3.3), we observed a significant population of $CD3^{-}CD4^{+}$ cells assuming follicular aggregation. As these cells appear in both $Rag1^{-/-}$, pmel and TRP1 spleens, it is possible that they reside in follicle devoid of T and B cells, or alternatively, they may be instrumental in recruiting T and B cells to the follicles in the spleen. When we adoptively transferred WT splenocytes into $Rag1^{-/-}$ mice, we observed accumulation of $CD3^{+}$ T cells and $CD19^{+}$ B cells in the vicinity of these follicles (Figure 3.8D-J), suggesting that these $CD3^{-}CD4^{+}$ cells may mediate the recruitment and potential development of B cells. These findings will need confirmation from future studies.

The presence of these $CD3^{-}CD4^{+}$ cells in the spleen outlines the importance of

multiplex staining to reliably study various immune cell populations. We were able to apply the technique in a multiplex platform to examine multiple parameters simultaneously in fixed specimens of murine spleens (Figure 3.6A-I), as well as two orthotopically implanted tumor cell lines (Figure 3.9A-G). To study these sensitive epitopes such as CD4 and CD8α in a multiplex platform, a mild antigen-stripping solution such as glycine is superior for proper preservation of signal compared to heat-mediated antigen stripping (Figure 3.5). We conclude that the pH10 stripping buffer is the optimal buffer solution for this T and B cell panel as it is able to efficiently remove previous antibody without adversely affecting the staining profile with subsequent antibodies. However, stronger stripping solution may be needed for antibodies with stronger affinity, such as F4/80 for macrophages. This can be accomplished with the addition of SDS and acidic pH, which provides a harsher environment for enhanced antibody stripping.

The ability to use this multiplex immunohistochemistry platform to stain different populations of immune cells within the tumor microenvironment provides both quantity and spatial relationships that are informative. It is also important to be able to examine functionality of these cells and we have begun to examine this using granzyme B expression in CD8 T cells (Figure 3.10).

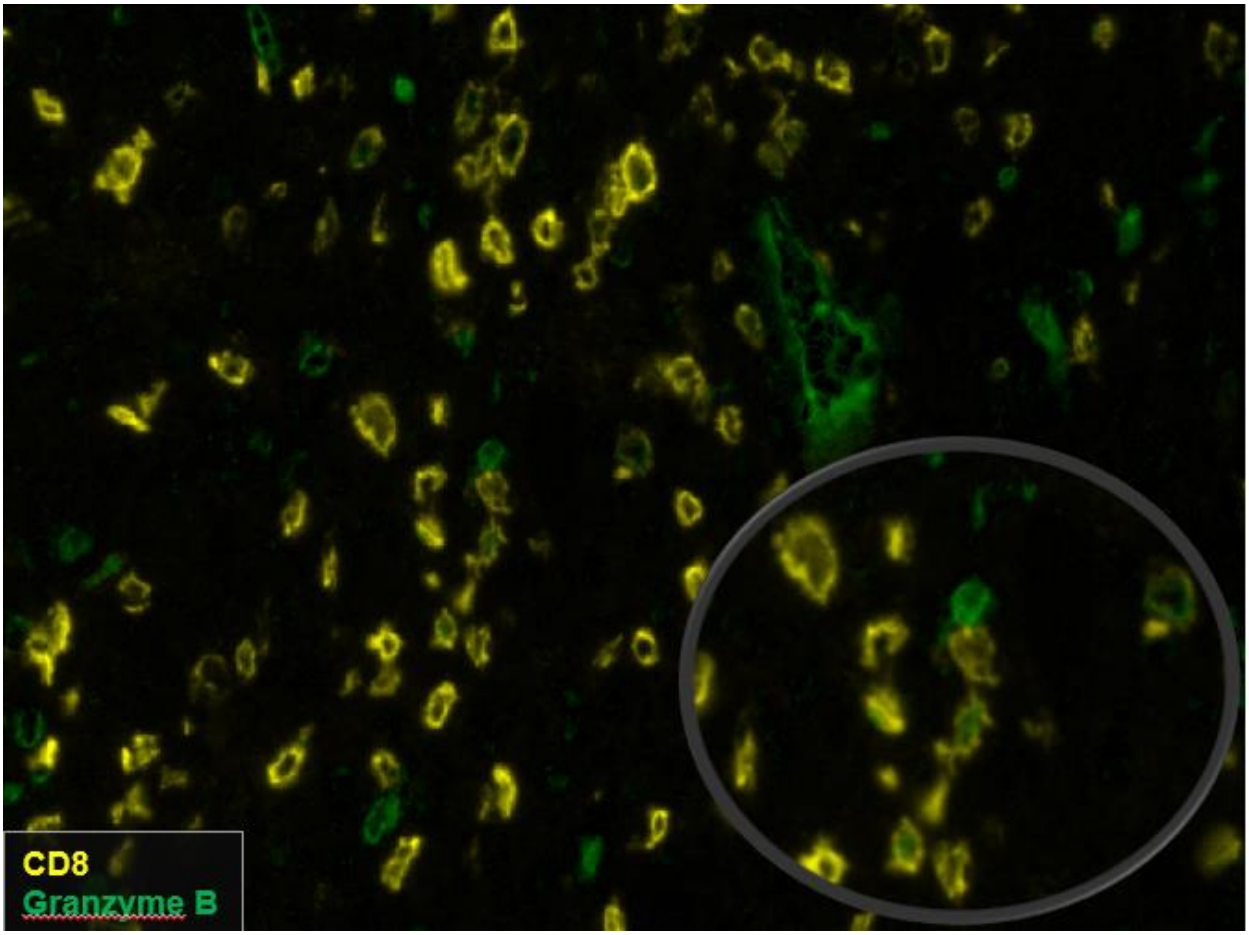

Figure 3.10: A subset of CD8+ T cells express granzyme B. Immunostaining of CD3 (not shown), CD8 (yellow), granzyme B (green) was done in SCCVII tumor sections fixed with zinc-based buffer. Heat mediated antigen-retrieval was performed before granzyme B staining.

A current limitation we have encountered is the lack of effective antibodies to study cytokines expressed by these cells. Genomic approaches may be an alternative to address some of these limitations. Zinc-based fixation has not been shown to adversely affect the quality of DNA and RNA in the sample[182, 192] and we have had preliminary success analyzing mRNA expression profiles in murine tumors fixed with zinc-based buffer (data not shown).

To our knowledge, our study is the first to report on the capability of performing

multiplex IHC with CD4, CD8 and CD19 to identify basic T and B cell populations in zinc-fixed-paraffin-embedded murine tissues. Importantly, this method provides the ability to examine the spatial interactions and relationships between multiple parameters on a single tissue section. Additionally, this approach will likely allow for the utilization of additional antibodies that are traditionally reserved for flow cytometry and frozen-section to be used on paraffin-embedded samples.

Respective contributions

I designed and performed most experiments in this chapter. SJ helped with experimental design, adoptive T cell transfer experiment, and flow cytometry staining. CBB reviewed and verified all IHC staining.

Chapter 4: Multiparametric immune staging of non-HPV head and neck squamous cell cancer

Abstract

Background: Changes in the composition and function of innate and adaptive immune cells in the tumor microenvironment represent crucial hallmarks for initiation and progression of cancer. In oral squamous cell carcinoma (OSCC) the composition, frequency and location of peri- and intra-tumoral immune cells, but also expression of HLA class I antigens and other components of the antigen processing machinery (APM) by tumor cells play an important role in the control of HPV-positive tumors, but the prognostic and therapeutic impact of these parameters in HPV-negative OSCC has not yet been clarified.

Materials and methods: For simultaneous characterization of peri- and intra-tumoral T cell subtypes (CD3, CD8, FoxP3, CD163) including their topographic localization, together with analysis of PD-L1 expression by tumour cells multi-spectral imaging was performed on sections obtained from 119 patients with HPV-negative OSCC. In addition, protein expression of three components of the HLA class I APM (ß$_2$-microglobulin (β_2-m), MHC class I heavy chain (HC) and large multifunctional peptidase (LMP)10 was analyzed by conventional immunohistochemistry. Finally, the data obtained were correlated with clinical and prognostic parameters.

Results: Independent from accepted progression markers like TNM classification and tumor grading high number of peri-tumoral $CD8^+$ T cells in close distance to the tumor cells paired with the absence of surrounding $FoxP3^+$ and/or $PD\text{-}L1^+$

cells and low expression of β_2-m, MHC class I HC and LMP10 defined a tumor subgroup with prolonged overall survival (OS; $P<0.01$). A multivariable cumulative “suppression index” (CSI) scoring system allowed to separate OSCC patients with a 5-year overall survival rate (OSR) of 90% and 20%, respectively.

Conclusion: To our knowledge this is the first application of multispectral imaging describing the relevance of simultaneous evaluation of immune cell – tumor interactions and their use as prognostic biomarkers in evaluating OSCC patients’ outcome. Simultaneous analysis of immune cell infiltration and HLA class I APM component expression by tumor cells even improved the prognostic impact of the multispectral data.

Introduction

Oral squamous cell carcinoma (OSCC) represents a leading cause of cancer worldwide with significant mortality and morbidity. In contrast to other head and neck squamous cell cancer (HNSCC) subtypes, most OSCC are attributed to smoking and alcohol, while an association of this disease with HPV infection is rare [193-196]. Despite novel insights into the molecular basis of HNSCC current therapies do not offer a significant improvement in overall survival (OS) over the last decade[197].

Since the traditionally used risk stratification based on tumor size, lymph node and distant metastasis (TNM staging) and histological grading alone is not sufficient to predict the individual prognosis of OSCC patients[198, 199], additional prognostic biomarkers are urgently required. The adverse prognostic impact of some tumor markers, like the carcinoembryonic antigen (CEA), the cancer antigen (CA) 19-9, CA125, CA15-3 and the squamous cell carcinoma (SCC) antigen is already known since decades[200]. Local tumor hypoxia influencing the expression of hypoxia-inducible factor (HIF) 1α and other hypoxia-associated proteins also has an adverse impact on prognosis[198, 201]. Furthermore, the composition of peri-tumoral immune cell infiltration has been suggested as novel prognostic marker and potential therapeutic target in several tumor entities. Already twenty years ago it was reported that tumor patients with high tumor burden and nodal spread had decreased T cell cytokine release upon their stimulation with the highest depression occurring at most proximal tumor draining lymph nodes[46, 47]. More recently published data indicated that the degree of

immune dysfunction was significantly correlated with a negative clinical outcome[202, 203]. In HNSCC, the prognostic role of immune cells was determined in both peripheral blood and tumor infiltrating immune cells. In peripheral blood mononuclear cells (PBMC) a reduced frequency and activity of immune effector cells and an increased frequency of regulatory T cells (Treg), tumor-associated macrophages (TAM) and myeloid-derived suppressor cells (MDSC) could be correlated with early recurrence and worse prognosis [204-206]. For other solid tumor entities in particular colorectal cancer the adaptive immune reaction composed of T lymphocytes (CD3) with cytotoxic (CD8) and memory (CD45RO) phenotype, located intra-tumoral and peri-tumoral at the invasive margin (IM) represented a significant parameter to predict recurrence and survival of patients [17, 18]. This classification was termed "immunoscore" and provides a score based on the number of $CD3^+$ and $CD8^+$ lymphocytes in the center and in the IM regions of tumors. The prognostic value of various tumor-infiltrating immune cell populations in patients with HNSCC was also determined demonstrating a correlation of a strong $CD3^+$ and $CD8^+$ T cell infiltrate as well as a high frequency of $CD4^+$ $CD69^+$ T cells with an increased OS of these patients [45, 207, 208]. Discrepant results exist on the frequency of $CD4^+$ $CD25^+$ $FoxP3^+$ Tregs and their link to prognosis [209-211]. In contrast absent or low expression of the ζ chain of the T cell receptor (TCR) and a low density of dendritic cells (DCs) was correlated with a poor survival and a high risk of recurrence[212-214].

For most tumor entities it is generally accepted that tumor cells develop different strategies leading to tumor escape from immune surveillance. These mechanisms include downregulation of tumor antigen (TA) expression on their cell surface, loss or a reduced expression of MHC (major histocompatibility complex) class I molecules and components of the antigen processing and presentation machinery (APM) like the MHC class I HC, β_2-m, proteasomal subunits and the peptide transporter associated with antigen processing (TAP), increased expression of immunosuppressive molecules, like co-inhibitory molecules of the B7 family e.g. the programmed death-like receptor ligand 1 (PD-L1) as well as the non-classical HLA class I antigens HLA-G and HLA-E [215-218]. Reversal of the immune escape phenotype by targeting the immune check points with antibodies directed against PD-1 or PD-L1 demonstrated promising efficacy for the treatment of HNSCC [219].

One major disadvantage of studies concerning immune surveillance of HNSCC is that many of these studies either focused on HPV^+ oropharyngeal cancers or did not distinguish its cohorts based on the patients' HPV status despite HPV^+ OSCC exhibit a distinct gene and immune signature compared to HPV^- counterparts [220]. HPV^+ OSCC are associated with much brisker infiltrates of T and B cells, higher levels of interferon (IFN)-gamma secretion, and enhanced CD8 to FoxP3 ratios [45, 221]. These features are might be a response to the presence of viral antigens and may translate into enhanced anti-tumor immune responses [51-55].

So far, a detailed analysis of HPV$^-$ oral cavity SCC regarding immune cell infiltrations, tumor specific strategies for immune escape and association of these parameters with clinical parameters has not been performed. Therefore, the aim of this study was to get better insights into these processes concerning their impact on prognosis, which might help to select patients for specific immunotherapies in particular those with poorer outcome. In order to analyze the different components of immune surveillance players together on one tissue slide multiplex immunohistochemistry (IHC), a powerful method for studying multiple immune subpopulations, tumor cells and cell-to-cell relationship as already been evaluated for melanoma was employed [24,13].

Material and methods

Patient selection

151 patients from University of Halle and 12 patients from Providence with HNSCC were selected for this study. 48 patients were dropped from the study due to HPV-positivity, lack of invasive margin, or difficulties with staining. The features of the cohort are shown in Figure S1.

A

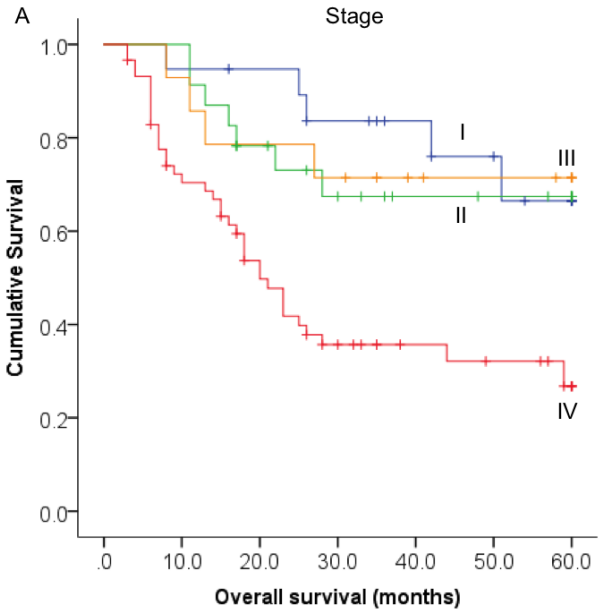

B

Case Summaries

	Age (Years)	Follow-up (Months)	Stage	Grade
N	108	119	115	88
Median	58.000	26.000	4.000	2.000
Minimum	25.0	3.0	1.0	1.0
Maximum	83.0	60.0	4.0	3.0

% Male	75.9
% Received radiation	62.0
% Received chemotherapy	40.0
% HPV-negative cases	100.0
% Survival at last followup	51.8

Figure 4.1: Patient characteristics. A) Kaplan-Meier survival curve of patients by their stage. B) Summaries of patient characteristics, treatment, and follow-up.

Brightfield Immunohistochemistry

For bright field immunohistochemistry (IHC), following monoclonal antibodies (mAb) were used: NAMB (b_2-m; SP09-36), HC10 (HLA class I HC; HSP09-35) and TO-7 (LMP10; SP08-225). Tissue samples were deparaffinized with xylol and transferred via alcohol into aqua dest. Antigen decloaking was performed by steaming the slides with a preheated T-EDTA buffer (ZUC029-500, 1:10 dissolved, Zytomed Systems) at pH 9,0 and 98°C for 20 minutes in an oven (Braun, type 3216). After cooling down for 20 minutes and rinsing with aqua dest slides were blocked for 7-10 minutes with 3% H_2O_2. After another rinsing step and application of washing buffer (ZUC202-2500, 1:20 solution, Zytochem Plus HRP Kit / Plus Polymer System, Zytomed) the antibodies (β_2-m at 1:50, HC10 at 1:2500 and LMP10 at 1:200 dilution) were added dropwise on the tissue area

and incubated for 30 minutes at room temperature (RT). Antibody removal was performed by vacuum followed by a washing step. Then slides were incubated with a biotinylated secondary antibody (Broad Spectrum, Zytochem Plus HRP Kit, Zytomed) for 15 minutes at RT, rinsed with washing buffer followed by 15 minutes of incubation with horse radish peroxidase (HRP; Zytochem Plus HRP, Zytomed). The epitopes were visualized with DAB (10 minutes of DAB Substrate Kit, Zytomed). After further rinsing steps (aqua dest), the slides were counterstained with hemalaun (Dr. K. Hollborn & sons) for 30 seconds, transferred into xylol and covered (Eukitt, ORSAtec) for bright field analysis. Staining results were semi-quantitatively evaluated utilizing the international rating score (IRS) as described by Remmele and co-authors[222] determining staining intensity (0-negative, 1-low, 2-moderate, 3-strong positive) and percentage of stained cells (0-negative, 1- <10%, 2- 10-50, 3- 51-80, 4- >80%), the IRS score is then the product of the two. All tissue samples were independently categorized by two pathologists.

Multiplex Immunohistochemistry

Slides were deparaffinized and antigen retrieved with Citra (Biogenex) buffer. Slides were sequentially stained as previously described (Feng, Puri et al, 2015) with PD-L1 (E1L3N, Cell signaling), CD8 (M239, Spring Bioscience), FoxP3 (236A/E7, Abcam), CD3 (2GV6, Ventana), CD163 (MRQ26, Ventana), cytokeratin (AE1/AE3, DAKO) and DAPI (Invitrogen). TSA-Cy5 (PerkinElmer),

TSA-Cy3 (PerkinElmer), TSA-FITC (PerkinElmer), TSA-Alexa594 (Life Technologies), TSA-Biotin-Alexa514 (PerkinElmer, Life Technologies), and TSA-Coumarin (PerkinElmer) were applied to each antibody respectively. Slides were imaged using PerkinElmer Vectra platform. Similar to the "hotspot" analysis established previously[18], three 20x fields from the invasive margin were selected based on highest lymphocytic infiltrate. Images were analyzed in small batches using PerkinElmer inForm and R script for cell phenotype enumeration and relationship analysis.

Statistical analysis

Kaplan-Meyer survival curve were established using SPSS statistical software V23. For each analysis, a median cutoff is used, log-rank and Breslow tests were performed and P value from the most appropriate test was reported. For suppression index studies, we assigned a binary value for each category using median cutoff and summed all the values to calculate the suppression index score. The P value represents the difference between the lowest and highest SI scores.

Results

Location of $CD8^+$ T cells at the tumor invasive margin predict overall survival in HPV-negative OSCC

Within a tumor tissue the invasive margin represents an immunologic important zone, where invading tumor cells interact with surrounding tissues and environment. As already shown for colorectal cancer (CRC), such tumor-immune cell interactions have the potential to decide on outcome of patients – independent from other prognosis factors[223]. Immunoscore studies on CRC and lung cancer revealed that one of the most important components of the tumor micro milieu is the density of $CD8^+$ T cells, but every tumor entity has to be considered separately [157, 224-226]. In HPV^- OSCC, the invasive margins harbor a significantly denser immune cell infiltrate than the tumor centers, a difference that was more pronounced than in CRC (Figure 4.2A-C).

Therefore, the analyses were focused particularly at the invasive margins after staining tumor sections from 119 OSCC patients in two centers with 7 different markers (Figure 4.3). The invasive margins were further divided into tumor and stromal components before the immune population subsets in both compartments were objectively assessed (Figure 4.3).

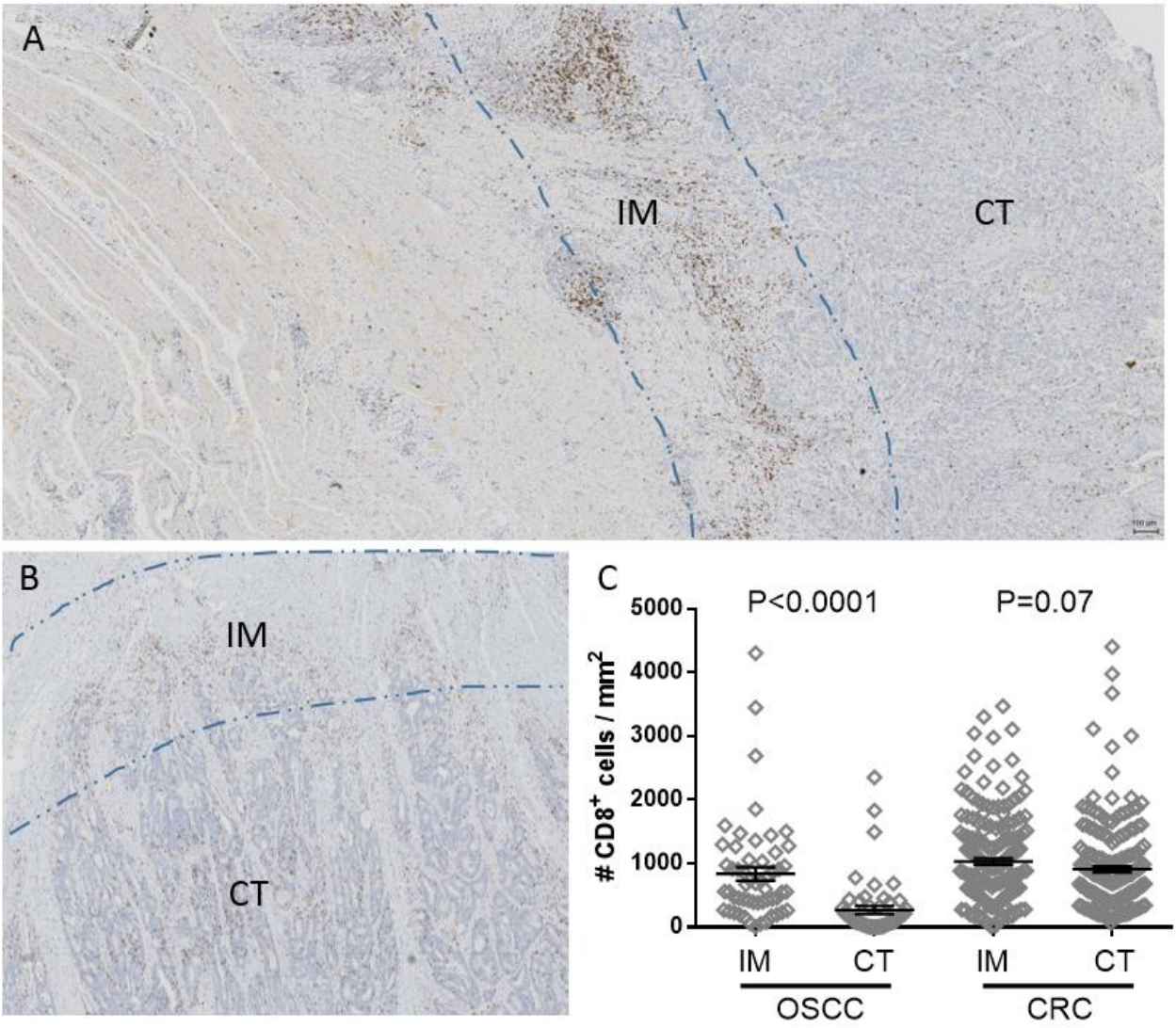

Figure 4.2: Difference in the location of immune infiltrate between OSCC and colorectal cancer. A) Representative example of CD8 infiltrate for OSCC B) Representative example of CD8 infiltrate for colorectal cancer C) Enumeration of immune infiltrates using Definiens platform. IM: Invasive Margin, CT: Center of Tumor

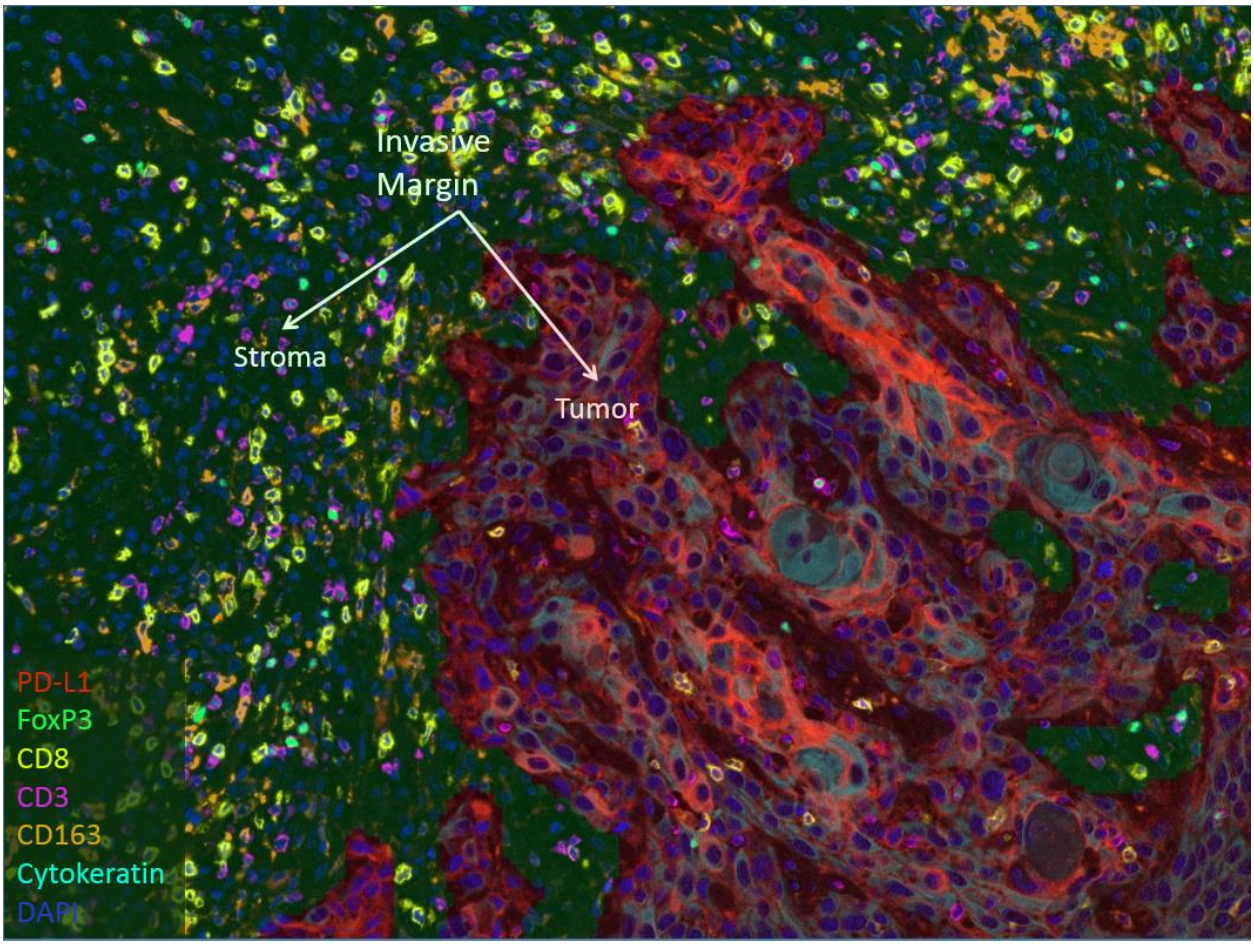

Figure 4.3: Example of staining and tumor-stromal recognition for OSCC specimens. Tissue sections were stained with 7 different markers, 20x images with highest immune infiltrate were taken at the invasive margin, which is further separated into tumor and stromal components. Red overlay – recognized by software as tumor; green overlay – recognized by the software as stroma.

Consistent with the concept of CD8 T cells playing a central role in prognosis and response to therapy, we found a direct correlation between the density of $CD3^+CD8^+$ T cells and a favorable overall survival (Figure 4.4A, D). More strikingly, by sub-compartmentalizing the invasive margin, the density of $CD8^+$ T cells in proximate vicinity of tumor cells has a greater impact on overall survival compared to $CD8^+$ T cells in greater distance to the tumor cells (Figure 4.4A, D). These data suggest that even within the IM the relative location of $CD8^+$ T cells is

important, and may be an indicator of an overall favorable immune signature at the IM.

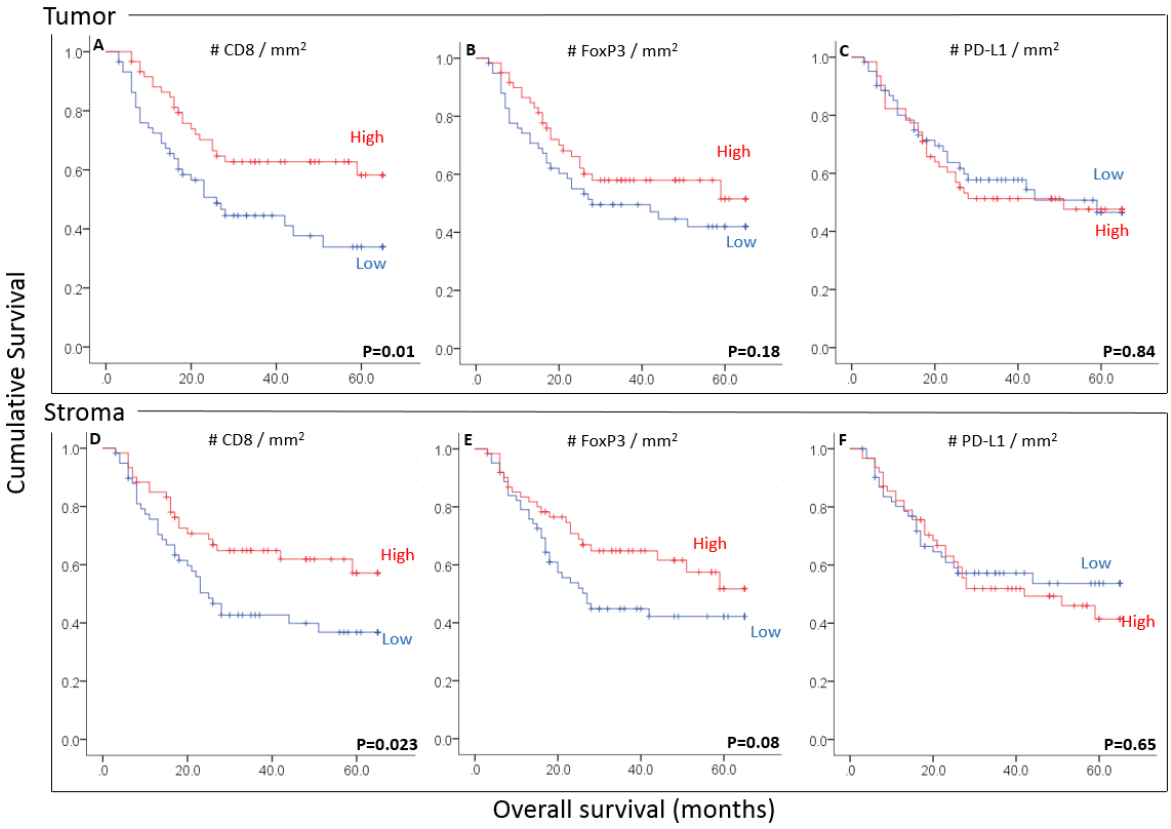

Figure 4.4: Impact of densities of immune infiltrate at the invasive margin on overall survival. Densities of CD8, FoxP3 and PD-L1 at both tumor and stroma of the invasive margin were enumerated using PerkinElmer inForm software. A median cutoff is used to separate high and low infiltrate. Log-rank statistics are performed to determine significance.

Suppressive factors at the invasive margin play an important role in overall survival

Interestingly, our analysis revealed a positive association between the number of $CD3^+$ $FoxP3^+$ T cells in the stroma and OSCC patients' outcome (Figure 4.4E). Similar findings have been reported in CRC, HPV^+ oropharyngeal SCC and gastric cancer [227, 228]. Based on a positive correlation between the Treg influx and $CD8^+$ T cell infiltrate (Figure 4.5), it was assumed that a portion of these Tregs

recruited to the tumor microenvironment (TME) either do not repress tumor antigen-specific T cells or exert diminished suppression due to increased distance.

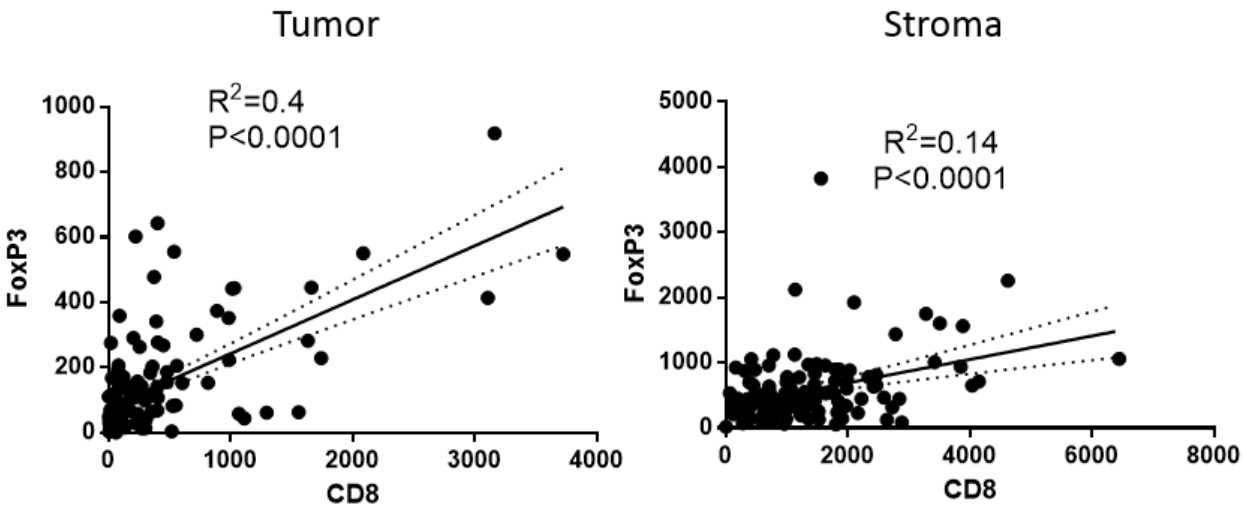

Figure 4.5: Correlation between FoxP3 and CD8 infiltrate at the invasive margin. Densities of cells were enumerated using PerkinElmer inForm and linear regression and significance were established using Prism.

To support this hypothesis that different levels of suppression exist dependent on their precise localization within the TME, the density of $FoxP3^+$ T cells was determined only within 30µm of $CD8^+$ T cells (our method is illustrated in Figure 4.6), a distance that was established based on the preliminary analysis of 34 patients of our cohort (Figure 4.7).

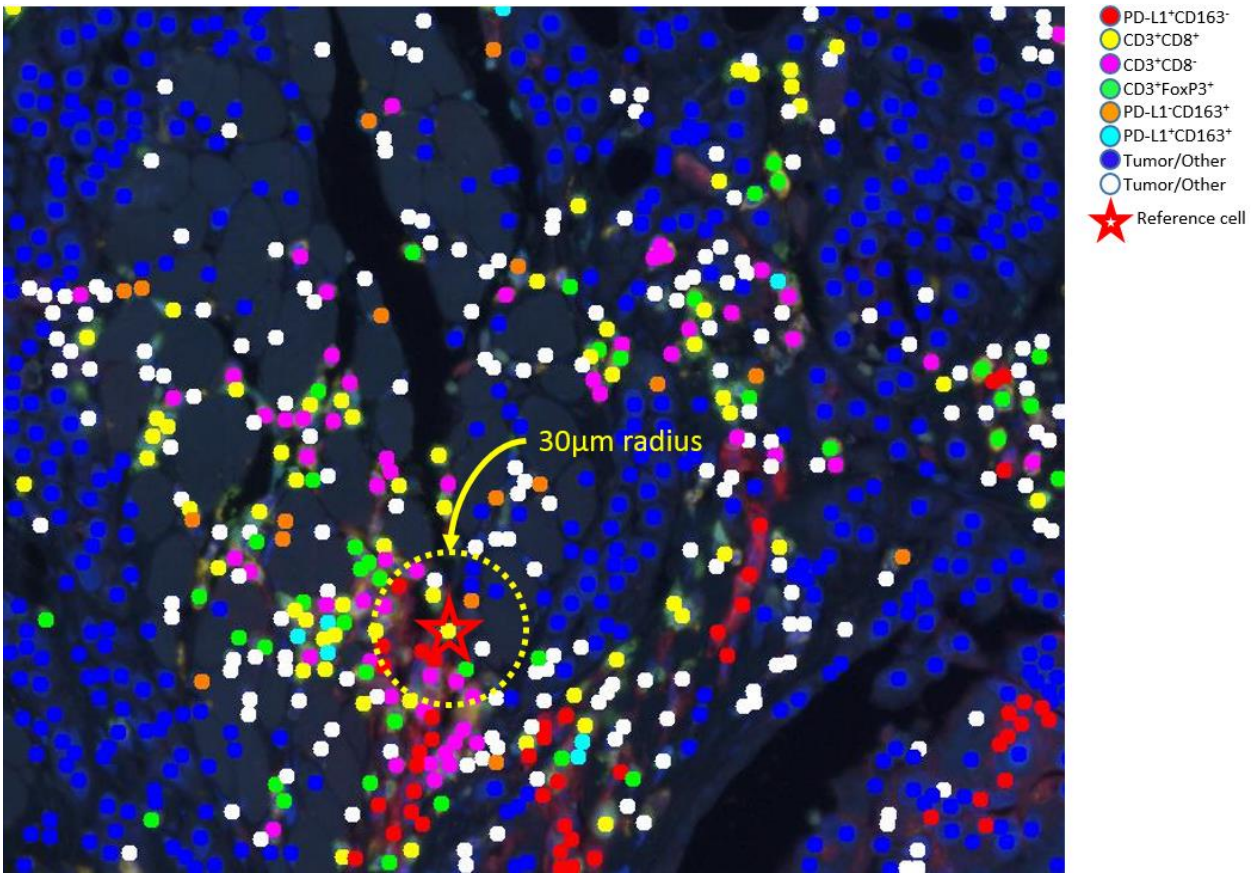

Figure 4.6: Example of relationship analysis. A reference cell (star) is picked and cell types were enumerated within a certain distance and the overall relationship parameter is an average of all numbers in the entire 20x field.

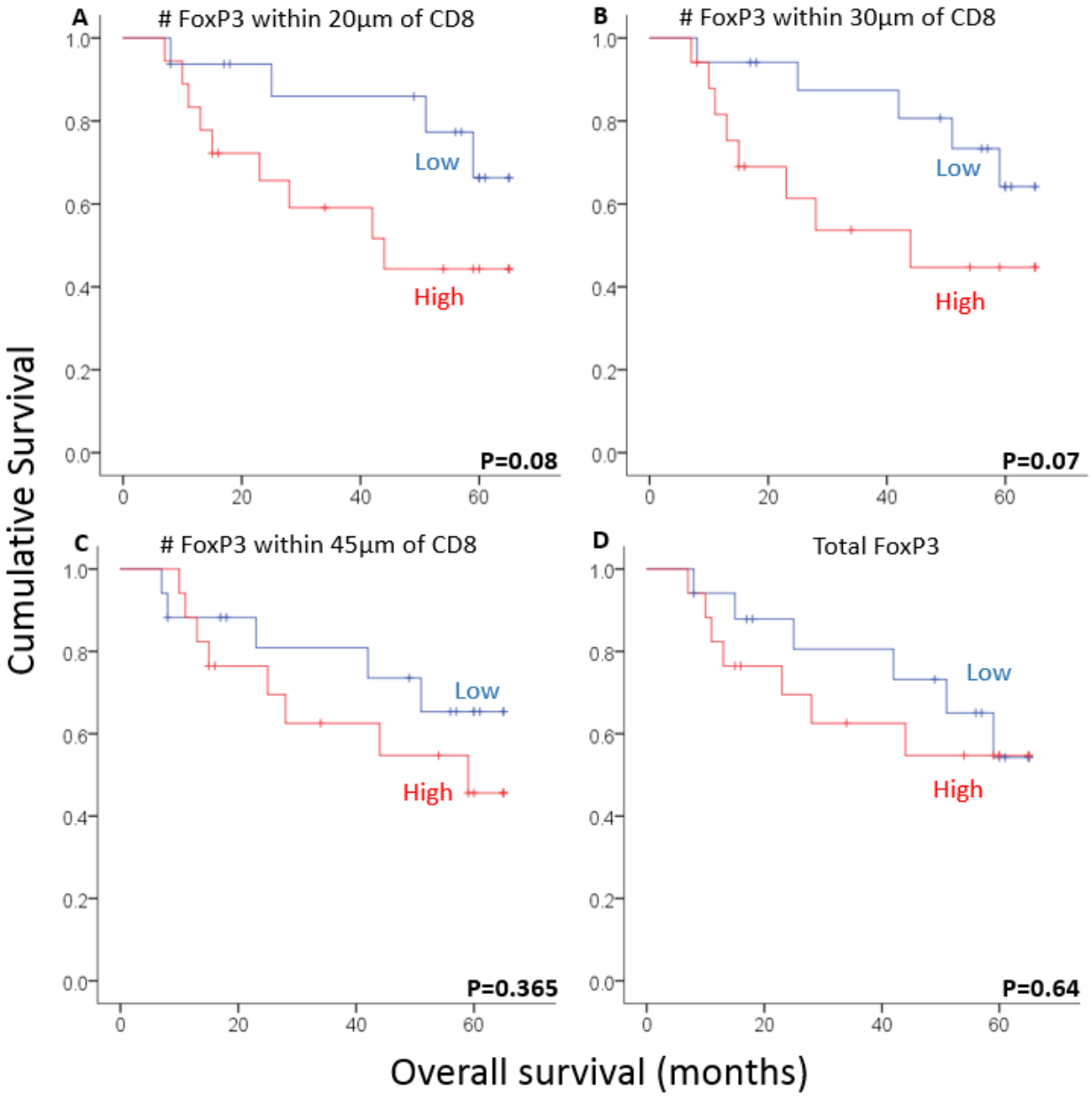

Figure 4.7: Comparison between numbers of FoxP3 within different distances of $CD8^+$ T cell. Four different distances were compared using inForm platform combined with R-script provided by PerkinElmer. The average numbers of $FoxP3^+$ T cells within 20, 30, and 45 microns of CD8, as well as total number of $FoxP3^+$ T cells were calculated and normalized to total number of $CD8^+$ T cells. A median cutoff is used to establish the Kaplan-Meier survival curve. N=34 for this preliminary cohort.

When normalized to the density of $CD8^+$ T cells prognostic separation of the patients was superior using this approach: we were able to further separate patients when compared to analyses of the density of either $CD8^+$ T cells or

Tregs alone (Figure 4.8A, D); this observation was not found by analysis of all Tregs (Figure 4.9A, C, E, G). Consistent with Treg biology this difference suggests that Tregs more proximal to $CD8^+$ T cells may exhibit an enhanced suppressive function.

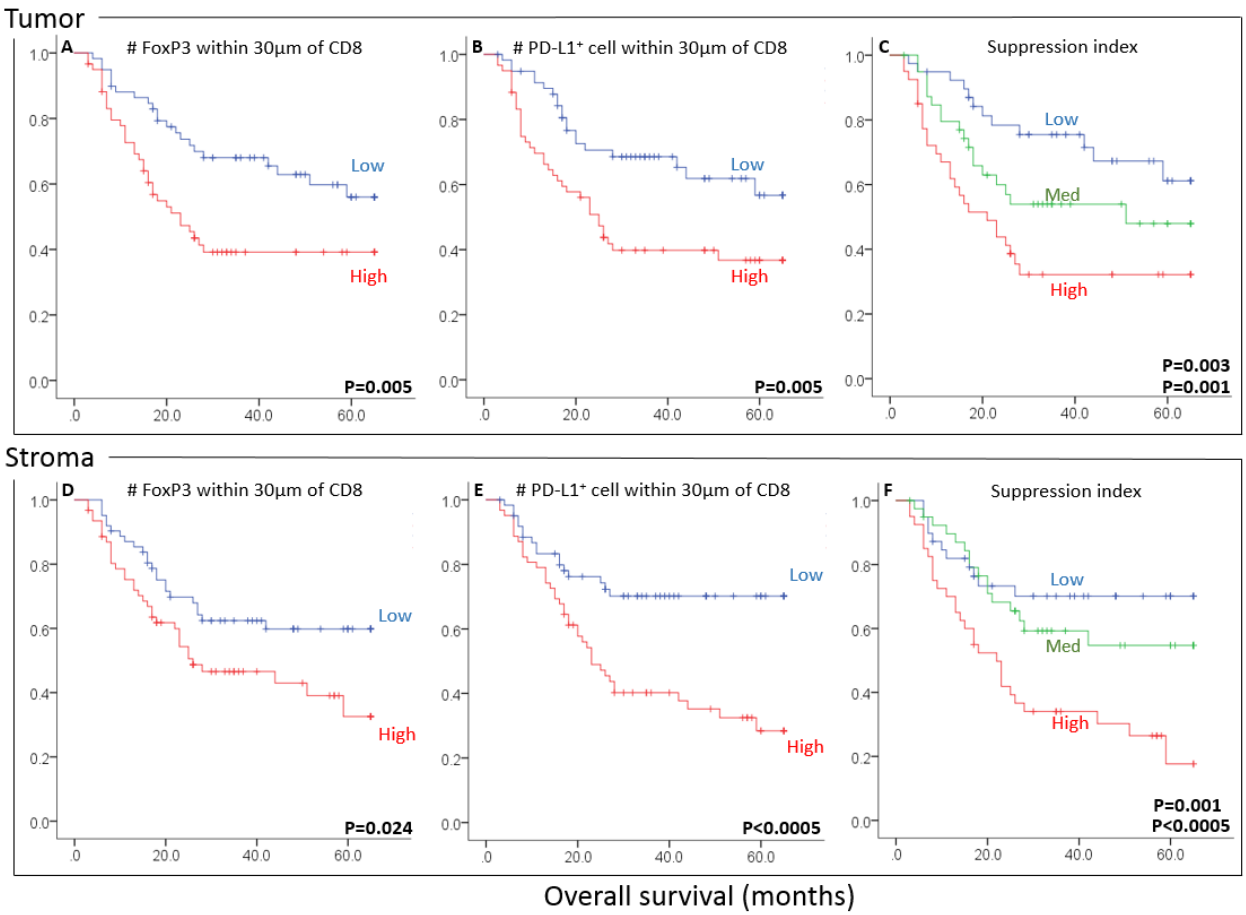

Figure 4.8: Impact of relationship and suppression index on prognosis. A,B,D,E) Numbers of $FoxP3^+$ and $PD\text{-}L1^+$ cells within 30 micron of CD8 were determined using PerkinElmer inForm and R-script and are normalized to number of $CD8^+$ T cells. A median cutoff is used to separate high and low infiltrate. C,F) the expression based on median cutoff of FoxP3 and PD-L1 are added together and ranked from high (score of 2), med (score of 1) and low (score of 0). Log-rank statistics are performed to determine significance.

We have also examined the impact of PD-L1 on prognosis. Previous reports in a Chinese cohort suggest PD-L1 may be inversely correlated with outcome in HNSCC[229], however, we did not see a difference in our cohort. This could be a

result of distinct etiology of carcinogenesis between the Chinese population and European population[230]. Importantly, in HNSCC, PD-L1 expression in the tumor can be both cytokine induced or constitutively expressed through aberrant signaling pathways[231]. While PD-L1 upregulation as a response to increased interferon-gamma levels in the tumor microenvironment may indicate favorable prognosis, constitutive PD-L1 expression on the other hand, is thought to be associated with poor outcome. We have enumerated the number of PD-L1 expressing cells within 30µm of CD8 T cells. Normalizing this to the number of CD8 T cells allows us to indirectly evaluate the impact of PD-L1 as a function of CD8 T cell on overall survival. We found that patients with high number of PD-L1 relative to CD8 performed more poorly than patients with low number of PD-L1 relative to CD8 (Figure 4.8B, E). This suggest that for the tumors with high PD-L1 in the absence of CD8, there might be aberrant signaling pathways resulting in constitutive activation of PD-L1, leading to worse outcome; while for the tumors with high PD-L1 in the presence of higher $CD8^+$ T cell infiltrate, the PD-L1 upregulation may be an indicator of an anti-tumor immune response, thus correlating with improved overall survival. Interestingly, contrary to Tregs, we did not see any difference between the PD-L1 within 30µm of CD8 compared to total numbers of PD-L1 expressing cells (Figure 4.9B, D, F, H), this suggests that the PD-L1 upregulation is largely uniform at the invasive margin.

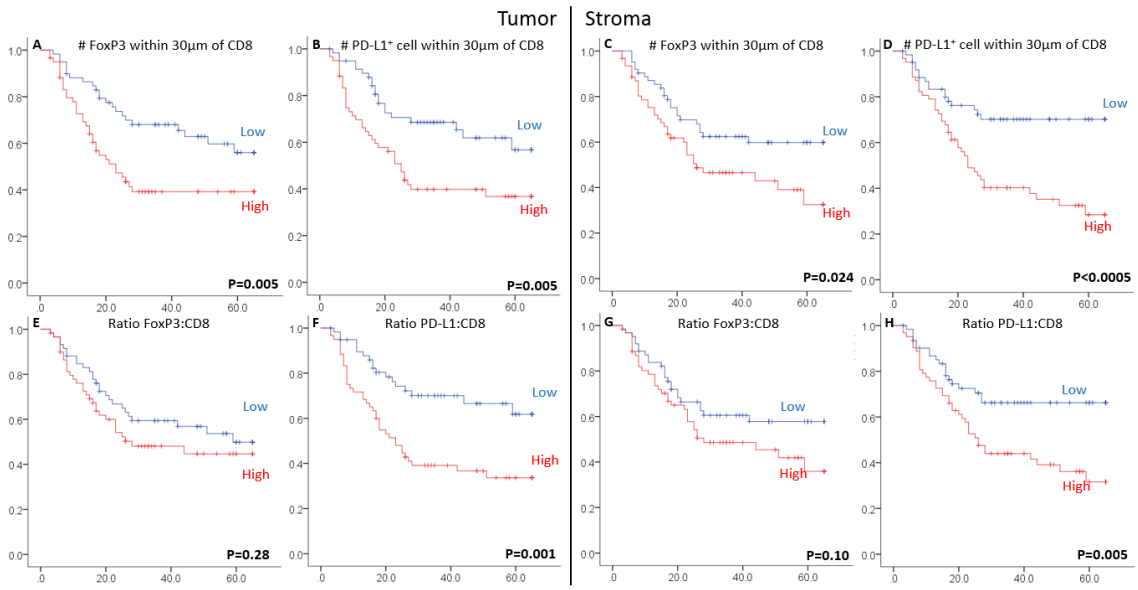

Figure 4.9: Distance of FoxP3 to CD8 is more important on prognosis than distance of PD-L1 to CD8. Comparisons were made between the 30 micron distance and overall ratio for FoxP3 (A,E,C,G) and PD-L1 (B,F,D,H) in both tumor and stroma of the invasive margin. Log-rank statistics are performed to determine significance.

Our previous work in melanoma demonstrate that combining CD8:FoxP3 and CD8:PD-L1 ratios are important in predicting culturing success of tumor-infiltrating lymphocytes[24]. We conveyed similar concept to HPV-negative HNSCC and coined the term “suppression index (**SI**)”, which takes into consideration both FoxP3 and PD-L1 within 30µm of CD8 normalized to CD8. Our results showed that by combining both suppressors, we are able to separate out the patients with around 70% and those with around 30% 5-year survival (Figure 4.8C, F). To examine the effect of tumor staging on relationships, we separated our cohort into 2 general groups based on their overall survival (Figure 4.1A). Patients with stage III disease were grouped with stage I and II based on their 70% 5-year overall survival in our particular cohort. We found in patients with stage I-III OSCC, the effect of suppression index in the stroma is highly predictive of overall

survival: patients with lowest suppression index achieved almost 90% 5-year survival, compared to less than 40% for patients with highest suppression index (Figure 4.10A-F). In patients with stage IV disease, the relationship parameters and suppression index in both the tumor and stroma seem also to be predictive of outcome, with more separation observed in the tumor compartment (Figure 4.11A-F).

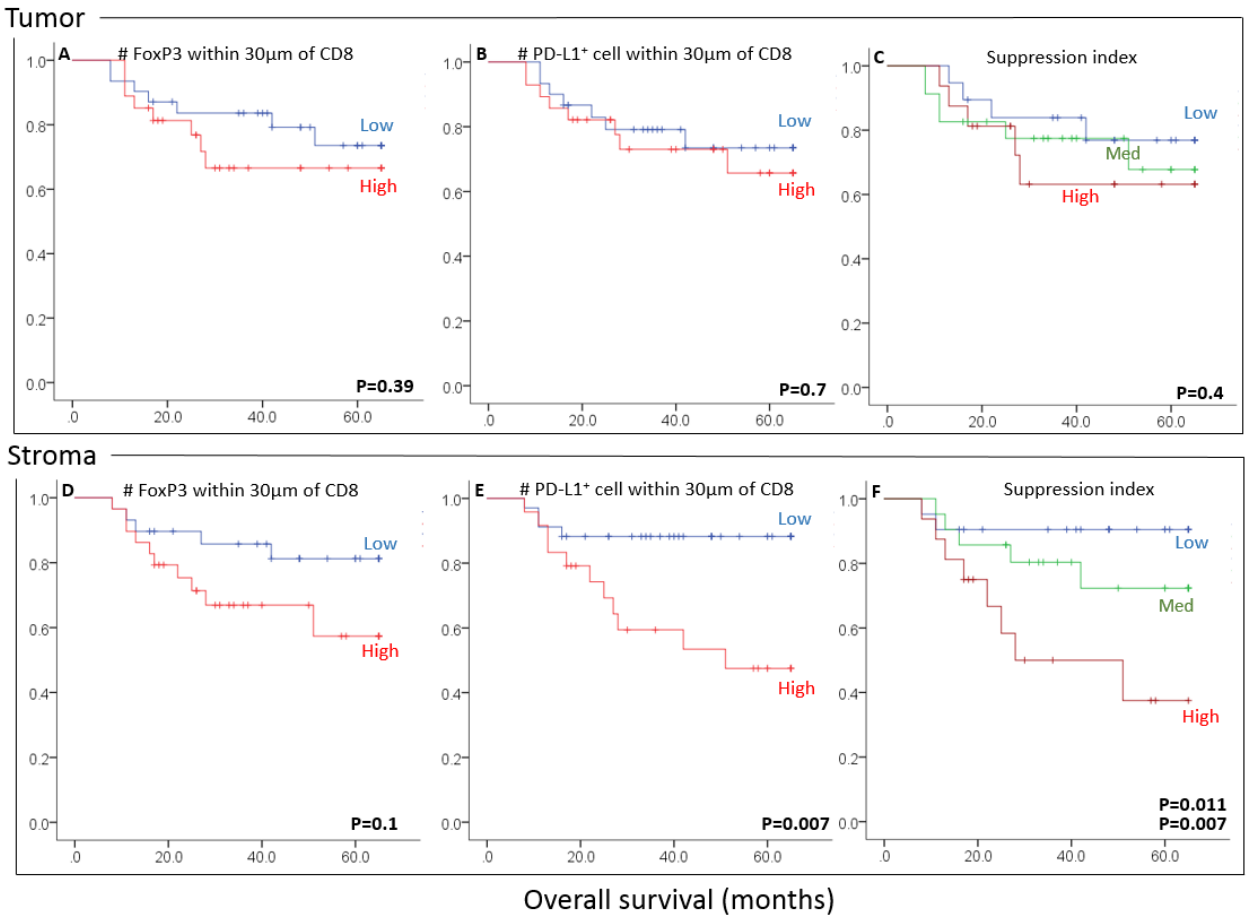

Figure 4.10: Stromal suppression index is more important on patient prognosis in Stage I-III patients. Distance parameters and suppression indices were performed on both tumor and stroma of invasive margin for stage I-III patients, median cutoff is used to establish high (above median) and low (below median). For C and F, the expression based on median cutoff of FoxP3 and PD-L1 are added together and ranked from high (score of 2), med (score of 1) and low (score of 0). Log-rank statistics are performed to determine significance.

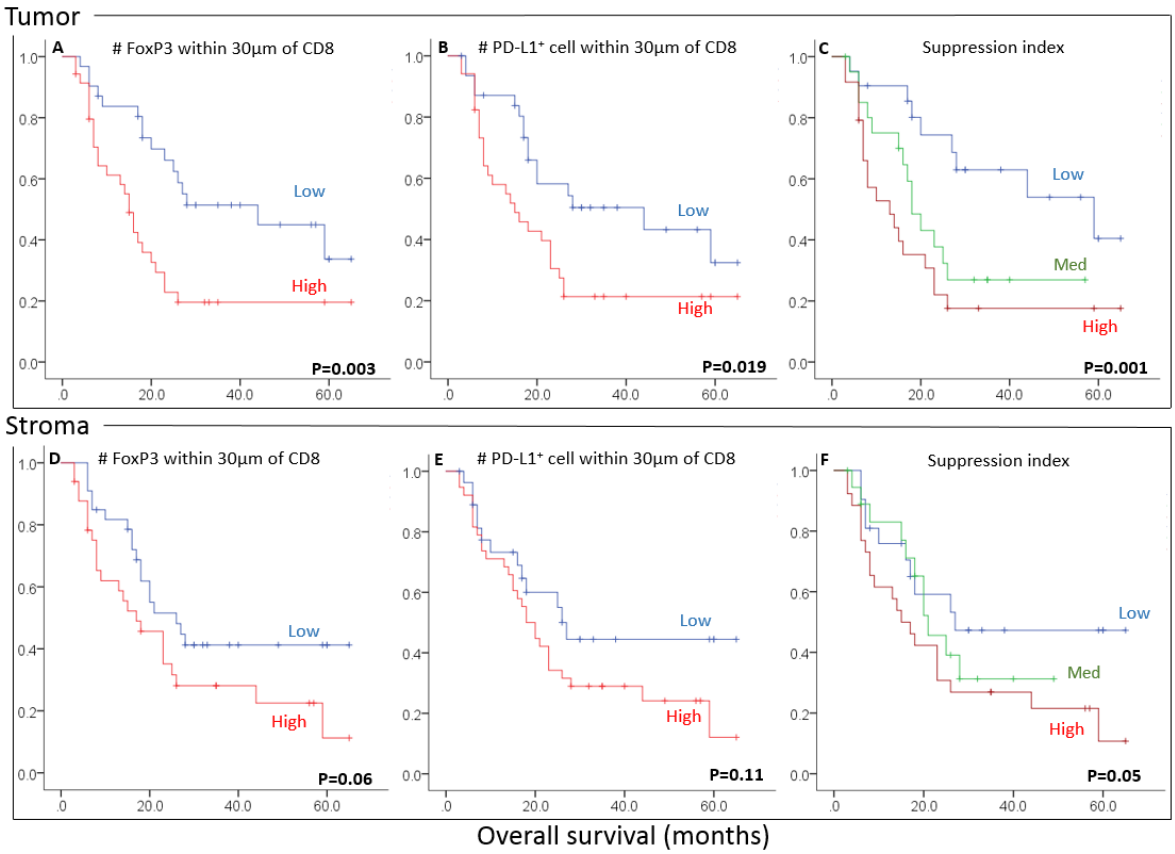

Figure 4.11: Both tumor and stromal component are important on patient prognosis in Stage IV patients. Distance parameters and suppression indices were performed on both tumor and stroma of invasive margin for stage IV patients, median cutoff is used to establish high (above median) and low (below median). For C and F, the expression based on median cutoff of FoxP3 and PD-L1 are added together and ranked from high (score of 2), med (score of 1) and low (score of 0). Log-rank statistics are performed to determine significance.

Cumulative suppression index scoring system as a means to evaluate both tumor and stromal components is prognostic in OSCC

Stemmed from the concept Galon and colleagues have established previously in colon studies, we combined the SIs from both the tumor and stroma at the invasive margin into a cumulative SI (**CSI,** Figure 4.12A). This results in identification of patients with over 90% 5-year survival and those with only 20% 5-year survival in our entire cohort (Figure 6B). To further strengthen our CSI scoring system, we have examined the expression of antigen presentation

machinery (APM) components such as class I heavy chain and b_2-microglobulin in our cohort using an “immunoreactivity score (IRS)” previously established to clinically assess the intensity of hormonal receptors in breast cancer. We found that interestingly, cytoplasmic expression of these APM components inversely correlated with overall survival (Figure 4.12C). We speculate that higher cytoplasmic expression may indicate a defect in the pathway that traps these components in the cytoplasm, leading to decrease in T cell mediated killing. Combining it with CIS resulted in further increase in patient survival with CSI of 0 and 1 achieving 90-100% 5-year survival and those with CSI 5 and 6 achieving 0-20% 5-year survival (Figure 4.12D). When we evaluated the effect of CSI on different tumor stages, we found that in patients with stage I-III disease, a CSI score of 0 achieved 100% survival in our cohort (Figure 4.12E); however, no other improvement was observed compared to the stroma alone (Figure 4.10F, 4.12E). Similar results were observed by considering just stage I-II patients (data not shown). In patients with stage IV disease, we were able to separate patients with CSI score of 0 having 60% 5-year survival, and those with score of IV rapidly succumb to their disease (Figure 4.12F). Our findings indicate that even for patients with late stage HPV-negative OSCC, relationship parameters between immune populations are still prognostic. We believe that this type of analysis including multiple relationships parameters and resistance mechanisms evaluated independently is an important step forward. It allows us to establish an immune signature that separates the patients with good outcome from those with poor outcome.

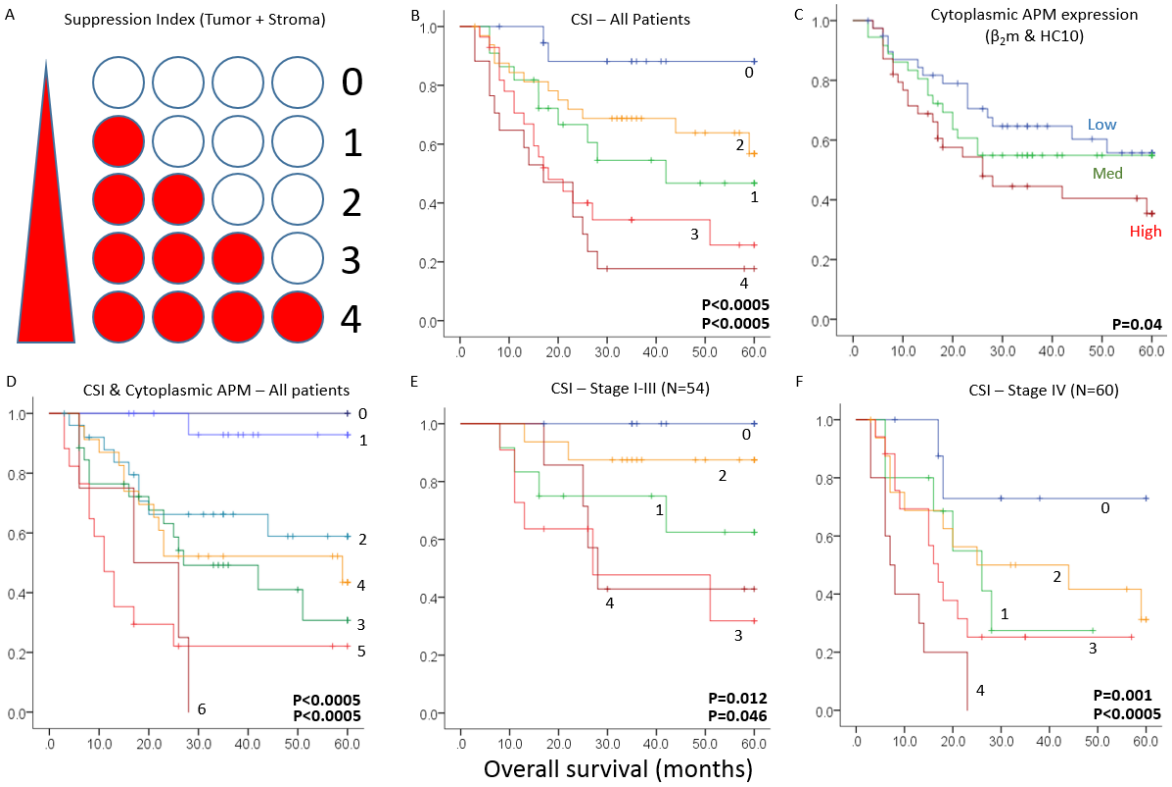

Figure 4.12: Cumulative suppression index is important in determining patient prognosis. A) model B) Entire cohort, scores were summed from each individual component using median cutoff as seen in the model C) APM components (beta-2 microglobulin and heavy chain), scores from each component using a median cutoff and compiled into low (score of 0), med (score of 1) and high (score of 2) D) CSI with APM components, scores from each component using median cutoff were added, ranging from score of 0 (below median for every category), and score of 6 (above median for every category) E) CSI for patients with stage I-III disease F) CSI for patients with stage IV disease. Log-rank statistics are performed to determine significance, the top p-value refers to all comparisons, the bottom p-value refers to the difference between the lowest and highest score.

Discussion

To the best of our knowledge this is one of the first immune profiling studies that objectively assessed not only the frequency and composition of the immune cell infiltrate, but rather also cell-cell relationships and further correlated these data to clinical parameters. Compared to conventional single-color IHC, multiplex IHC offers the ability to stain multiple parameters on a single section for the analysis of the quantity and localization of cells as well as their interactions [13]. This type of

multidimensional analysis was applied to an in-depth study of tumor cells and the TME followed by correlation of these data with OSCC patients' survival.

As recently demonstrated in various studies density, composition and localization of immune cell infiltrates, in particular $CD8^+$ T cells, have prognostic relevance in different solid cancers, which led to the development of the immunoscore as an important independent prognosis index in CRC[232-234]. In HNSCC, numbers of various immune subsets have been correlated with clinical outcome[235, 236], but the majority of these reports either focused exclusively on HPV^+ HNSCC or did not distinguish patient populations based on HPV status. However, high throughput analysis revealed that HPV^+ and HPV^- HNSCC are distinct clinical entities, which have distinct molecular features and an altered immune phenotype characterized by $CD8^+$ T cell infiltration[236]. To date our study represents one of the largest HPV OSCC studies consisting of more than 120 patients from two centers. Immunoscore data were generated using multiplex imaging, a novel technique that has shown promise for analyzing multiple parameters from a single FFPE section[24, 237]. Consistent with other reports, our results indicated a favorable association between $CD8^+$ T cell density and OSCC patients' survival. By focusing exclusively on $CD8^+$ T cell infiltrates in the tumor, we were able to identify long term survivors, independent of the tumor stage suggesting a prognostic value of the immune cell repertoire in the TME. In addition, PD-L1 expression was analyzed in our tumor samples, which has recently been shown to be inversely correlated with the outcome of HNSCC patients of a Chinese cohort [229]. These discrepant results might be due to the

distinct etiology of carcinogenesis between the Chinese, North American and European population [45]. In HNSCC, PD-L1 expression can be induced by cytokines secreted from immune cells or constitutively expressed due to aberrant signaling pathways [46]. While upregulation of PD-L1 as a response to the IFN-γ levels in the TME has a favorable prognosis, basal PD-L1 expression of tumors is linked to a worse patients' prognosis.

Based on our previous data in melanoma, we additionally analyzed the spatial relationships between $CD8^+$ T cells and immune suppressors and the role of the distance between different immune cell subsets and/or tumor cells for prognosis. Adapted from on optimal separation of a test cohort of 34 patients (Figure 4.7), which led to the generation of a suppression index scoring system consisting of neighboring effector and suppressor cells FoxP3 and PD-L1 expression was analyzed within a 3-lymphocytes-wide distance (30µm). Using this approach, patients with a low suppression index survived much longer compared to those with a high suppression index, while the OS for those with intermediate suppression index fell right in the middle. When separating the patients by tumor stages the stromal SI was more important in stage I-III, the tumor SI appeared to be more important in stage IV patients. These data lead to the hypothesis that in earlier tumor stages, the peri-tumoral immune infiltrate acts to contain the tumor. While in late stage patients often with nodal invasion, high levels of intra-tumoral immune infiltrate represent a favorable signature that aids to clear the remaining tumor after surgical resection. By combining the suppression indices from both tumor and stroma, we were able to further separate the overall survival based on

their cumulative suppression index scores in both early and late stage patients with HPV^- OSCC. The power of this index was further strengthened by taking into consideration the cytoplasmic expression of MHC class I components, which by themselves inversely correlate with overall survival.

To further strengthen our CSI scoring system, the expression of APM components, such as MHC class I HC, β_2-m and LMP10 was determined in our cohort using an "immunoreactivity score (IRS)" previously established to score hormone receptor intensity[222]. The cytoplasmic expression of these APM components inversely correlated with OS of OSCC patients (Figure 6C). We speculate that higher cytoplasmic expression of HC and β_2-m may indicate a defect in the export of MHC class I molecules to the cell surface as shown in virus-infected cells. This result in lower MHC class I surface expression, which could be associated with reduced T cell-mediated killing. An altered MHC class I APM component expression has been also shown to be associated with a reduced patients' survival in HNSCC, but also in other tumor entities[238, 239]. Although the underlying molecular mechanisms of the altered APM component expression has not been analyzed in detail, deregulation rather than structural abnormalities appear to be the cause. This assumption is further strengthened by the fact that deficient β_2-m expression in HNSCC is not due to mutations in this gene. By combining multiple parameters including the study of immune suppressive factors in a $CD8^+$ T cell centric way, patients with 80% to 100% 5-year survival could be identified and distinguished from those who rapidly

progressed with 0% 2-year survival. Our study not only confirms the importance of $CD8^+$ T cells in prognosis, but also highlights the complexity of the tumor microenvironment suggesting that the consideration of multiple parameters is necessary in order to better identify the patients requiring aggressive treatment. However, our study has some limitations: Some tumor samples from patients with stage IV disease exhibit a very high $CD8^+$ T cell infiltrate and a very favorable CSI score. In contrast to our prediction, these patients rapidly progressed suggesting that the immune suppressive panel analyzed is insufficient to identify additional suppressive mechanisms that exist to dampen a strong anti-tumor response. Furthermore, the scoring system used does not address patients with intermediate scores. Incorporation of HLA class I APM component analysis improved the prognostic power of the SI, but still does not fully allow us to separate these patients. One might consider extending the analysis for other APM components to increase the prognostic relevance of these markers. Thus going from CSI of 0 to 1a small change at the invasive margin can cause drastic shifts in pathways and immune contextures postulating that additional markers should be further analyzed to tease apart what is happening at the invasive margin.

Overall, these data signify the importance of T cell responses in HPV^- OSCC and provide a rationale for the utilization of multiplex imaging in identifying the patients that may require treatment intensification or enrollment into clinical trials.

Respective contributions

I designed and performed most experiments in this chapter. Daniel Bethmann, Barbara Seliger et al. provided the HNSCC slides for staining and performed the APM analyses. CBB reviewed and verified all IHC staining.

Chapter 5 (Appendix): Immunoprofiling to monitor changes in tumor microenvironment following immunotherapy

One of the powerful applications of immune profiling, as mentioned in the introduction, is to evaluate changes in the tumor-immune interactions following treatment with immunotherapy. This appendix will touch on both changes following immunotherapy in human and murine cancers.

Appendix 1: Changes in tumor microenvironment in murine tumors following treatment with DRibble vaccine and STING ligand.

Autophagy, the process by which cells recycle cellular components through autophagolysosomal fusion, is essential in the immune recognition of cancer[132-134]. We and others have shown that tumor autophagy is necessary for tumor-specific T cell priming through the induction of cross-presentation of tumor antigens by DCs[135, 136]. In addition, tumor-derived autophagosomes contain SLiPs and DRiPs, which represent the major source of proteins for MHC class I-restricted self-peptides[137, 138]. Acting together, these two characteristics make autophagosomes an ideal vaccine encompassing a highly enriched antigen repertoire for the cross-priming of CD8+ T cells. We have developed a method to harvest these autophagosomes through the simultaneous inhibition of the proteasome with bortezomib to induce autophagosome formation, and inhibition of autophagolysosomal fusion with ammonium chloride, leading to intracellular and extracellular accrual of these autophagosomes[139]. These autophagosomes are then collected by centrifugation, and we have demonstrated their protective and therapeutic efficacy in 7 pre-clinical sarcoma and carcinoma models[135, 139,

[140]. Our work has resulted in an ongoing multicenter phase II clinical trial in patients with non-small cell lung cancer (NCT01909752), and a trial planned in HNSCC. Since much of DRibbles' activity is heavily dependent on cross-presentation by cells of the innate immune system, it is possible that activation of the STING pathway may further enhance DRibbles' therapeutic efficacy. STING is a receptor that resides in both the cytoplasm and the endoplasmic reticulum of most cells. Macrophages and DCs are potently activated by STING ligands such as cyclic dinucleotides (CDN)[240-243]. Tumor cells can also express STING receptor to various degree, and in HNSCC, there is a positive correlation between STING receptor expression and CD8 T cell infiltrate (Figure A1-1).

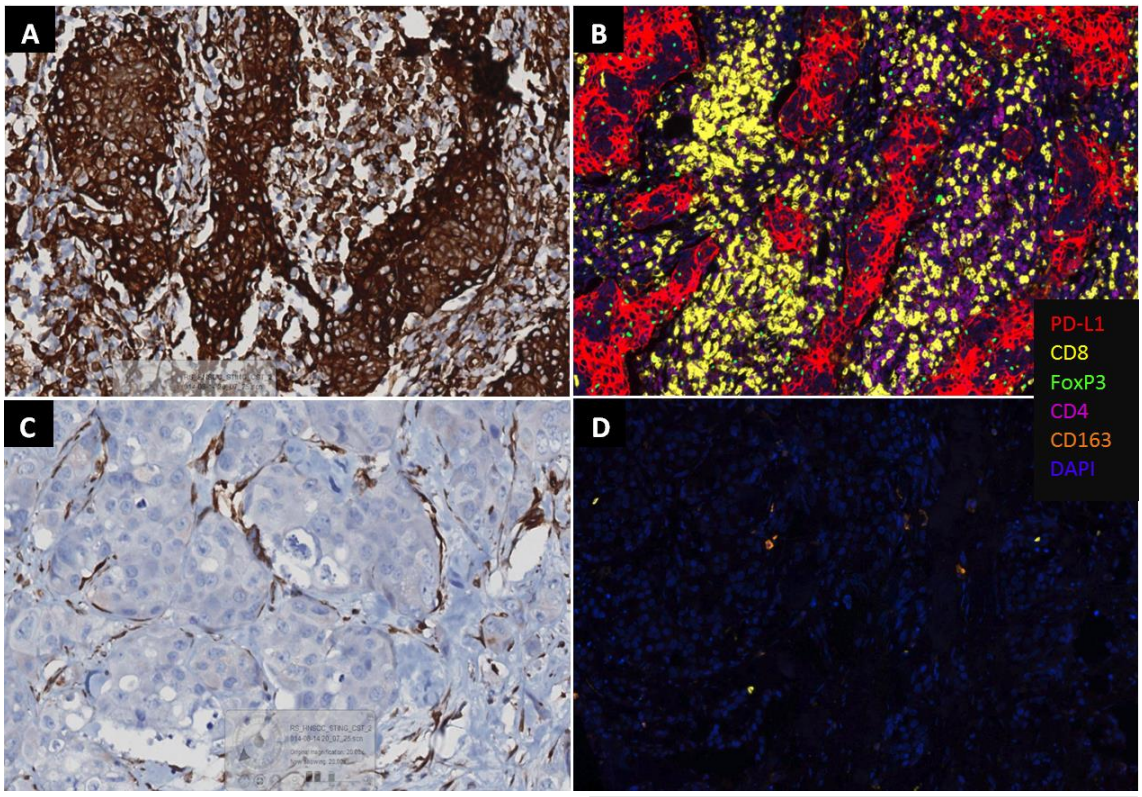

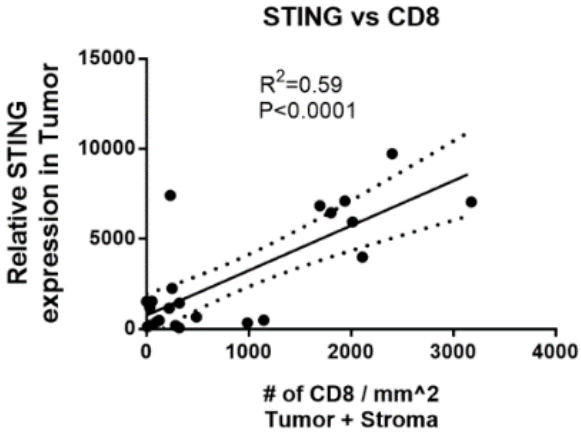

Figure 5-1: STING Expression significantly correlates with CD8$^+$ T cell infiltrate in 22 Patients with HNSCC
A, C: High and low STING expression (brown) in patient #1 and #2, respectively. *B, D*: 6-plex multispectral staining using PerkinElmer platform in patient #1 and #2, respectively. *E*: correlation between STING expression in the tumor and number of CD8$^+$ T cell infiltrate. Quantification is done using Definiens' Tissue Studio (STING), and PerkinElmer (CD8).

Central to its role in innate immunity to infection, the binding of CDN to STING receptor induces type I interferon secretion[241, 244-247], and this reverses macrophages that already exhibit an anti-inflammatory (M2) biased activation status back to a more pro-inflammatory (M1) phenotype[248]. Consistent with a pro-inflammatory signature, my preliminary results suggest that CDN significantly enhances the secretion of IL-12, a pro-inflammatory "signal 3" critical for T cell

proliferation and function[249-252], from both M1 and M2 macrophages differentiated in vitro with γ-interferon (IFNγ) and IL-4, respectively (Fig. A1-1).

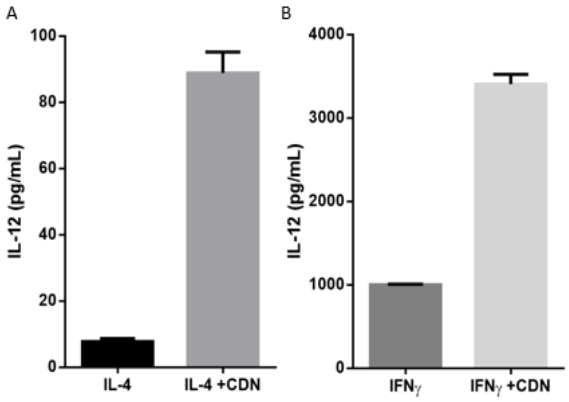

Figure 5-2: Augmentation of IL-12 release from differentiated macrophages by CDN. BMDMs are cultured in M-CSF and differentiated *in vitro* with (*A*) IL-4 and (*B*) IFNγ with vehicle or CDN. IL-12 level in the media is quantified by ELISA 24 hours later.

In this way CDNs can repolarize the milieu of antigen presentation, as suppressive factors such as IL-10 and Arg1 become less abundant in the local environment and pro-inflammatory factors increase. The consequence of such polarization can increase T cell priming and proliferation[177, 253]. Therefore, I hypothesize that the stimulation of macrophages and DCs with CDN will increase antigen cross-presentation of DRibbles, leading to tumor-specific T cell activation and subsequent tumor rejection. To test the impact of DRibbles and CDN on T cell infiltrate, tumors were established by the injection of $5x10^5$ SCCVII cells subcutaneously on the posterior cervical region of C3H/HeJ mice and were allowed to reach 5mm in diameter. PBS, DRibbles, CDN, or combination DRibbles and CDN were delivered to inguinal lymph nodes bilaterally. Tumors were resected 7 days post injection and bisected. Half of the tumor were fixed in zinc fixation buffer for IHC and other half were enzymatically digested for flow

cytometry. The results show that combining DRibbles with CDN may increase in CD8 T cell infiltrate and proliferation in the tumor, and enhance $CD8^+$ T cell to FoxP3 ratio (Figure A1-3).

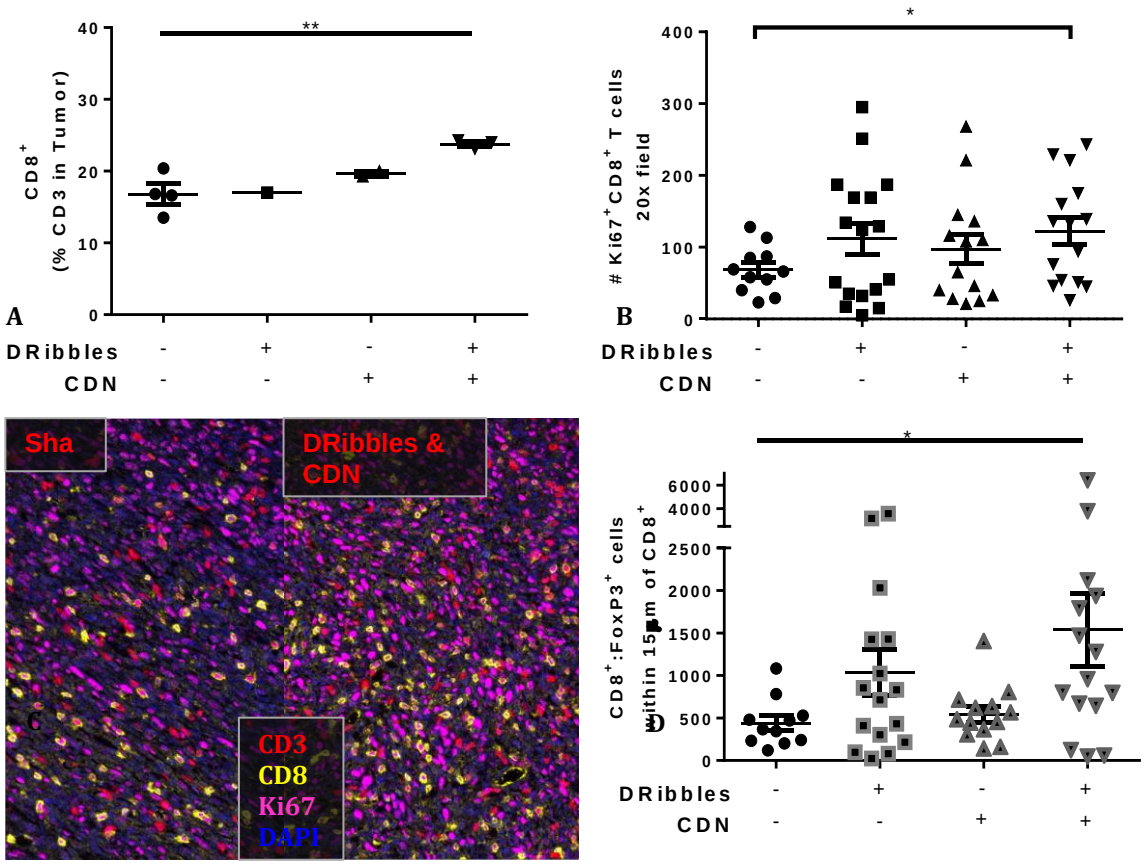

Figure 5-3: Characterization of tumor-infiltrating immune cells after DRibble and CDN therapy. A) Flow cytometry analysis, N=max 4 per group. B) IHC analysis of proliferating CD8 T cells, N=5 per group. C) Representative images of immunostaining of T cells. D) Ratio of CD8 to # of FoxP3 within 15 microns of a CD8 T cell.

Appendix 2: Changes in tumor microenvironment in melanoma following treatment with oncolytic virus CVA21[#]

CAVATAK is an oncolytic strain of coxsackievirus A21 (CVA21), preclinical models demonstrated that intratumoral injection of CVA21 results in tumor-

specific viral in-situ proliferation and lysis of melanoma both *in vitro* and *in vivo*[254]. A phase II study was performed in collaboration with Viralytics to assess the safety and efficacy of CVA21 in patients with advanced melanoma that have injectable cutaneous metastases. Overall response rate in the study per irRECIST 1.1 criteria is 30%. The aim of our study is to understand the effect of the treatment on immune infiltrate. We utilized both multiplex imaging to evaluate different aspects of immune function at baseline, and at day 8 post injection. We found that there is no significant difference between disease-controlling responders and progressors in their immune infiltrate density at baseline (Figure A1B). However, in the disease-controlling responders, injection of oncolytic virus results in significant increase in both CD8+ T cells and PD-L1 expression in the tumor, suggesting potentially an anti-tumor response and the release of interferon-gamma. This change was not observed in the progressors, as demonstrated by Pt 03-042 in Figure A1A, and A1B. Our result is the first step towards understanding the effects of oncolytic virus CVA21 on the tumor microenvironment and we hope to identify in the future resistance mechanisms that prevent an increase in the T cell infiltrate following administration of CVA21.

Originally presented in ASCO 2016 J Clin Oncol 33, 2015 (suppl; abstr 9030)

A

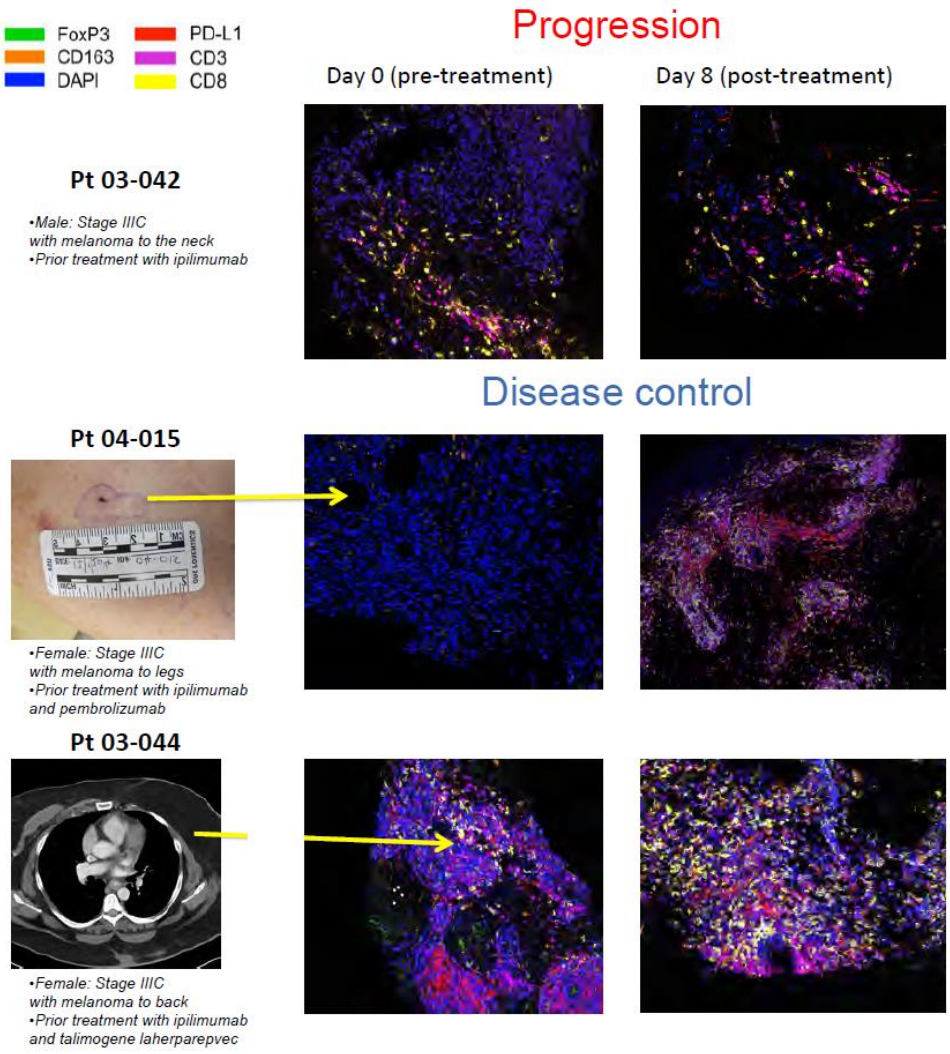

B

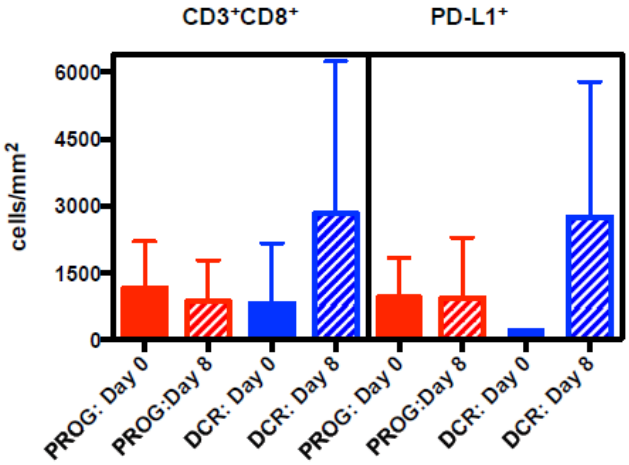

Figure 5-4: Changes in immune infiltrate post CVA21 injection
A) 3 example patients with before/after multiplex imaging B) summary of 8 patients. PROG: progressors, DCR: patients whose disease were controlled

Chapter 6: Summary and Conclusions

Objective assessment of the immune component of the tumor microenvironment represents a key advancement in standardization and biomarker development. The work presented in this thesis highlights the importance of multiparametric analysis and assessing cell-cell relationships. Pre-clinically, by combining a zinc-based tissue fixation method with a glycine-based antigen-retrieval solution, we have successfully established a multiplex IHC platform to assess T and B cell distributions in murine tissue. We have also provided evidence for the value of multiparametric analysis by identifying follicular aggregation of $CD3^{-}CD4^{+}CD11c^{+}$ cells in murine $RAG1^{-/-}$ spleen and their replacement by T and B cells following adoptive transfer of splenocytes from wild-type animals. In cancer models, we could identify $CD4^{+}F4/80^{+}$ macrophages and $CD8^{+}FoxP3^{+}$ cells that were abundant in certain tumors such as FAT, a cell line derived from MMTV-PyMT spontaneous mammary carcinoma. The functions of these cells are poorly understood and they are difficult to isolate and study using conventional IHC or flow cytometry. Understanding changes to these populations and the resulting shift in cytokine and T cell infiltrate by multiplex IHC following treatment may give us insight into the mechanisms of tumor rejection by these therapies. Overall, the multiplex IHC platform represents a step forward in objective assessment of immune populations in the tumor microenvironment following therapy. The combination of zinc-fixation and mild antigen-stripping solution also expands the possibility of using antibodies traditionally reserved for frozen section or flow cytometry for multiplex IHC studies; and the contextual information provided by

IHC can complement flow cytometry. This is especially advantageous for the study of immune subsets such as resident memory T cells that can't be efficiently isolated out, or when the tissue sample is too small to be used in flow cytometry.

Applying multiparametric analysis to clinical samples yields promise for biomarker development. In melanoma, we demonstrated that CD8:FoxP3 ratio can predict the success in culturing tumor-infiltrating lymphocytes; and combining it with CD8:PD-L1 ratio, we were able to achieve 100% sensitivity and specificity in our small cohort. This is important for two reasons. Our technique may allow for better selection of patients with a more favorable immune signature who would more likely benefit from TIL therapy. Secondly, checkpoint blockade therapy is one of the most promising treatments for patients with solid tumors. But response to agents such as anti-PD-1 and anti-PD-L1 is limited to patients with pre-existing immune response[20, 21]. Being able to culture tumor-reactive lymphocytes from patients' tumors could be an important indicator of the likelihood of a pre-existing anti-cancer immune response. Thus, while the density of $CD8^+$ T cells has been shown to be a powerful marker in predicting response to anti-PD-1 therapy in a small cohort of patients[20], it is possible that including Tregs and PD-L1 may further enhance the prediction for response to anti-PD-1 therapy.

We further investigated the distances between CD8, Treg and PD-L1 in the tumor microenvironment in HPV-negative HNSCC. Consistent with our data in

melanoma, a high CD8:PD-L1 ratio correlated with a prolonged overall survival in HPV-negative HNSCC. However, when we examined the ratio of CD8:FoxP3, we found that the numbers of Treg within a 30-micron radius of CD8, but not total Treg, were prognostic. This observation that higher densities of Tregs close to CD8 correlated with worse outcome suggests differential suppression of T cells by Tregs in HNSCC. Consistent with our interpretation, studies by others have shown that a significant part of Treg-mediated T cell inhibition is contact-mediated, such as through CTLA-4, CD73/CD39, direct cytolysis or gap junctions[255, 256].

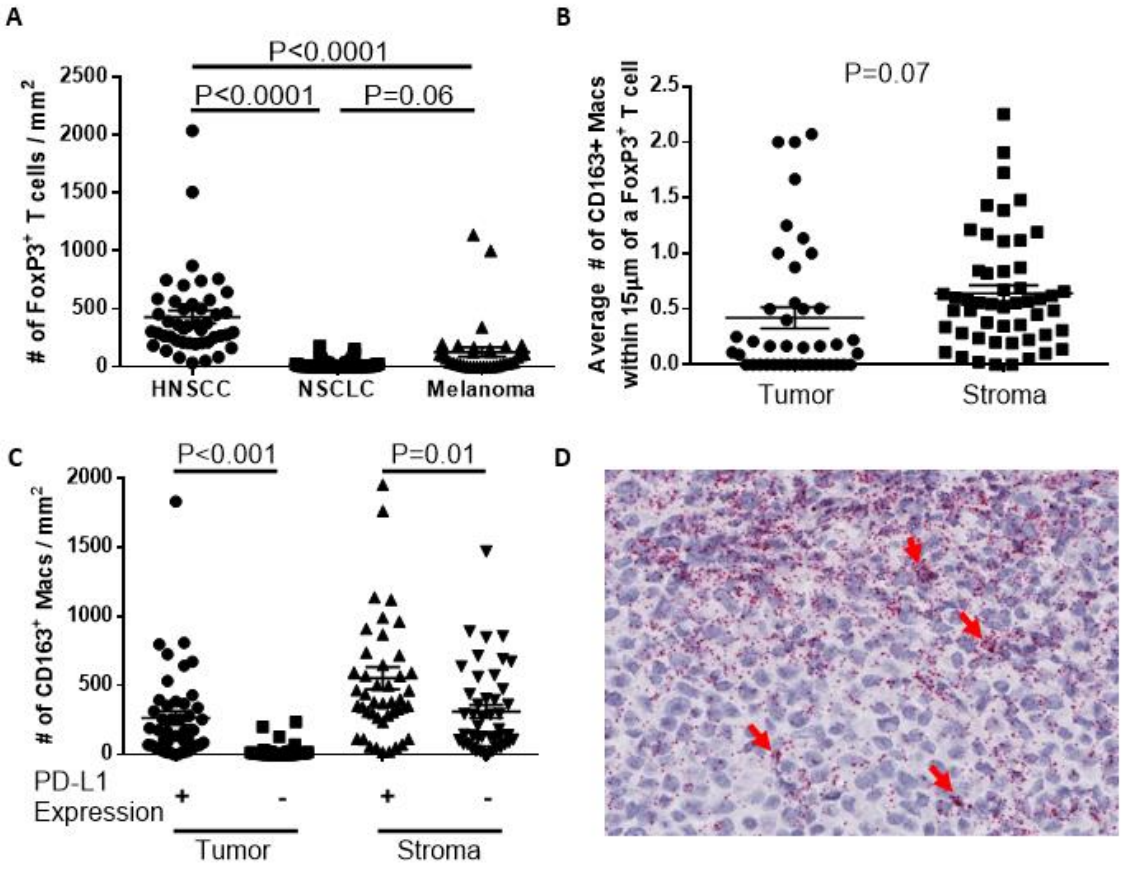

Figure 6-1: CD163+ macrophages exist in close proximity to FoxP3+ Tregs. A) Numbers of FoxP3$^+$ Tregs per mm^2 in different types of cancer. B) Average numbers of CD163$^+$ macrophages within 15-micron of Treg in both tumor and

stroma in HPV-negative HNSCC. C) Differences in PD-L1 expression of $CD163^+$ macrophages in both tumor and stroma. D) In-situ hybridization of TGF-beta shown in red, arrows pointing to cells resemble macrophages.

Additionally, HPV-negative HNSCC is one of the cancers with the highest FoxP3 infiltrate (Figure 6-1A), but it is unclear whether this process is mediated through chemokine induced migration, or *in situ* conversion. Studies from Gajewski's group demonstrated that for inflamed tumors, CD8 mediates Treg migration through CCR4 binding chemokines, while other studies suggest potential for highly suppressive iTreg conversion *in situ* through TGF-beta[8, 257]. Examining the location of the $FoxP3^+$ T cells intratumorally revealed their close proximity to PD-L1+ macrophages: on average, there is one $CD163^+$ macrophage within 15-microns of every other Treg (Figure 6-1B,C). Could these macrophages mediate the conversion of these Tregs through the secretion of TGF-beta? We probed for TGF-beta using in-situ hybridization methods and found aggregates of TGF-beta in cells resembling macrophages. Methodology to perform both ISH and multiplex IHC on a single slide is underway and can help to determine if the PD-L1+ CD163+ macrophages adjacent to FoxP3 are secreting TGF-beta and mediating the conversion of these Tregs. Combining TGF-beta inhibitors with other modalities such as radiation and OX40 agonist has demonstrated efficacy in preclinical models[9, 10] and our data could provide another rationale for use of TGF-beta signaling blockade in HNSCC, reducing Treg burden and enhancing T cell function.

Combination of relationships, such as CD8:FoxP3 with CD8:PD-L1, in melanoma showed better prediction of TIL culture success than either parameter alone. Using this concept in HNSCC to develop of a "suppression index" (SI), we can separate patients with less than 20% 5-year overall survival with those achieving over 80% 5-year survival. It is important to realize that the survival benefit is primarily driven by CD8 T cell infiltrate. In other words, tumors with low CD8 density have high suppression indices (above median) regardless of PD-L1 and Treg level, whereas tumors with very high levels of CD8 infiltrate have low suppression indices even if they also have high FoxP3 infiltrate and PD-L1 expression. Because of this, the suppression index fails to address the rare patients with some of the highest CD8 T cell infiltrate who progress rapidly. For these particular patients, preliminary analysis of their tumors with activated caspase 3 and XIAP, a suppressor of caspase activation, revealed high XIAP expressions and almost complete absences of nuclear cleaved caspase 3. Furthermore, these patients also have increased expression of cytoplasmic class I antigen-presentation machinery with a concurrent decrease of membrane class I expression. All of these factors suggest that despite high T cell infiltrate for these particular patients, defects in signaling pathways prevent them from eliminating the cancer. To stratify these rare patients, additional markers of immune resistance and escape are much needed. Novel technologies such as NanoString and RNAseq can help uncover these mechanisms of immune resistance and escape.

For the majority of patients, our results can potentially be important in patient care. Patients with more “hot” tumors and low suppression indices may potentially benefit from less intensive therapy and avoid treatment associated adverse effects. Conversely, patients with “cold” tumors characterized by high suppression indices may need more aggressive therapies to improve their overall survival. Some therapies such as oncolytic virus and anti-OX40 may convert a “cold” tumor with a high suppression index into an “inflamed tumor” with a low suppression index. Neoadjuvant treatment with these particular therapies, based on results from our suppression index study, may provide survival benefit for patients with high SI. Incorporation of multiplex IHC to study immune parameters in tumor biopsies at baseline is key in such trials, as it can not only help assess clinical outcome of the patients on therapy, but also evaluate the potential mechanism of action of the therapeutic agents, advancing treatment strategies and improving patient care.

References

[1] Lloyd, O. C. (1969) Regression of malignant melanoma as a manifestation of a cellular immunity response, *Proceedings of the Royal Society of Medicine 62*, 543-545.

[2] Schreiber, R. D., Old, L. J., and Smyth, M. J. (2011) Cancer immunoediting: integrating immunity's roles in cancer suppression and promotion, *Science 331*, 1565-1570.

[3] Dunn, G. P., Bruce, A. T., Ikeda, H., Old, L. J., and Schreiber, R. D. (2002) Cancer immunoediting: from immunosurveillance to tumor escape, *Nature immunology 3*, 991-998.

[4] Mittal, D., Gubin, M. M., Schreiber, R. D., and Smyth, M. J. (2014) New insights into cancer immunoediting and its three component phases--elimination, equilibrium and escape, *Current opinion in immunology 27*, 16-25.

[5] Dunn, G. P., Old, L. J., and Schreiber, R. D. (2004) The three Es of cancer immunoediting, *Annual review of immunology 22*, 329-360.

[6] Shankaran, V., Ikeda, H., Bruce, A. T., White, J. M., Swanson, P. E., Old, L. J., and Schreiber, R. D. (2001) IFNgamma and lymphocytes prevent primary tumour development and shape tumour immunogenicity, *Nature 410*, 1107-1111.

[7] Kim, R., Emi, M., and Tanabe, K. (2007) Cancer immunoediting from immune surveillance to immune escape, *Immunology 121*, 1-14.

[8] Spranger, S., Spaapen, R. M., Zha, Y., Williams, J., Meng, Y., Ha, T. T., and Gajewski, T. F. (2013) Up-regulation of PD-L1, IDO, and T(regs) in the melanoma tumor microenvironment is driven by CD8(+) T cells, *Science translational medicine 5*, 200ra116.

[9] Triplett, T. A., Tucker, C. G., Triplett, K. C., Alderman, Z., Sun, L., Ling, L. E., Akporiaye, E. T., and Weinberg, A. D. (2015) STAT3 Signaling Is Required for Optimal Regression of Large Established Tumors in Mice Treated with Anti-OX40 and TGFbeta Receptor Blockade, *Cancer immunology research 3*, 526-535.

[10] Young, K. H., Newell, P., Cottam, B., Friedman, D., Savage, T., Baird, J. R., Akporiaye, E., Gough, M. J., and Crittenden, M. (2014) TGFbeta inhibition prior to hypofractionated radiation enhances efficacy in preclinical models, *Cancer immunology research 2*, 1011-1022.

[11] Ruffell, B., Chang-Strachan, D., Chan, V., Rosenbusch, A., Ho, C. M., Pryer, N., Daniel, D., Hwang, E. S., Rugo, H. S., and Coussens, L. M. (2014) Macrophage IL-10 blocks CD8+ T cell-dependent responses to chemotherapy by suppressing IL-12 expression in intratumoral dendritic cells, *Cancer cell 26*, 623-637.

[12] Strachan, D. C., Ruffell, B., Oei, Y., Bissell, M. J., Coussens, L. M., Pryer, N., and Daniel, D. (2013) CSF1R inhibition delays cervical and mammary tumor growth in murine models by attenuating the turnover of tumor-associated macrophages and enhancing infiltration by CD8 T cells, *Oncoimmunology 2*, e26968.

[13] Stack, E. C., Wang, C., Roman, K. A., and Hoyt, C. C. (2014) Multiplexed immunohistochemistry, imaging, and quantitation: a review, with an assessment of Tyramide signal amplification, multispectral imaging and multiplex analysis, *Methods 70*, 46-58.

[14] Oble, D. A., Loewe, R., Yu, P., and Mihm, M. C., Jr. (2009) Focus on TILs: prognostic significance of tumor infiltrating lymphocytes in human melanoma, *Cancer Immun 9*, 3.

[15] Taylor, R. C., Patel, A., Panageas, K. S., Busam, K. J., and Brady, M. S. (2007) Tumor-infiltrating lymphocytes predict sentinel lymph node positivity in patients with cutaneous melanoma, *J Clin Oncol 25*, 869-875.

[16] Holman, C. D., James, I. R., Heenan, P. J., Matz, L. R., Blackwell, J. B., Kelsall, G. R., Singh, A., and ten Seldam, R. E. (1982) An improved method of analysis of observer variation between pathologists, *Histopathology 6*, 581-589.

[17] Broussard, E. K., and Disis, M. L. (2011) TNM staging in colorectal cancer: T is for T cell and M is for memory, *Journal of clinical oncology : official journal of the American Society of Clinical Oncology 29*, 601-603.

[18] Galon, J., Costes, A., Sanchez-Cabo, F., Kirilovsky, A., Mlecnik, B., Lagorce-Pages, C., Tosolini, M., Camus, M., Berger, A., Wind, P., Zinzindohoue, F., Bruneval, P., Cugnenc, P. H., Trajanoski, Z., Fridman, W. H., and Pages, F. (2006) Type, density, and location of immune cells within human colorectal tumors predict clinical outcome, *Science 313*, 1960-1964.

[19] Pardoll, D. M. (2012) The blockade of immune checkpoints in cancer immunotherapy, *Nature reviews. Cancer 12*, 252-264.

[20] Tumeh, P. C., Harview, C. L., Yearley, J. H., Shintaku, I. P., Taylor, E. J., Robert, L., Chmielowski, B., Spasic, M., Henry, G., Ciobanu, V., West, A. N., Carmona, M., Kivork, C., Seja, E., Cherry, G., Gutierrez, A. J., Grogan, T. R., Mateus, C., Tomasic, G., Glaspy, J. A., Emerson, R. O., Robins, H., Pierce, R. H., Elashoff, D. A., Robert, C., and Ribas, A. (2014) PD-1 blockade induces responses by inhibiting adaptive immune resistance, *Nature 515*, 568-571.

[21] Herbst, R. S., Soria, J. C., Kowanetz, M., Fine, G. D., Hamid, O., Gordon, M. S., Sosman, J. A., McDermott, D. F., Powderly, J. D., Gettinger, S. N., Kohrt, H. E., Horn, L., Lawrence, D. P., Rost, S., Leabman, M., Xiao, Y., Mokatrin, A., Koeppen, H., Hegde, P. S., Mellman, I., Chen, D. S., and Hodi, F. S. (2014) Predictive correlates of response to the anti-PD-L1 antibody MPDL3280A in cancer patients, *Nature 515*, 563-567.

[22] Roy S. Herbst, Jean-Charles Soria, Marcin Kowanetz, Gregg D. Fine, Omid Hamid, Michael S. Gordon, Jeffery A. Sosman, David F. McDermott, John D. Powderly, Scott N. Gettinger, Holbrook E. K. Kohrt, Leora Horn, Donald P. Lawrence, Sandra Rost, Maya Leabman, Yuanyuan Xiao, Ahmad Mokatrin, Hartmut Koeppen, Priti S. Hegde, Ira Mellman, Daniel S. Chen, and F. Stephen Hodi. (2014) Predictive correlates of response to the anti-PD-L1 antibody MPDL3280A in cancer patients, *Nature 515*, 563-567.

[23] Stack, E. C., Wang, C., Roman, K. A., and Hoyt, C. C. (2014) Multiplexed immunohistochemistry, imaging, and quantitation: A review, with an assessment of Tyramide signal amplification, multispectral imaging and multiplex analysis, *Methods*.

[24] Feng, Z., Puri, S., Moudgil, T., Wood, W., Hoyt, C. C., Wang, C., Urba, W. J., Curti, B. D., Bifulco, C. B., and Fox, B. A. (2015) Multispectral imaging of formalin-fixed tissue predicts ability to generate tumor-infiltrating lymphocytes from melanoma, *Journal for immunotherapy of cancer 3*, 47.

[25] Takahiro Tsujikawa, R. N. B., Vahid Azimi, El Edward Rassi, Daniel R Clayburgh, Sushil Kumar, Andrew J Gunderson, Molly F Kresz-Martin, Paul W Flint and Lisa M Coussens. (2015) Multiplex immunohistochemistry for immune profiling of HPV-associated head and neck cancer, *JITC 3(Suppl 2):P419*.

[26] Dudley, M. E., Wunderlich, J. R., Shelton, T. E., Even, J., and Rosenberg, S. A. (2003) Generation of tumor-infiltrating lymphocyte cultures for use in adoptive transfer therapy for melanoma patients, *Journal of immunotherapy 26*, 332-342.

[27] Wu, R., Forget, M. A., Chacon, J., Bernatchez, C., Haymaker, C., Chen, J. Q., Hwu, P., and Radvanyi, L. G. (2012) Adoptive T-cell therapy using autologous tumor-infiltrating lymphocytes for metastatic melanoma: current status and future outlook, *Cancer journal 18*, 160-175.

[28] LaCelle, M. G., Jensen, S. M., and Fox, B. A. (2009) Partial CD4 depletion reduces regulatory T cells induced by multiple vaccinations and restores therapeutic efficacy, *Clinical cancer research : an official journal of the American Association for Cancer Research 15*, 6881-6890.

[29] Valzasina, B., Guiducci, C., Dislich, H., Killeen, N., Weinberg, A. D., and Colombo, M. P. (2005) Triggering of OX40 (CD134) on CD4(+)CD25+ T cells blocks their inhibitory activity: a novel regulatory role for OX40 and its comparison with GITR, *Blood 105*, 2845-2851.

[30] Weinberg, A. D., Morris, N. P., Kovacsovics-Bankowski, M., Urba, W. J., and Curti, B. D. (2011) Science gone translational: the OX40 agonist story, *Immunological reviews 244*, 218-231.

[31] Woo, E. Y., Yeh, H., Chu, C. S., Schlienger, K., Carroll, R. G., Riley, J. L., Kaiser, L. R., and June, C. H. (2002) Cutting edge: Regulatory T cells from lung cancer patients directly inhibit autologous T cell proliferation, *Journal of immunology 168*, 4272-4276.

[32] Dudley, M. E. (2011) Adoptive cell therapy for patients with melanoma, *Journal of Cancer 2*, 360-362.

[33] Klapper, J. A., Downey, S. G., Smith, F. O., Yang, J. C., Hughes, M. S., Kammula, U. S., Sherry, R. M., Royal, R. E., Steinberg, S. M., and Rosenberg, S. (2008) High-dose interleukin-2 for the treatment of metastatic renal cell carcinoma : a retrospective analysis of response and survival in patients treated in the surgery branch at the National Cancer Institute between 1986 and 2006, *Cancer 113*, 293-301.

[34] Rosenberg, S. A., Yang, J. C., Sherry, R. M., Kammula, U. S., Hughes, M. S., Phan, G. Q., Citrin, D. E., Restifo, N. P., Robbins, P. F., Wunderlich, J. R., Morton, K. E., Laurencot, C. M., Steinberg, S. M., White, D. E., and Dudley, M. E. (2011) Durable complete responses in heavily pretreated patients with metastatic melanoma using T-cell transfer immunotherapy, *Clinical cancer research : an official journal of the American Association for Cancer Research 17*, 4550-4557.

[35] Dudley, M. E., Gross, C. A., Somerville, R. P., Hong, Y., Schaub, N. P., Rosati, S. F., White, D. E., Nathan, D., Restifo, N. P., Steinberg, S. M., Wunderlich, J. R., Kammula, U. S., Sherry, R. M., Yang, J. C., Phan, G. Q., Hughes, M. S., Laurencot, C. M., and Rosenberg, S. A. (2013) Randomized selection design trial evaluating CD8+-enriched versus unselected tumor-infiltrating lymphocytes for adoptive cell therapy for patients with melanoma, *Journal of clinical oncology : official journal of the American Society of Clinical Oncology 31*, 2152-2159.

[36] Junker, N., Andersen, M. H., Wenandy, L., Dombernowsky, S. L., Kiss, K., Sorensen, C. H., Therkildsen, M. H., Von Buchwald, C., Andersen, E., Straten, P. T., and Svane, I. M. (2011) Bimodal ex vivo expansion of T cells from patients with head and neck squamous cell carcinoma: a prerequisite for adoptive cell transfer, *Cytotherapy 13*, 822-834.

[37] Ohtani, T., Yamada, Y., Furuhashi, A., Ohmura, Y., Nakamura, S., Kato, H., Yoshikawa, K., and Kazaoka, Y. (2014) Activated cytotoxic T-lymphocyte immunotherapy is effective for advanced oral and maxillofacial cancers, *International journal of oncology 45*, 2051-2057.

[38] Yannelli, J. R., Hyatt, C., McConnell, S., Hines, K., Jacknin, L., Parker, L., Sanders, M., and Rosenberg, S. A. (1996) Growth of tumor-infiltrating lymphocytes from human solid

cancers: summary of a 5-year experience, *International journal of cancer. Journal international du cancer 65*, 413-421.
[39] Mehra, R., Cohen, R. B., and Burtness, B. A. (2008) The role of cetuximab for the treatment of squamous cell carcinoma of the head and neck, *Clinical advances in hematology & oncology : H&O 6*, 742-750.
[40] Argiris, A., Karamouzis, M. V., Raben, D., and Ferris, R. L. (2008) Head and neck cancer, *Lancet 371*, 1695-1709.
[41] Wong, R. J., and Shah, J. P. (2010) The role of the head and neck surgeon in contemporary multidisciplinary treatment programs for advanced head and neck cancer, *Current opinion in otolaryngology & head and neck surgery 18*, 79-82.
[42] Pignon, J. P., le Maitre, A., Maillard, E., Bourhis, J., and Group, M.-N. C. (2009) Meta-analysis of chemotherapy in head and neck cancer (MACH-NC): an update on 93 randomised trials and 17,346 patients, *Radiotherapy and oncology : journal of the European Society for Therapeutic Radiology and Oncology 92*, 4-14.
[43] Young, M. R., Wright, M. A., Lozano, Y., Matthews, J. P., Benefield, J., and Prechel, M. M. (1996) Mechanisms of immune suppression in patients with head and neck cancer: influence on the immune infiltrate of the cancer, *International journal of cancer. Journal international du cancer 67*, 333-338.
[44] Balermpas, P., Rodel, F., Weiss, C., Rodel, C., and Fokas, E. (2014) Tumor-infiltrating lymphocytes favor the response to chemoradiotherapy of head and neck cancer, *Oncoimmunology 3*, e27403.
[45] Pretscher, D., Distel, L. V., Grabenbauer, G. G., Wittlinger, M., Buettner, M., and Niedobitek, G. (2009) Distribution of immune cells in head and neck cancer: CD8+ T-cells and CD20+ B-cells in metastatic lymph nodes are associated with favourable outcome in patients with oro- and hypopharyngeal carcinoma, *BMC cancer 9*, 292.
[46] Wanebo, H. J., Jun, M. Y., Strong, E. W., and Oettgen, H. (1975) T-cell deficiency in patients with squamous cell cancer of the head and neck, *American journal of surgery 130*, 445-451.
[47] Wang, M. B., Lichtenstein, A., and Mickel, R. A. (1991) Hierarchical immunosuppression of regional lymph nodes in patients with head and neck squamous cell carcinoma, *Otolaryngology--head and neck surgery : official journal of American Academy of Otolaryngology-Head and Neck Surgery 105*, 517-527.
[48] Gillison, M. L., Koch, W. M., Capone, R. B., Spafford, M., Westra, W. H., Wu, L., Zahurak, M. L., Daniel, R. W., Viglione, M., Symer, D. E., Shah, K. V., and Sidransky, D. (2000) Evidence for a causal association between human papillomavirus and a subset of head and neck cancers, *Journal of the National Cancer Institute 92*, 709-720.
[49] Lindeberg, H., Fey, S. J., Ottosen, P. D., and Mose Larsen, P. (1988) Human papilloma virus (HPV) and carcinomas of the head and neck, *Clinical otolaryngology and allied sciences 13*, 447-454.
[50] Loning, T., Meichsner, M., Milde-Langosch, K., Hinze, H., Orlt, I., Hormann, K., Sesterhenn, K., Becker, J., and Reichart, P. (1987) HPV DNA detection in tumours of the head and neck: a comparative light microscopy and DNA hybridization study, *ORL; journal for oto-rhino-laryngology and its related specialties 49*, 259-269.
[51] Stransky, N., Egloff, A. M., Tward, A. D., Kostic, A. D., Cibulskis, K., Sivachenko, A., Kryukov, G. V., Lawrence, M. S., Sougnez, C., McKenna, A., Shefler, E., Ramos, A. H., Stojanov, P., Carter, S. L., Voet, D., Cortes, M. L., Auclair, D., Berger, M. F., Saksena, G., Guiducci, C., Onofrio, R. C., Parkin, M., Romkes, M., Weissfeld, J. L., Seethala, R. R., Wang, L., Rangel-Escareno, C., Fernandez-Lopez, J. C., Hidalgo-Miranda, A., Melendez-Zajgla, J., Winckler,

W., Ardlie, K., Gabriel, S. B., Meyerson, M., Lander, E. S., Getz, G., Golub, T. R., Garraway, L. A., and Grandis, J. R. (2011) The mutational landscape of head and neck squamous cell carcinoma, *Science 333*, 1157-1160.

[52] Koch, W. M., Lango, M., Sewell, D., Zahurak, M., and Sidransky, D. (1999) Head and neck cancer in nonsmokers: a distinct clinical and molecular entity, *The Laryngoscope 109*, 1544-1551.

[53] Wilczynski, S. P., Lin, B. T., Xie, Y., and Paz, I. B. (1998) Detection of human papillomavirus DNA and oncoprotein overexpression are associated with distinct morphological patterns of tonsillar squamous cell carcinoma, *The American journal of pathology 152*, 145-156.

[54] King, E. V., Ottensmeier, C. H., and Thomas, G. J. (2014) The immune response in HPV oropharyngeal cancer, *Oncoimmunology 3*, e27254.

[55] Wansom, D., Light, E., Worden, F., Prince, M., Urba, S., Chepeha, D. B., Cordell, K., Eisbruch, A., Taylor, J., D'Silva, N., Moyer, J., Bradford, C. R., Kurnit, D., Kumar, B., Carey, T. E., and Wolf, G. T. (2010) Correlation of cellular immunity with human papillomavirus 16 status and outcome in patients with advanced oropharyngeal cancer, *Archives of otolaryngology--head & neck surgery 136*, 1267-1273.

[56] Wolchok, J. D., Kluger, H., Callahan, M. K., Postow, M. A., Rizvi, N. A., Lesokhin, A. M., Segal, N. H., Ariyan, C. E., Gordon, R. A., Reed, K., Burke, M. M., Caldwell, A., Kronenberg, S. A., Agunwamba, B. U., Zhang, X., Lowy, I., Inzunza, H. D., Feely, W., Horak, C. E., Hong, Q., Korman, A. J., Wigginton, J. M., Gupta, A., and Sznol, M. (2013) Nivolumab plus ipilimumab in advanced melanoma, *The New England journal of medicine 369*, 122-133.

[57] Hodi, F. S., O'Day, S. J., McDermott, D. F., Weber, R. W., Sosman, J. A., Haanen, J. B., Gonzalez, R., Robert, C., Schadendorf, D., Hassel, J. C., Akerley, W., van den Eertwegh, A. J., Lutzky, J., Lorigan, P., Vaubel, J. M., Linette, G. P., Hogg, D., Ottensmeier, C. H., Lebbe, C., Peschel, C., Quirt, I., Clark, J. I., Wolchok, J. D., Weber, J. S., Tian, J., Yellin, M. J., Nichol, G. M., Hoos, A., and Urba, W. J. (2010) Improved survival with ipilimumab in patients with metastatic melanoma, *The New England journal of medicine 363*, 711-723.

[58] Brahmer, J., Reckamp, K. L., Baas, P., Crino, L., Eberhardt, W. E., Poddubskaya, E., Antonia, S., Pluzanski, A., Vokes, E. E., Holgado, E., Waterhouse, D., Ready, N., Gainor, J., Aren Frontera, O., Havel, L., Steins, M., Garassino, M. C., Aerts, J. G., Domine, M., Paz-Ares, L., Reck, M., Baudelet, C., Harbison, C. T., Lestini, B., and Spigel, D. R. (2015) Nivolumab versus Docetaxel in Advanced Squamous-Cell Non-Small-Cell Lung Cancer, *The New England journal of medicine 373*, 123-135.

[59] Parham, P., and Janeway, C. (2009) *The immune system*, 3rd ed., Garland Science, London ; New York.

[60] Curtsinger, J. M., Schmidt, C. S., Mondino, A., Lins, D. C., Kedl, R. M., Jenkins, M. K., and Mescher, M. F. (1999) Inflammatory cytokines provide a third signal for activation of naive CD4+ and CD8+ T cells, *Journal of immunology 162*, 3256-3262.

[61] Valenzuela, J., Schmidt, C., and Mescher, M. (2002) The roles of IL-12 in providing a third signal for clonal expansion of naive CD8 T cells, *Journal of immunology 169*, 6842-6849.

[62] Powles, T., Eder, J. P., Fine, G. D., Braiteh, F. S., Loriot, Y., Cruz, C., Bellmunt, J., Burris, H. A., Petrylak, D. P., Teng, S. L., Shen, X., Boyd, Z., Hegde, P. S., Chen, D. S., and Vogelzang, N. J. (2014) MPDL3280A (anti-PD-L1) treatment leads to clinical activity in metastatic bladder cancer, *Nature 515*, 558-562.

[63] Iida, T., Ohno, H., Nakaseko, C., Sakuma, M., Takeda-Ezaki, M., Arase, H., Kominami, E., Fujisawa, T., and Saito, T. (2000) Regulation of cell surface expression of CTLA-4 by

secretion of CTLA-4-containing lysosomes upon activation of CD4+ T cells, *Journal of immunology 165*, 5062-5068.
[64] Guntermann, C., and Alexander, D. R. (2002) CTLA-4 suppresses proximal TCR signaling in resting human CD4(+) T cells by inhibiting ZAP-70 Tyr(319) phosphorylation: a potential role for tyrosine phosphatases, *Journal of immunology 168*, 4420-4429.
[65] van der Merwe, P. A., Bodian, D. L., Daenke, S., Linsley, P., and Davis, S. J. (1997) CD80 (B7-1) binds both CD28 and CTLA-4 with a low affinity and very fast kinetics, *The Journal of experimental medicine 185*, 393-403.
[66] Zamarin, D., Holmgaard, R. B., Subudhi, S. K., Park, J. S., Mansour, M., Palese, P., Merghoub, T., Wolchok, J. D., and Allison, J. P. (2014) Localized oncolytic virotherapy overcomes systemic tumor resistance to immune checkpoint blockade immunotherapy, *Science translational medicine 6*, 226ra232.
[67] Hurwitz, A. A., Yu, T. F., Leach, D. R., and Allison, J. P. (1998) CTLA-4 blockade synergizes with tumor-derived granulocyte-macrophage colony-stimulating factor for treatment of an experimental mammary carcinoma, *Proceedings of the National Academy of Sciences of the United States of America 95*, 10067-10071.
[68] Leach, D. R., Krummel, M. F., and Allison, J. P. (1996) Enhancement of antitumor immunity by CTLA-4 blockade, *Science 271*, 1734-1736.
[69] Romano, E., Kusio-Kobialka, M., Foukas, P. G., Baumgaertner, P., Meyer, C., Ballabeni, P., Michielin, O., Weide, B., Romero, P., and Speiser, D. E. (2015) Ipilimumab-dependent cell-mediated cytotoxicity of regulatory T cells ex vivo by nonclassical monocytes in melanoma patients, *Proceedings of the National Academy of Sciences of the United States of America 112*, 6140-6145.
[70] Agata, Y., Kawasaki, A., Nishimura, H., Ishida, Y., Tsubata, T., Yagita, H., and Honjo, T. (1996) Expression of the PD-1 antigen on the surface of stimulated mouse T and B lymphocytes, *International immunology 8*, 765-772.
[71] Sheppard, K. A., Fitz, L. J., Lee, J. M., Benander, C., George, J. A., Wooters, J., Qiu, Y., Jussif, J. M., Carter, L. L., Wood, C. R., and Chaudhary, D. (2004) PD-1 inhibits T-cell receptor induced phosphorylation of the ZAP70/CD3zeta signalosome and downstream signaling to PKCtheta, *FEBS letters 574*, 37-41.
[72] Yang, W., Chen, P. W., Li, H., Alizadeh, H., and Niederkorn, J. Y. (2008) PD-L1: PD-1 interaction contributes to the functional suppression of T-cell responses to human uveal melanoma cells in vitro, *Investigative ophthalmology & visual science 49*, 2518-2525.
[73] Li, B., VanRoey, M., Wang, C., Chen, T. H., Korman, A., and Jooss, K. (2009) Anti-programmed death-1 synergizes with granulocyte macrophage colony-stimulating factor--secreting tumor cell immunotherapy providing therapeutic benefit to mice with established tumors, *Clinical cancer research : an official journal of the American Association for Cancer Research 15*, 1623-1634.
[74] Mangsbo, S. M., Sandin, L. C., Anger, K., Korman, A. J., Loskog, A., and Totterman, T. H. (2010) Enhanced tumor eradication by combining CTLA-4 or PD-1 blockade with CpG therapy, *Journal of immunotherapy 33*, 225-235.
[75] Nomi, T., Sho, M., Akahori, T., Hamada, K., Kubo, A., Kanehiro, H., Nakamura, S., Enomoto, K., Yagita, H., Azuma, M., and Nakajima, Y. (2007) Clinical significance and therapeutic potential of the programmed death-1 ligand/programmed death-1 pathway in human pancreatic cancer, *Clinical cancer research : an official journal of the American Association for Cancer Research 13*, 2151-2157.

[76] Iwai, Y., Terawaki, S., and Honjo, T. (2005) PD-1 blockade inhibits hematogenous spread of poorly immunogenic tumor cells by enhanced recruitment of effector T cells, *International immunology 17*, 133-144.

[77] Curran, M. A., Montalvo, W., Yagita, H., and Allison, J. P. (2010) PD-1 and CTLA-4 combination blockade expands infiltrating T cells and reduces regulatory T and myeloid cells within B16 melanoma tumors, *Proceedings of the National Academy of Sciences of the United States of America 107*, 4275-4280.

[78] Brahmer, J. R., Drake, C. G., Wollner, I., Powderly, J. D., Picus, J., Sharfman, W. H., Stankevich, E., Pons, A., Salay, T. M., McMiller, T. L., Gilson, M. M., Wang, C., Selby, M., Taube, J. M., Anders, R., Chen, L., Korman, A. J., Pardoll, D. M., Lowy, I., and Topalian, S. L. (2010) Phase I study of single-agent anti-programmed death-1 (MDX-1106) in refractory solid tumors: safety, clinical activity, pharmacodynamics, and immunologic correlates, *Journal of clinical oncology : official journal of the American Society of Clinical Oncology 28*, 3167-3175.

[79] Topalian, S. L., Hodi, F. S., Brahmer, J. R., Gettinger, S. N., Smith, D. C., McDermott, D. F., Powderly, J. D., Carvajal, R. D., Sosman, J. A., Atkins, M. B., Leming, P. D., Spigel, D. R., Antonia, S. J., Horn, L., Drake, C. G., Pardoll, D. M., Chen, L., Sharfman, W. H., Anders, R. A., Taube, J. M., McMiller, T. L., Xu, H., Korman, A. J., Jure-Kunkel, M., Agrawal, S., McDonald, D., Kollia, G. D., Gupta, A., Wigginton, J. M., and Sznol, M. (2012) Safety, activity, and immune correlates of anti-PD-1 antibody in cancer, *The New England journal of medicine 366*, 2443-2454.

[80] Lipson, E. J., Sharfman, W. H., Drake, C. G., Wollner, I., Taube, J. M., Anders, R. A., Xu, H., Yao, S., Pons, A., Chen, L., Pardoll, D. M., Brahmer, J. R., and Topalian, S. L. (2013) Durable cancer regression off-treatment and effective reinduction therapy with an anti-PD-1 antibody, *Clinical cancer research : an official journal of the American Association for Cancer Research 19*, 462-468.

[81] Berger, R., Rotem-Yehudar, R., Slama, G., Landes, S., Kneller, A., Leiba, M., Koren-Michowitz, M., Shimoni, A., and Nagler, A. (2008) Phase I safety and pharmacokinetic study of CT-011, a humanized antibody interacting with PD-1, in patients with advanced hematologic malignancies, *Clinical cancer research : an official journal of the American Association for Cancer Research 14*, 3044-3051.

[82] Hamid, O., Robert, C., Daud, A., Hodi, F. S., Hwu, W. J., Kefford, R., Wolchok, J. D., Hersey, P., Joseph, R. W., Weber, J. S., Dronca, R., Gangadhar, T. C., Patnaik, A., Zarour, H., Joshua, A. M., Gergich, K., Elassaiss-Schaap, J., Algazi, A., Mateus, C., Boasberg, P., Tumeh, P. C., Chmielowski, B., Ebbinghaus, S. W., Li, X. N., Kang, S. P., and Ribas, A. (2013) Safety and tumor responses with lambrolizumab (anti-PD-1) in melanoma, *The New England journal of medicine 369*, 134-144.

[83] Larkin, J., Chiarion-Sileni, V., Gonzalez, R., Grob, J. J., Cowey, C. L., Lao, C. D., Schadendorf, D., Dummer, R., Smylie, M., Rutkowski, P., Ferrucci, P. F., Hill, A., Wagstaff, J., Carlino, M. S., Haanen, J. B., Maio, M., Marquez-Rodas, I., McArthur, G. A., Ascierto, P. A., Long, G. V., Callahan, M. K., Postow, M. A., Grossmann, K., Sznol, M., Dreno, B., Bastholt, L., Yang, A., Rollin, L. M., Horak, C., Hodi, F. S., and Wolchok, J. D. (2015) Combined Nivolumab and Ipilimumab or Monotherapy in Untreated Melanoma, *The New England journal of medicine 373*, 23-34.

[84] Callahan, M. K., and Wolchok, J. D. (2013) At the bedside: CTLA-4- and PD-1-blocking antibodies in cancer immunotherapy, *Journal of leukocyte biology 94*, 41-53.

[85] Freeman, G. J., Long, A. J., Iwai, Y., Bourque, K., Chernova, T., Nishimura, H., Fitz, L. J., Malenkovich, N., Okazaki, T., Byrne, M. C., Horton, H. F., Fouser, L., Carter, L., Ling, V.,

Bowman, M. R., Carreno, B. M., Collins, M., Wood, C. R., and Honjo, T. (2000) Engagement of the PD-1 immunoinhibitory receptor by a novel B7 family member leads to negative regulation of lymphocyte activation, *The Journal of experimental medicine 192*, 1027-1034.

[86] Chen, J., Feng, Y., Lu, L., Wang, H., Dai, L., Li, Y., and Zhang, P. (2012) Interferon-gamma-induced PD-L1 surface expression on human oral squamous carcinoma via PKD2 signal pathway, *Immunobiology 217*, 385-393.

[87] Muhlbauer, M., Fleck, M., Schutz, C., Weiss, T., Froh, M., Blank, C., Scholmerich, J., and Hellerbrand, C. (2006) PD-L1 is induced in hepatocytes by viral infection and by interferon-alpha and -gamma and mediates T cell apoptosis, *Journal of hepatology 45*, 520-528.

[88] Terawaki, S., Chikuma, S., Shibayama, S., Hayashi, T., Yoshida, T., Okazaki, T., and Honjo, T. (2011) IFN-alpha directly promotes programmed cell death-1 transcription and limits the duration of T cell-mediated immunity, *Journal of immunology 186*, 2772-2779.

[89] Akbay, E. A., Koyama, S., Carretero, J., Altabef, A., Tchaicha, J. H., Christensen, C. L., Mikse, O. R., Cherniack, A. D., Beauchamp, E. M., Pugh, T. J., Wilkerson, M. D., Fecci, P. E., Butaney, M., Reibel, J. B., Soucheray, M., Cohoon, T. J., Janne, P. A., Meyerson, M., Hayes, D. N., Shapiro, G. I., Shimamura, T., Sholl, L. M., Rodig, S. J., Freeman, G. J., Hammerman, P. S., Dranoff, G., and Wong, K. K. (2013) Activation of the PD-1 pathway contributes to immune escape in EGFR-driven lung tumors, *Cancer discovery 3*, 1355-1363.

[90] Roy S. Herbst, M. S. G., Gregg Daniel Fine, Jeffrey Alan Sosman, Jean-Charles Soria, Omid Hamid, John D. Powderly, Howard A. Burris, Ahmad Mokatrin, Marcin Kowanetz, Maya Leabman, Maria Anderson, Daniel S. Chen and F. Stephen Hodi. (2013) A study of MPDL3280A, an engineered PD-L1 antibody in patients with locally advanced or metastatic tumors., *J Clin Oncol (Meeting Abstracts) 31*.

[91] Brahmer, J. R., Tykodi, S. S., Chow, L. Q., Hwu, W. J., Topalian, S. L., Hwu, P., Drake, C. G., Camacho, L. H., Kauh, J., Odunsi, K., Pitot, H. C., Hamid, O., Bhatia, S., Martins, R., Eaton, K., Chen, S., Salay, T. M., Alaparthy, S., Grosso, J. F., Korman, A. J., Parker, S. M., Agrawal, S., Goldberg, S. M., Pardoll, D. M., Gupta, A., and Wigginton, J. M. (2012) Safety and activity of anti-PD-L1 antibody in patients with advanced cancer, *The New England journal of medicine 366*, 2455-2465.

[92] Leisha A. Emens, F. S. B., Philippe Cassier, Jean-Pierre Delord, Joseph Paul Eder, Marcella Fasso, Yuanyuan Xiao, Yan Wang, Luciana Molinero, Daniel S. Chen, Ian Krop. (2015) Inhibition of PD-L1 by MPDL3280A leads to clinical activity in patients with metastatic triple-negative breast cancer (TNBC) *Proceedings of the 106th Annual Meeting of the American Association for Cancer Research Abstract #2859*.

[93] Alexander I. Spira, K. P., Julien Mazières, Johan F. Vansteenkiste, Achim Rittmeyer, Marcus Ballinger, Daniel Waterkamp, Marcin Kowanetz, Ahmad Mokatrin, Louis Fehrenbacher. (2015) Efficacy, safety and predictive biomarker results from a randomized phase II study comparing MPDL3280A vs docetaxel in 2L/3L NSCLC (POPLAR), *J Clin Oncol 33, 2015 (suppl; abstr 8010)*.

[94] Hadrup, S., Donia, M., and Thor Straten, P. (2013) Effector CD4 and CD8 T cells and their role in the tumor microenvironment, *Cancer microenvironment : official journal of the International Cancer Microenvironment Society 6*, 123-133.

[95] Rosenberg, S. A., Lotze, M. T., Muul, L. M., Chang, A. E., Avis, F. P., Leitman, S., Linehan, W. M., Robertson, C. N., Lee, R. E., Rubin, J. T., and et al. (1987) A progress report on the treatment of 157 patients with advanced cancer using lymphokine-activated killer cells

and interleukin-2 or high-dose interleukin-2 alone, *The New England journal of medicine 316*, 889-897.
[96] Mocellin, S., Pasquali, S., Rossi, C. R., and Nitti, D. (2010) Interferon alpha adjuvant therapy in patients with high-risk melanoma: a systematic review and meta-analysis, *Journal of the National Cancer Institute 102*, 493-501.
[97] Malek, T. R. (2008) The biology of interleukin-2, *Annual review of immunology 26*, 453-479.
[98] Scheffold, A., Huhn, J., and Hofer, T. (2005) Regulation of CD4+CD25+ regulatory T cell activity: it takes (IL-)two to tango, *European journal of immunology 35*, 1336-1341.
[99] Atkins, M. B., Lotze, M. T., Dutcher, J. P., Fisher, R. I., Weiss, G., Margolin, K., Abrams, J., Sznol, M., Parkinson, D., Hawkins, M., Paradise, C., Kunkel, L., and Rosenberg, S. A. (1999) High-dose recombinant interleukin 2 therapy for patients with metastatic melanoma: analysis of 270 patients treated between 1985 and 1993, *Journal of clinical oncology : official journal of the American Society of Clinical Oncology 17*, 2105-2116.
[100] Fisher, R. I., Rosenberg, S. A., and Fyfe, G. (2000) Long-term survival update for high-dose recombinant interleukin-2 in patients with renal cell carcinoma, *The cancer journal from Scientific American 6 Suppl 1*, S55-57.
[101] Payne, R., Glenn, L., Hoen, H., Richards, B., Smith, J. W., 2nd, Lufkin, R., Crocenzi, T. S., Urba, W. J., and Curti, B. D. (2014) Durable responses and reversible toxicity of high-dose interleukin-2 treatment of melanoma and renal cancer in a Community Hospital Biotherapy Program, *Journal for immunotherapy of cancer 2*, 13.
[102] Atkins, M. B., Kunkel, L., Sznol, M., and Rosenberg, S. A. (2000) High-dose recombinant interleukin-2 therapy in patients with metastatic melanoma: long-term survival update, *The cancer journal from Scientific American 6 Suppl 1*, S11-14.
[103] Wanebo, H. J., Jones, T., Pace, R., Cantrell, R., and Levine, P. (1989) Immune restoration with interleukin-2 in patients with squamous cell carcinoma of the head and neck, *American journal of surgery 158*, 356-360.
[104] Cortesina, G., De Stefani, A., Galeazzi, E., Bussi, M., Giordano, C., Cavallo, G. P., Jemma, C., Vai, S., Forni, G., and Valente, G. (1991) The effect of preoperative local interleukin-2 (IL-2) injections in patients with head and neck squamous cell carcinoma. An immunological study, *Acta oto-laryngologica 111*, 428-433.
[105] Cortesina, G., De Stefani, A., Galeazzi, E., Cavallo, G. P., Badellino, F., Margarino, G., Jemma, C., and Forni, G. (1994) Temporary regression of recurrent squamous cell carcinoma of the head and neck is achieved with a low but not with a high dose of recombinant interleukin 2 injected perilymphatically, *British journal of cancer 69*, 572-576.
[106] Cortesina, G., De Stefani, A., Galeazzi, E., Cavallo, G. P., Jemma, C., Giovarelli, M., Vai, S., and Forni, G. (1991) Interleukin-2 injected around tumor-draining lymph nodes in head and neck cancer, *Head & neck 13*, 125-131.
[107] De Stefani, A., Valente, G., Forni, G., Lerda, W., Ragona, R., and Cortesina, G. (1996) Treatment of oral cavity and oropharynx squamous cell carcinoma with perilymphatic interleukin-2: clinical and pathologic correlations, *Journal of immunotherapy with emphasis on tumor immunology : official journal of the Society for Biological Therapy 19*, 125-133.
[108] Saito, T., Kakiuti, H., Kuki, K., Yokota, M., Jinnin, T., Kimura, T., Fujiwara, K., Yoda, J., Kunimoto, M., Arai, H., and et al. (1989) [Clinical evaluation of local administration of RIL-2 in head and neck cancer], *Nihon Jibiinkoka Gakkai kaiho 92*, 1265-1270.
[109] Wei, S., Kryczek, I., Edwards, R. P., Zou, L., Szeliga, W., Banerjee, M., Cost, M., Cheng, P., Chang, A., Redman, B., Herberman, R. B., and Zou, W. (2007) Interleukin-2

administration alters the CD4+FOXP3+ T-cell pool and tumor trafficking in patients with ovarian carcinoma, *Cancer research 67*, 7487-7494.
[110] Belardelli, F., Ferrantini, M., Proietti, E., and Kirkwood, J. M. (2002) Interferon-alpha in tumor immunity and immunotherapy, *Cytokine & growth factor reviews 13*, 119-134.
[111] Trinchieri, G. (2010) Type I interferon: friend or foe?, *The Journal of experimental medicine 207*, 2053-2063.
[112] van Herpen, C. M., van der Laak, J. A., de Vries, I. J., van Krieken, J. H., de Wilde, P. C., Balvers, M. G., Adema, G. J., and De Mulder, P. H. (2005) Intratumoral recombinant human interleukin-12 administration in head and neck squamous cell carcinoma patients modifies locoregional lymph node architecture and induces natural killer cell infiltration in the primary tumor, *Clinical cancer research : an official journal of the American Association for Cancer Research 11*, 1899-1909.
[113] van Herpen, C. M., van der Voort, R., van der Laak, J. A., Klasen, I. S., de Graaf, A. O., van Kempen, L. C., de Vries, I. J., Boer, T. D., Dolstra, H., Torensma, R., van Krieken, J. H., Adema, G. J., and De Mulder, P. H. (2008) Intratumoral rhIL-12 administration in head and neck squamous cell carcinoma patients induces B cell activation, *International journal of cancer. Journal international du cancer 123*, 2354-2361.
[114] Piconese, S., Valzasina, B., and Colombo, M. P. (2008) OX40 triggering blocks suppression by regulatory T cells and facilitates tumor rejection, *The Journal of experimental medicine 205*, 825-839.
[115] Jensen, S. M., Maston, L. D., Gough, M. J., Ruby, C. E., Redmond, W. L., Crittenden, M., Li, Y., Puri, S., Poehlein, C. H., Morris, N., Kovacsovics-Bankowski, M., Moudgil, T., Twitty, C., Walker, E. B., Hu, H. M., Urba, W. J., Weinberg, A. D., Curti, B., and Fox, B. A. (2010) Signaling through OX40 enhances antitumor immunity, *Seminars in oncology 37*, 524-532.
[116] Curti, B. D., Kovacsovics-Bankowski, M., Morris, N., Walker, E., Chisholm, L., Floyd, K., Walker, J., Gonzalez, I., Meeuwsen, T., Fox, B. A., Moudgil, T., Miller, W., Haley, D., Coffey, T., Fisher, B., Delanty-Miller, L., Rymarchyk, N., Kelly, T., Crocenzi, T., Bernstein, E., Sanborn, R., Urba, W. J., and Weinberg, A. D. (2013) OX40 is a potent immune-stimulating target in late-stage cancer patients, *Cancer research 73*, 7189-7198.
[117] Futagawa, T., Akiba, H., Kodama, T., Takeda, K., Hosoda, Y., Yagita, H., and Okumura, K. (2002) Expression and function of 4-1BB and 4-1BB ligand on murine dendritic cells, *International immunology 14*, 275-286.
[118] Cheuk, A. T., Mufti, G. J., and Guinn, B. A. (2004) Role of 4-1BB:4-1BB ligand in cancer immunotherapy, *Cancer gene therapy 11*, 215-226.
[119] Mittler, R. S., Bailey, T. S., Klussman, K., Trailsmith, M. D., and Hoffmann, M. K. (1999) Anti-4-1BB monoclonal antibodies abrogate T cell-dependent humoral immune responses in vivo through the induction of helper T cell anergy, *The Journal of experimental medicine 190*, 1535-1540.
[120] Foell, J., Strahotin, S., O'Neil, S. P., McCausland, M. M., Suwyn, C., Haber, M., Chander, P. N., Bapat, A. S., Yan, X. J., Chiorazzi, N., Hoffmann, M. K., and Mittler, R. S. (2003) CD137 costimulatory T cell receptor engagement reverses acute disease in lupus-prone NZB x NZW F1 mice, *The Journal of clinical investigation 111*, 1505-1518.
[121] Chen, S., Lee, L. F., Fisher, T. S., Jessen, B., Elliott, M., Evering, W., Logronio, K., Tu, G. H., Tsaparikos, K., Li, X., Wang, H., Ying, C., Xiong, M., VanArsdale, T., and Lin, J. C. (2015) Combination of 4-1BB agonist and PD-1 antagonist promotes antitumor effector/memory CD8 T cells in a poorly immunogenic tumor model, *Cancer immunology research 3*, 149-160.

[122] Vinay, D. S., and Kwon, B. S. (2012) Immunotherapy of cancer with 4-1BB, *Molecular cancer therapeutics 11*, 1062-1070.
[123] David L. Bajor, R. M., Matthew J. Riese, Lee P. Richman, Xiaowei Xu, Drew A. Torigian, Erietta Stelekati, Martha Sweeney, Brendan Sullivan, Lynn M. Schuchter, Ravi Amaravadi, E. John Wherry, Robert H. Vonderheide. (2015) Combination of agonistic CD40 monoclonal antibody CP-870,893 and anti-CTLA-4 antibody tremelimumab in patients with metastatic melanoma *Proceedings of the 106th Annual Meeting of the American Association for Cancer Research, Philadelphia, PA*.
[124] Hu, X., Chakraborty, N. G., Sporn, J. R., Kurtzman, S. H., Ergin, M. T., and Mukherji, B. (1996) Enhancement of cytolytic T lymphocyte precursor frequency in melanoma patients following immunization with the MAGE-1 peptide loaded antigen presenting cell-based vaccine, *Cancer research 56*, 2479-2483.
[125] Barve, M., Bender, J., Senzer, N., Cunningham, C., Greco, F. A., McCune, D., Steis, R., Khong, H., Richards, D., Stephenson, J., Ganesa, P., Nemunaitis, J., Ishioka, G., Pappen, B., Nemunaitis, M., Morse, M., Mills, B., Maples, P. B., Sherman, J., and Nemunaitis, J. J. (2008) Induction of immune responses and clinical efficacy in a phase II trial of IDM-2101, a 10-epitope cytotoxic T-lymphocyte vaccine, in metastatic non-small-cell lung cancer, *Journal of clinical oncology : official journal of the American Society of Clinical Oncology 26*, 4418-4425.
[126] Schwartzentruber, D. J., Lawson, D. H., Richards, J. M., Conry, R. M., Miller, D. M., Treisman, J., Gailani, F., Riley, L., Conlon, K., Pockaj, B., Kendra, K. L., White, R. L., Gonzalez, R., Kuzel, T. M., Curti, B., Leming, P. D., Whitman, E. D., Balkissoon, J., Reintgen, D. S., Kaufman, H., Marincola, F. M., Merino, M. J., Rosenberg, S. A., Choyke, P., Vena, D., and Hwu, P. (2011) gp100 peptide vaccine and interleukin-2 in patients with advanced melanoma, *The New England journal of medicine 364*, 2119-2127.
[127] Kantoff, P. W., Higano, C. S., Shore, N. D., Berger, E. R., Small, E. J., Penson, D. F., Redfern, C. H., Ferrari, A. C., Dreicer, R., Sims, R. B., Xu, Y., Frohlich, M. W., Schellhammer, P. F., and Investigators, I. S. (2010) Sipuleucel-T immunotherapy for castration-resistant prostate cancer, *The New England journal of medicine 363*, 411-422.
[128] Aris, M., Zubieta, M. R., Colombo, M., Arriaga, J. M., Bianchini, M., Alperovich, M., Bravo, A. I., Barrio, M. M., and Mordoh, J. (2012) MART-1- and gp100-expressing and -non-expressing melanoma cells are equally proliferative in tumors and clonogenic in vitro, *The Journal of investigative dermatology 132*, 365-374.
[129] Dranoff, G. (2002) GM-CSF-based cancer vaccines, *Immunological reviews 188*, 147-154.
[130] Srivatsan, S., Patel, J. M., Bozeman, E. N., Imasuen, I. E., He, S., Daniels, D., and Selvaraj, P. (2014) Allogeneic tumor cell vaccines: the promise and limitations in clinical trials, *Human vaccines & immunotherapeutics 10*, 52-63.
[131] Lutz, E., Yeo, C. J., Lillemoe, K. D., Biedrzycki, B., Kobrin, B., Herman, J., Sugar, E., Piantadosi, S., Cameron, J. L., Solt, S., Onners, B., Tartakovsky, I., Choi, M., Sharma, R., Illei, P. B., Hruban, R. H., Abrams, R. A., Le, D., Jaffee, E., and Laheru, D. (2011) A lethally irradiated allogeneic granulocyte-macrophage colony stimulating factor-secreting tumor vaccine for pancreatic adenocarcinoma. A Phase II trial of safety, efficacy, and immune activation, *Annals of surgery 253*, 328-335.
[132] Levine, B. (2006) Unraveling the role of autophagy in cancer, *Autophagy 2*, 65-66.
[133] Eskelinen, E. L. (2011) The dual role of autophagy in cancer, *Current opinion in pharmacology 11*, 294-300.
[134] Mathew, R., Karantza-Wadsworth, V., and White, E. (2007) Role of autophagy in cancer, *Nature reviews. Cancer 7*, 961-967.

[135] Li, Y., Wang, L. X., Yang, G., Hao, F., Urba, W. J., and Hu, H. M. (2008) Efficient cross-presentation depends on autophagy in tumor cells, *Cancer research 68*, 6889-6895.
[136] Li, Y., Wang, L. X., Pang, P., Twitty, C., Fox, B. A., Aung, S., Urba, W. J., and Hu, H. M. (2009) Cross-presentation of tumor associated antigens through tumor-derived autophagosomes, *Autophagy 5*, 576-577.
[137] Dolan, B. P., Li, L., Veltri, C. A., Ireland, C. M., Bennink, J. R., and Yewdell, J. W. (2011) Distinct pathways generate peptides from defective ribosomal products for CD8+ T cell immunosurveillance, *Journal of immunology 186*, 2065-2072.
[138] Yewdell, J. W., Anton, L. C., and Bennink, J. R. (1996) Defective ribosomal products (DRiPs): a major source of antigenic peptides for MHC class I molecules?, *Journal of immunology 157*, 1823-1826.
[139] Twitty, C. G., Jensen, S. M., Hu, H. M., and Fox, B. A. (2011) Tumor-derived autophagosome vaccine: induction of cross-protective immune responses against short-lived proteins through a p62-dependent mechanism, *Clinical cancer research : an official journal of the American Association for Cancer Research 17*, 6467-6481.
[140] Li, Y., Wang, L. X., Pang, P., Cui, Z., Aung, S., Haley, D., Fox, B. A., Urba, W. J., and Hu, H. M. (2011) Tumor-derived autophagosome vaccine: mechanism of cross-presentation and therapeutic efficacy, *Clinical cancer research : an official journal of the American Association for Cancer Research 17*, 7047-7057.
[141] A. Chaturvedi, E. E., W. Anderson and M. Gillison. (2007) Incidence trends for human papillomavirus-related (HPV-R) and unrelated (HPV-U) head and neck squamous cell carcinomas (HNSCC) in the United States (US) *J Clin Oncol (Meeting Abstracts) 25*.
[142] Chaturvedi, A. K. (2012) Epidemiology and clinical aspects of HPV in head and neck cancers, *Head and neck pathology 6 Suppl 1*, S16-24.
[143] Paavonen, J., Jenkins, D., Bosch, F. X., Naud, P., Salmeron, J., Wheeler, C. M., Chow, S. N., Apter, D. L., Kitchener, H. C., Castellsague, X., de Carvalho, N. S., Skinner, S. R., Harper, D. M., Hedrick, J. A., Jaisamrarn, U., Limson, G. A., Dionne, M., Quint, W., Spiessens, B., Peeters, P., Struyf, F., Wieting, S. L., Lehtinen, M. O., Dubin, G., and group, H. P. s. (2007) Efficacy of a prophylactic adjuvanted bivalent L1 virus-like-particle vaccine against infection with human papillomavirus types 16 and 18 in young women: an interim analysis of a phase III double-blind, randomised controlled trial, *Lancet 369*, 2161-2170.
[144] Villa, L. L., Costa, R. L., Petta, C. A., Andrade, R. P., Paavonen, J., Iversen, O. E., Olsson, S. E., Hoye, J., Steinwall, M., Riis-Johannessen, G., Andersson-Ellstrom, A., Elfgren, K., Krogh, G., Lehtinen, M., Malm, C., Tamms, G. M., Giacoletti, K., Lupinacci, L., Railkar, R., Taddeo, F. J., Bryan, J., Esser, M. T., Sings, H. L., Saah, A. J., and Barr, E. (2006) High sustained efficacy of a prophylactic quadrivalent human papillomavirus types 6/11/16/18 L1 virus-like particle vaccine through 5 years of follow-up, *British journal of cancer 95*, 1459-1466.
[145] Rizvi, N. A., Hellmann, M. D., Snyder, A., Kvistborg, P., Makarov, V., Havel, J. J., Lee, W., Yuan, J., Wong, P., Ho, T. S., Miller, M. L., Rekhtman, N., Moreira, A. L., Ibrahim, F., Bruggeman, C., Gasmi, B., Zappasodi, R., Maeda, Y., Sander, C., Garon, E. B., Merghoub, T., Wolchok, J. D., Schumacher, T. N., and Chan, T. A. (2015) Cancer immunology. Mutational landscape determines sensitivity to PD-1 blockade in non-small cell lung cancer, *Science 348*, 124-128.
[146] Cross, M. (2011) ERG oncoprotein overexpression in prostate cancer. Multiplex IHC adds to diagnostic prowess and efficiency of laboratory, *MLO: medical laboratory observer 43*, 22, 42.

[147] Rosenberg, S. A., Restifo, N. P., Yang, J. C., Morgan, R. A., and Dudley, M. E. (2008) Adoptive cell transfer: a clinical path to effective cancer immunotherapy, *Nature reviews. Cancer 8*, 299-308.
[148] Barth, R. J., Jr., Mule, J. J., Spiess, P. J., and Rosenberg, S. A. (1991) Interferon gamma and tumor necrosis factor have a role in tumor regressions mediated by murine CD8+ tumor-infiltrating lymphocytes, *The Journal of experimental medicine 173*, 647-658.
[149] Prieto, P. A., Durflinger, K. H., Wunderlich, J. R., Rosenberg, S. A., and Dudley, M. E. (2010) Enrichment of CD8+ cells from melanoma tumor-infiltrating lymphocyte cultures reveals tumor reactivity for use in adoptive cell therapy, *Journal of immunotherapy 33*, 547-556.
[150] Church, S. E., Jensen, S. M., Antony, P. A., Restifo, N. P., and Fox, B. A. (2014) Tumor-specific CD4+ T cells maintain effector and memory tumor-specific CD8+ T cells, *European journal of immunology 44*, 69-79.
[151] Hu, H. M., Winter, H., Urba, W. J., and Fox, B. A. (2000) Divergent roles for CD4+ T cells in the priming and effector/memory phases of adoptive immunotherapy, *Journal of immunology 165*, 4246-4253.
[152] Rosenberg, S. A., and Lotze, M. T. (1986) Cancer immunotherapy using interleukin-2 and interleukin-2-activated lymphocytes, *Annual review of immunology 4*, 681-709.
[153] Rosenberg, S. A., Packard, B. S., Aebersold, P. M., Solomon, D., Topalian, S. L., Toy, S. T., Simon, P., Lotze, M. T., Yang, J. C., Seipp, C. A., and et al. (1988) Use of tumor-infiltrating lymphocytes and interleukin-2 in the immunotherapy of patients with metastatic melanoma. A preliminary report, *The New England journal of medicine 319*, 1676-1680.
[154] Rosenberg, S. A., Spiess, P., and Lafreniere, R. (1986) A new approach to the adoptive immunotherapy of cancer with tumor-infiltrating lymphocytes, *Science 233*, 1318-1321.
[155] Hom, S. S., Schwartzentruber, D. J., Rosenberg, S. A., and Topalian, S. L. (1993) Specific release of cytokines by lymphocytes infiltrating human melanomas in response to shared melanoma antigens, *Journal of immunotherapy with emphasis on tumor immunology : official journal of the Society for Biological Therapy 13*, 18-30.
[156] Riddell, S. R., and Greenberg, P. D. (1990) The use of anti-CD3 and anti-CD28 monoclonal antibodies to clone and expand human antigen-specific T cells, *Journal of immunological methods 128*, 189-201.
[157] Fridman, W. H., Pages, F., Sautes-Fridman, C., and Galon, J. (2012) The immune contexture in human tumours: impact on clinical outcome, *Nature reviews. Cancer 12*, 298-306.
[158] Hillen, F., Baeten, C. I., van de Winkel, A., Creytens, D., van der Schaft, D. W., Winnepenninckx, V., and Griffioen, A. W. (2008) Leukocyte infiltration and tumor cell plasticity are parameters of aggressiveness in primary cutaneous melanoma, *Cancer immunology, immunotherapy : CII 57*, 97-106.
[159] Ladanyi, A., Somlai, B., Gilde, K., Fejos, Z., Gaudi, I., and Timar, J. (2004) T-cell activation marker expression on tumor-infiltrating lymphocytes as prognostic factor in cutaneous malignant melanoma, *Clinical cancer research : an official journal of the American Association for Cancer Research 10*, 521-530.
[160] Erdag, G., Schaefer, J. T., Smolkin, M. E., Deacon, D. H., Shea, S. M., Dengel, L. T., Patterson, J. W., and Slingluff, C. L., Jr. (2012) Immunotype and immunohistologic characteristics of tumor-infiltrating immune cells are associated with clinical outcome in metastatic melanoma, *Cancer research 72*, 1070-1080.
[161] Aebersold, P., Hyatt, C., Johnson, S., Hines, K., Korcak, L., Sanders, M., Lotze, M., Topalian, S., Yang, J., and Rosenberg, S. A. (1991) Lysis of autologous melanoma cells by tumor-infiltrating lymphocytes: association with clinical response, *Journal of the National Cancer Institute 83*, 932-937.

[162] Clevenger, J., Joseph, C., Dawlett, M., Guo, M., and Gong, Y. (2014) Reliability of immunostaining using pan-melanoma cocktail, SOX10, and microphthalmia transcription factor in confirming a diagnosis of melanoma on fine-needle aspiration smears, *Cancer cytopathology 122*, 779-785.

[163] Yao, X., Ahmadzadeh, M., Lu, Y. C., Liewehr, D. J., Dudley, M. E., Liu, F., Schrump, D. S., Steinberg, S. M., Rosenberg, S. A., and Robbins, P. F. (2012) Levels of peripheral CD4(+)FoxP3(+) regulatory T cells are negatively associated with clinical response to adoptive immunotherapy of human cancer, *Blood 119*, 5688-5696.

[164] Antony, P. A., Piccirillo, C. A., Akpinarli, A., Finkelstein, S. E., Speiss, P. J., Surman, D. R., Palmer, D. C., Chan, C. C., Klebanoff, C. A., Overwijk, W. W., Rosenberg, S. A., and Restifo, N. P. (2005) CD8+ T cell immunity against a tumor/self-antigen is augmented by CD4+ T helper cells and hindered by naturally occurring T regulatory cells, *Journal of immunology 174*, 2591-2601.

[165] Pyonteck, S. M., Akkari, L., Schuhmacher, A. J., Bowman, R. L., Sevenich, L., Quail, D. F., Olson, O. C., Quick, M. L., Huse, J. T., Teijeiro, V., Setty, M., Leslie, C. S., Oei, Y., Pedraza, A., Zhang, J., Brennan, C. W., Sutton, J. C., Holland, E. C., Daniel, D., and Joyce, J. A. (2013) CSF-1R inhibition alters macrophage polarization and blocks glioma progression, *Nature medicine 19*, 1264-1272.

[166] Ries, C. H., Cannarile, M. A., Hoves, S., Benz, J., Wartha, K., Runza, V., Rey-Giraud, F., Pradel, L. P., Feuerhake, F., Klaman, I., Jones, T., Jucknischke, U., Scheiblich, S., Kaluza, K., Gorr, I. H., Walz, A., Abiraj, K., Cassier, P. A., Sica, A., Gomez-Roca, C., de Visser, K. E., Italiano, A., Le Tourneau, C., Delord, J. P., Levitsky, H., Blay, J. Y., and Ruttinger, D. (2014) Targeting tumor-associated macrophages with anti-CSF-1R antibody reveals a strategy for cancer therapy, *Cancer cell 25*, 846-859.

[167] Chacon, J. A., Sarnaik, A. A., Chen, J. Q., Creasy, C., Kale, C., Robinson, J., Weber, J., Hwu, P., Pilon-Thomas, S., and Radvanyi, L. (2015) Manipulating the tumor microenvironment ex vivo for enhanced expansion of tumor-infiltrating lymphocytes for adoptive cell therapy, *Clinical cancer research : an official journal of the American Association for Cancer Research 21*, 611-621.

[168] John, L. B., Kershaw, M. H., and Darcy, P. K. (2013) Blockade of PD-1 immunosuppression boosts CAR T-cell therapy, *Oncoimmunology 2*, e26286.

[169] Radvanyi, L., Pilon-Thomas, S., Peng, W., Sarnaik, A., Mule, J. J., Weber, J., and Hwu, P. (2013) Antagonist antibodies to PD-1 and B7-H1 (PD-L1) in the treatment of advanced human cancer--letter, *Clinical cancer research : an official journal of the American Association for Cancer Research 19*, 5541.

[170] Collings, L. A., Poulter, L. W., and Janossy, G. (1984) The demonstration of cell surface antigens on T cells, B cells and accessory cells in paraffin-embedded human tissues, *Journal of immunological methods 75*, 227-239.

[171] Gendelman, H. E., Moench, T. R., Narayan, O., and Griffin, D. E. (1983) Selection of a fixative for identifying T cell subsets, B cells, and macrophages in paraffin-embedded mouse spleen, *Journal of immunological methods 65*, 137-145.

[172] Rehg, J. E., Bush, D., and Ward, J. M. (2012) The utility of immunohistochemistry for the identification of hematopoietic and lymphoid cells in normal tissues and interpretation of proliferative and inflammatory lesions of mice and rats, *Toxicologic pathology 40*, 345-374.

[173] Whiteland, J. L., Nicholls, S. M., Shimeld, C., Easty, D. L., Williams, N. A., and Hill, T. J. (1995) Immunohistochemical detection of T-cell subsets and other leukocytes in paraffin-embedded rat and mouse tissues with monoclonal antibodies, *The journal of*

histochemistry and cytochemistry : official journal of the Histochemistry Society 43, 313-320.

[174] Hicks, D. J., Johnson, L., Mitchell, S. M., Gough, J., Cooley, W. A., La Ragione, R. M., Spencer, Y. I., and Wangoo, A. (2006) Evaluation of zinc salt based fixatives for preserving antigenic determinants for immunohistochemical demonstration of murine immune system cell markers, *Biotechnic & histochemistry : official publication of the Biological Stain Commission 81*, 23-30.

[175] Beckstead, J. H. (1994) A simple technique for preservation of fixation-sensitive antigens in paraffin-embedded tissues, *The journal of histochemistry and cytochemistry : official journal of the Histochemistry Society 42*, 1127-1134.

[176] Steinert, E. M., Schenkel, J. M., Fraser, K. A., Beura, L. K., Manlove, L. S., Igyarto, B. Z., Southern, P. J., and Masopust, D. (2015) Quantifying Memory CD8 T Cells Reveals Regionalization of Immunosurveillance, *Cell 161*, 737-749.

[177] Winter, H., Hu, H. M., Poehlein, C. H., Huntzicker, E., Osterholzer, J. J., Bashy, J., Lashley, D., Lowe, B., Yamada, J., Alvord, G., Urba, W. J., and Fox, B. A. (2003) Tumour-induced polarization of tumour vaccine-draining lymph node T cells to a type 1 cytokine profile predicts inherent strong immunogenicity of the tumour and correlates with therapeutic efficacy in adoptive transfer studies, *Immunology 108*, 409-419.

[178] Khurana, D., Martin, E. A., Kasperbauer, J. L., O'Malley, B. W., Jr., Salomao, D. R., Chen, L., and Strome, S. E. (2001) Characterization of a spontaneously arising murine squamous cell carcinoma (SCC VII) as a prerequisite for head and neck cancer immunotherapy, *Head & neck 23*, 899-906.

[179] Borowitz, M. J., Croker, B. P., and Burchette, J. (1982) Immunocytochemical detection of lymphocyte surface antigens in fixed tissue sections, *The journal of histochemistry and cytochemistry : official journal of the Histochemistry Society 30*, 171-174.

[180] McLean, I. W., and Nakane, P. K. (1974) Periodate-lysine-paraformaldehyde fixative. A new fixation for immunoelectron microscopy, *The journal of histochemistry and cytochemistry : official journal of the Histochemistry Society 22*, 1077-1083.

[181] Brenes, F., Harris, S., Paz, M. O., Petrovic, L. M., and Scheuer, P. J. (1986) PLP fixation for combined routine histology and immunocytochemistry of liver biopsies, *Journal of clinical pathology 39*, 459-463.

[182] Wester, K., Asplund, A., Backvall, H., Micke, P., Derveniece, A., Hartmane, I., Malmstrom, P. U., and Ponten, F. (2003) Zinc-based fixative improves preservation of genomic DNA and proteins in histoprocessing of human tissues, *Laboratory investigation; a journal of technical methods and pathology 83*, 889-899.

[183] Shortman, K., and Heath, W. R. (2010) The CD8+ dendritic cell subset, *Immunological reviews 234*, 18-31.

[184] Kim, M. Y., McConnell, F. M., Gaspal, F. M., White, A., Glanville, S. H., Bekiaris, V., Walker, L. S., Caamano, J., Jenkinson, E., Anderson, G., and Lane, P. J. (2007) Function of CD4+CD3- cells in relation to B- and T-zone stroma in spleen, *Blood 109*, 1602-1610.

[185] Kim, M. Y., Rossi, S., Withers, D., McConnell, F., Toellner, K. M., Gaspal, F., Jenkinson, E., Anderson, G., and Lane, P. J. (2008) Heterogeneity of lymphoid tissue inducer cell populations present in embryonic and adult mouse lymphoid tissues, *Immunology 124*, 166-174.

[186] Vremec, D., Pooley, J., Hochrein, H., Wu, L., and Shortman, K. (2000) CD4 and CD8 expression by dendritic cell subtypes in mouse thymus and spleen, *Journal of immunology 164*, 2978-2986.

[187] Esashi, E., Ito, H., Ishihara, K., Hirano, T., Koyasu, S., and Miyajima, A. (2004) Development of CD4+ macrophages from intrathymic T cell progenitors is induced by thymic epithelial cells, *Journal of immunology 173*, 4360-4367.

[188] Garon, E. B., Rizvi, N. A., Hui, R., Leighl, N., Balmanoukian, A. S., Eder, J. P., Patnaik, A., Aggarwal, C., Gubens, M., Horn, L., Carcereny, E., Ahn, M. J., Felip, E., Lee, J. S., Hellmann, M. D., Hamid, O., Goldman, J. W., Soria, J. C., Dolled-Filhart, M., Rutledge, R. Z., Zhang, J., Lunceford, J. K., Rangwala, R., Lubiniecki, G. M., Roach, C., Emancipator, K., Gandhi, L., and Investigators, K.-. (2015) Pembrolizumab for the treatment of non-small-cell lung cancer, *The New England journal of medicine 372*, 2018-2028.

[189] Marisa Dolled-Filhart, C. M. R., Grant Toland, Jeanette Musser, Gregory M. Lubiniecki, Gary Ponto, Kenneth Emancipator. (2015) Development of a PD-L1 immunohistochemistry (IHC) assay for use as a companion diagnostic for pembrolizumab (MK-3475) in non-small cell lung cancer (NSCLC). *J Clin Oncol 33, 2015 (suppl; abstr 11065)*.

[190] Winter, H., van den Engel, N. K., Ruttinger, D., Schmidt, J., Schiller, M., Poehlein, C. H., Lohe, F., Fox, B. A., Jauch, K. W., Hatz, R. A., and Hu, H. M. (2007) Therapeutic T cells induce tumor-directed chemotaxis of innate immune cells through tumor-specific secretion of chemokines and stimulation of B16BL6 melanoma to secrete chemokines, *Journal of translational medicine 5*, 56.

[191] Liu, J., Yuan, Y., Chen, W., Putra, J., Suriawinata, A. A., Schenk, A. D., Miller, H. E., Guleria, I., Barth, R. J., Huang, Y. H., and Wang, L. (2015) Immune-checkpoint proteins VISTA and PD-1 nonredundantly regulate murine T-cell responses, *Proceedings of the National Academy of Sciences of the United States of America 112*, 6682-6687.

[192] Lykidis, D., Van Noorden, S., Armstrong, A., Spencer-Dene, B., Li, J., Zhuang, Z., and Stamp, G. W. (2007) Novel zinc-based fixative for high quality DNA, RNA and protein analysis, *Nucleic acids research 35*, e85.

[193] Abreu, L. P., Kruger, E., and Tennant, M. (2010) Oral cancer in Western Australia, 1982-2006: a retrospective epidemiological study, *Journal of oral pathology & medicine : official publication of the International Association of Oral Pathologists and the American Academy of Oral Pathology 39*, 376-381.

[194] Listl, S., Jansen, L., Stenzinger, A., Freier, K., Emrich, K., Holleczek, B., Katalinic, A., Gondos, A., Brenner, H., and Group, G. C. S. W. (2013) Survival of patients with oral cavity cancer in Germany, *PloS one 8*, e53415.

[195] Rogers, S. N., Brown, J. S., Woolgar, J. A., Lowe, D., Magennis, P., Shaw, R. J., Sutton, D., Errington, D., and Vaughan, D. (2009) Survival following primary surgery for oral cancer, *Oral oncology 45*, 201-211.

[196] Zini, A., Czerninski, R., and Sgan-Cohen, H. D. (2010) Oral cancer over four decades: epidemiology, trends, histology, and survival by anatomical sites, *Journal of oral pathology & medicine : official publication of the International Association of Oral Pathologists and the American Academy of Oral Pathology 39*, 299-305.

[197] Pulte, D., and Brenner, H. (2010) Changes in survival in head and neck cancers in the late 20th and early 21st century: a period analysis, *The oncologist 15*, 994-1001.

[198] Lothaire, P., de Azambuja, E., Dequanter, D., Lalami, Y., Sotiriou, C., Andry, G., Castro, G., Jr., and Awada, A. (2006) Molecular markers of head and neck squamous cell carcinoma: promising signs in need of prospective evaluation, *Head & neck 28*, 256-269.

[199] Piazzolla, D., Palla, A. R., Pantoja, C., Canamero, M., de Castro, I. P., Ortega, S., Gomez-Lopez, G., Dominguez, O., Megias, D., Roncador, G., Luque-Garcia, J. L., Fernandez-Tresguerres, B., Fernandez, A. F., Fraga, M. F., Rodriguez-Justo, M., Manzanares, M., Sanchez-Carbayo, M., Garcia-Pedrero, J. M., Rodrigo, J. P., Malumbres, M., and Serrano,

M. (2014) Lineage-restricted function of the pluripotency factor NANOG in stratified epithelia, *Nature communications 5*, 4226.

[200] Zoller, J., Fiehn, W., Mende, U., and Hotz, G. (1990) [The diagnostic value of the tumor markers CEA, "Ca 19-9", "Ca 125", "Ca15-3" and "SCC" for the detection of recurrent tumors in patients with tumors of the head and neck], *Deutsche Zeitschrift fur Mund-, Kiefer- und Gesichts-Chirurgie 14*, 254-259.

[201] Oliveira, L. R., and Ribeiro-Silva, A. (2011) Prognostic significance of immunohistochemical biomarkers in oral squamous cell carcinoma, *International journal of oral and maxillofacial surgery 40*, 298-307.

[202] Duray, A., Demoulin, S., Hubert, P., Delvenne, P., and Saussez, S. (2010) Immune suppression in head and neck cancers: a review, *Clinical & developmental immunology 2010*, 701657.

[203] Bell, R. B., Leidner, R. S., Crittenden, M. R., Curti, B. D., Feng, Z., Montler, R., Gough, M. J., Fox, B. A., Weinberg, A. D., and Urba, W. J. (2016) OX40 signaling in head and neck squamous cell carcinoma: Overcoming immunosuppression in the tumor microenvironment, *Oral oncology 52*, 1-10.

[204] Badoual, C., Hans, S., Rodriguez, J., Peyrard, S., Klein, C., Agueznay Nel, H., Mosseri, V., Laccourreye, O., Bruneval, P., Fridman, W. H., Brasnu, D. F., and Tartour, E. (2006) Prognostic value of tumor-infiltrating CD4+ T-cell subpopulations in head and neck cancers, *Clinical cancer research : an official journal of the American Association for Cancer Research 12*, 465-472.

[205] Boucek, J., Mrkvan, T., Chovanec, M., Kuchar, M., Betka, J., Boucek, V., Hladikova, M., Betka, J., Eckschlager, T., and Rihova, B. (2010) Regulatory T cells and their prognostic value for patients with squamous cell carcinoma of the head and neck, *Journal of cellular and molecular medicine 14*, 426-433.

[206] Lau, K. M., Cheng, S. H., Lo, K. W., Lee, S. A., Woo, J. K., van Hasselt, C. A., Lee, S. P., Rickinson, A. B., and Ng, M. H. (2007) Increase in circulating Foxp3+CD4+CD25(high) regulatory T cells in nasopharyngeal carcinoma patients, *British journal of cancer 96*, 617-622.

[207] Balermpas, P., Michel, Y., Wagenblast, J., Seitz, O., Weiss, C., Rodel, F., Rodel, C., and Fokas, E. (2014) Tumour-infiltrating lymphocytes predict response to definitive chemoradiotherapy in head and neck cancer, *British journal of cancer 110*, 501-509.

[208] Russell, S., Angell, T., Lechner, M., Liebertz, D., Correa, A., Sinha, U., Kokot, N., and Epstein, A. (2013) Immune cell infiltration patterns and survival in head and neck squamous cell carcinoma, *Head & neck oncology 5*, 24.

[209] Lim, K. P., Chun, N. A., Ismail, S. M., Abraham, M. T., Yusoff, M. N., Zain, R. B., Ngeow, W. C., Ponniah, S., and Cheong, S. C. (2014) CD4+CD25hiCD127low regulatory T cells are increased in oral squamous cell carcinoma patients, *PloS one 9*, e103975.

[210] Schwarz, S., Butz, M., Morsczeck, C., Reichert, T. E., and Driemel, O. (2008) Increased number of CD25 FoxP3 regulatory T cells in oral squamous cell carcinomas detected by chromogenic immunohistochemical double staining, *Journal of oral pathology & medicine : official publication of the International Association of Oral Pathologists and the American Academy of Oral Pathology 37*, 485-489.

[211] Strauss, L., Bergmann, C., Szczepanski, M., Gooding, W., Johnson, J. T., and Whiteside, T. L. (2007) A unique subset of CD4+CD25highFoxp3+ T cells secreting interleukin-10 and transforming growth factor-beta1 mediates suppression in the tumor microenvironment, *Clinical cancer research : an official journal of the American Association for Cancer Research 13*, 4345-4354.

[212] Kulkarni, D. P., Wadia, P. P., Pradhan, T. N., Pathak, A. K., and Chiplunkar, S. V. (2009) Mechanisms involved in the down-regulation of TCR zeta chain in tumor versus peripheral blood of oral cancer patients, *International journal of cancer. Journal international du cancer 124*, 1605-1613.
[213] Reichert, T. E., Strauss, L., Wagner, E. M., Gooding, W., and Whiteside, T. L. (2002) Signaling abnormalities, apoptosis, and reduced proliferation of circulating and tumor-infiltrating lymphocytes in patients with oral carcinoma, *Clinical cancer research : an official journal of the American Association for Cancer Research 8*, 3137-3145.
[214] Reichert, T. E., Scheuer, C., Day, R., Wagner, W., and Whiteside, T. L. (2001) The number of intratumoral dendritic cells and zeta-chain expression in T cells as prognostic and survival biomarkers in patients with oral carcinoma, *Cancer 91*, 2136-2147.
[215] Bukur, J., Jasinski, S., and Seliger, B. (2012) The role of classical and non-classical HLA class I antigens in human tumors, *Seminars in cancer biology 22*, 350-358.
[216] Seliger, B. (2012) Novel insights into the molecular mechanisms of HLA class I abnormalities, *Cancer immunology, immunotherapy : CII 61*, 249-254.
[217] Seliger, B., and Quandt, D. (2012) The expression, function, and clinical relevance of B7 family members in cancer, *Cancer immunology, immunotherapy : CII 61*, 1327-1341.
[218] Whiteside, T. L. (2002) Tumor-induced death of immune cells: its mechanisms and consequences, *Seminars in cancer biology 12*, 43-50.
[219] Tanguy Y. Seiwert, R. I. H., Shilpa Gupta, Ranee Mehra, Makoto Tahara, Raanan Berger, Se-Hoon Lee, Barbara Burtness, Dung T. Le, Karl Heath, Amy Blum, Marisa Dolled-Filhart, Kenneth Emancipator, Kumudu Pathiraja, Jonathan D. Cheng, Laura Q. Chow. (2015) Antitumor activity and safety of pembrolizumab in patients (pts) with advanced squamous cell carcinoma of the head and neck (SCCHN): Preliminary results from KEYNOTE-012 expansion cohort., *J Clin Oncol 33, 2015 (suppl; abstr LBA6008)*.
[220] Schlecht, N. F., Burk, R. D., Adrien, L., Dunne, A., Kawachi, N., Sarta, C., Chen, Q., Brandwein-Gensler, M., Prystowsky, M. B., Childs, G., Smith, R. V., and Belbin, T. J. (2007) Gene expression profiles in HPV-infected head and neck cancer, *The Journal of pathology 213*, 283-293.
[221] Partlova, S., Boucek, J., Kloudova, K., Lukesova, E., Zabrodsky, M., Grega, M., Fucikova, J., Truxova, I., Tachezy, R., Spisek, R., and Fialova, A. (2015) Distinct patterns of intratumoral immune cell infiltrates in patients with HPV-associated compared to non-virally induced head and neck squamous cell carcinoma, *Oncoimmunology 4*, e965570.
[222] Remmele, W., and Stegner, H. E. (1987) [Recommendation for uniform definition of an immunoreactive score (IRS) for immunohistochemical estrogen receptor detection (ER-ICA) in breast cancer tissue], *Der Pathologe 8*, 138-140.
[223] Mlecnik, B., Bindea, G., Angell, H. K., Maby, P., Angelova, M., Tougeron, D., Church, S. E., Lafontaine, L., Fischer, M., Fredriksen, T., Sasso, M., Bilocq, A. M., Kirilovsky, A., Obenauf, A. C., Hamieh, M., Berger, A., Bruneval, P., Tuech, J. J., Sabourin, J. C., Le Pessot, F., Mauillon, J., Rafii, A., Laurent-Puig, P., Speicher, M. R., Trajanoski, Z., Michel, P., Sesboue, R., Frebourg, T., Pages, F., Valge-Archer, V., Latouche, J. B., and Galon, J. (2016) Integrative Analyses of Colorectal Cancer Show Immunoscore Is a Stronger Predictor of Patient Survival Than Microsatellite Instability, *Immunity 44*, 698-711.
[224] Halama, N., Michel, S., Kloor, M., Zoernig, I., Benner, A., Spille, A., Pommerencke, T., von Knebel, D. M., Folprecht, G., Luber, B., Feyen, N., Martens, U. M., Beckhove, P., Gnjatic, S., Schirmacher, P., Herpel, E., Weitz, J., Grabe, N., and Jaeger, D. (2011) Localization and density of immune cells in the invasive margin of human colorectal cancer liver

metastases are prognostic for response to chemotherapy, *Cancer research 71*, 5670-5677.

[225] Brambilla, E., Le Teuff, G., Marguet, S., Lantuejoul, S., Dunant, A., Graziano, S., Pirker, R., Douillard, J. Y., Le Chevalier, T., Filipits, M., Rosell, R., Kratzke, R., Popper, H., Soria, J. C., Shepherd, F. A., Seymour, L., and Tsao, M. S. (2016) Prognostic Effect of Tumor Lymphocytic Infiltration in Resectable Non-Small-Cell Lung Cancer, *Journal of clinical oncology : official journal of the American Society of Clinical Oncology 34*, 1223-1230.

[226] Middel, P., Brauneck, S., Meyer, W., and Radzun, H. J. (2010) Chemokine-mediated distribution of dendritic cell subsets in renal cell carcinoma, *BMC cancer 10*, 578.

[227] Shang, B., Liu, Y., Jiang, S. J., and Liu, Y. (2015) Prognostic value of tumor-infiltrating FoxP3+ regulatory T cells in cancers: a systematic review and meta-analysis, *Scientific reports 5*, 15179.

[228] Ma, G. F., Miao, Q., Liu, Y. M., Gao, H., Lian, J. J., Wang, Y. N., Zeng, X. Q., Luo, T. C., Ma, L. L., Shen, Z. B., Sun, Y. H., and Chen, S. Y. (2014) High FoxP3 expression in tumour cells predicts better survival in gastric cancer and its role in tumour microenvironment, *British journal of cancer 110*, 1552-1560.

[229] Lin, Y. M., Sung, W. W., Hsieh, M. J., Tsai, S. C., Lai, H. W., Yang, S. M., Shen, K. H., Chen, M. K., Lee, H., Yeh, K. T., and Chen, C. J. (2015) High PD-L1 Expression Correlates with Metastasis and Poor Prognosis in Oral Squamous Cell Carcinoma, *PloS one 10*, e0142656.

[230] Joshi, P., Dutta, S., Chaturvedi, P., and Nair, S. (2014) Head and neck cancers in developing countries, *Rambam Maimonides medical journal 5*, e0009.

[231] Ritprajak, P., and Azuma, M. (2015) Intrinsic and extrinsic control of expression of the immunoregulatory molecule PD-L1 in epithelial cells and squamous cell carcinoma, *Oral oncology 51*, 221-228.

[232] Maby, P., Tougeron, D., Hamieh, M., Mlecnik, B., Kora, H., Bindea, G., Angell, H. K., Fredriksen, T., Elie, N., Fauquembergue, E., Drouet, A., Leprince, J., Benichou, J., Mauillon, J., Le Pessot, F., Sesboue, R., Tuech, J. J., Sabourin, J. C., Michel, P., Frebourg, T., Galon, J., and Latouche, J. B. (2015) Correlation between Density of CD8+ T-cell Infiltrate in Microsatellite Unstable Colorectal Cancers and Frameshift Mutations: A Rationale for Personalized Immunotherapy, *Cancer research 75*, 3446-3455.

[233] Galon, J., Mlecnik, B., Bindea, G., Angell, H. K., Berger, A., Lagorce, C., Lugli, A., Zlobec, I., Hartmann, A., Bifulco, C., Nagtegaal, I. D., Palmqvist, R., Masucci, G. V., Botti, G., Tatangelo, F., Delrio, P., Maio, M., Laghi, L., Grizzi, F., Asslaber, M., D'Arrigo, C., Vidal-Vanaclocha, F., Zavadova, E., Chouchane, L., Ohashi, P. S., Hafezi-Bakhtiari, S., Wouters, B. G., Roehrl, M., Nguyen, L., Kawakami, Y., Hazama, S., Okuno, K., Ogino, S., Gibbs, P., Waring, P., Sato, N., Torigoe, T., Itoh, K., Patel, P. S., Shukla, S. N., Wang, Y., Kopetz, S., Sinicrope, F. A., Scripcariu, V., Ascierto, P. A., Marincola, F. M., Fox, B. A., and Pages, F. (2014) Towards the introduction of the 'Immunoscore' in the classification of malignant tumours, *The Journal of pathology 232*, 199-209.

[234] Bindea, G., Mlecnik, B., Tosolini, M., Kirilovsky, A., Waldner, M., Obenauf, A. C., Angell, H., Fredriksen, T., Lafontaine, L., Berger, A., Bruneval, P., Fridman, W. H., Becker, C., Pages, F., Speicher, M. R., Trajanoski, Z., and Galon, J. (2013) Spatiotemporal dynamics of intratumoral immune cells reveal the immune landscape in human cancer, *Immunity 39*, 782-795.

[235] Green, V. L., Michno, A., Stafford, N. D., and Greenman, J. (2013) Increased prevalence of tumour infiltrating immune cells in oropharyngeal tumours in comparison to other

subsites: relationship to peripheral immunity, *Cancer immunology, immunotherapy : CII 62*, 863-873.
[236] Ritta, M., De Andrea, M., Mondini, M., Mazibrada, J., Giordano, C., Pecorari, G., Garzaro, M., Landolfo, V., Schena, M., Chiusa, L., and Landolfo, S. (2009) Cell cycle and viral and immunologic profiles of head and neck squamous cell carcinoma as predictable variables of tumor progression, *Head & neck 31*, 318-327.
[237] de Winde, C. M., Zuidscherwoude, M., Vasaturo, A., van der Schaaf, A., Figdor, C. G., and van Spriel, A. B. (2015) Multispectral imaging reveals the tissue distribution of tetraspanins in human lymphoid organs, *Histochemistry and cell biology 144*, 133-146.
[238] Meissner, M., Reichert, T. E., Kunkel, M., Gooding, W., Whiteside, T. L., Ferrone, S., and Seliger, B. (2005) Defects in the human leukocyte antigen class I antigen processing machinery in head and neck squamous cell carcinoma: association with clinical outcome, *Clinical cancer research : an official journal of the American Association for Cancer Research 11*, 2552-2560.
[239] Bandoh, N., Ogino, T., Katayama, A., Takahara, M., Katada, A., Hayashi, T., and Harabuchi, Y. (2010) HLA class I antigen and transporter associated with antigen processing downregulation in metastatic lesions of head and neck squamous cell carcinoma as a marker of poor prognosis, *Oncology reports 23*, 933-939.
[240] Corrales, L., Woo, S., and Gajewski, T. (2013) Extremely potent immunotherapeutic activity of a STING agonist in the B16 melanoma model in vivo, *Journal for immunotherapy of cancer 1*.
[241] Ishikawa, H., Ma, Z., and Barber, G. N. (2009) STING regulates intracellular DNA-mediated, type I interferon-dependent innate immunity, *Nature 461*, 788-792.
[242] Huang, L., Li, L., Lemos, H., Chandler, P. R., Pacholczyk, G., Baban, B., Barber, G. N., Hayakawa, Y., McGaha, T. L., Ravishankar, B., Munn, D. H., and Mellor, A. L. (2013) Cutting edge: DNA sensing via the STING adaptor in myeloid dendritic cells induces potent tolerogenic responses, *Journal of immunology 191*, 3509-3513.
[243] Ishikawa, H., and Barber, G. N. (2008) STING is an endoplasmic reticulum adaptor that facilitates innate immune signalling, *Nature 455*, 674-678.
[244] Chandra, D., Quispe-Tintaya, W., Jahangir, A., Asafu-Adjei, D., Ramos, I., Sintim, H. O., Zhou, J., Hayakawa, Y., Karaolis, D. K., and Gravekamp, C. (2014) STING Ligand c-di-GMP Improves Cancer Vaccination against Metastatic Breast Cancer, *Cancer immunology research 2*, 901-910.
[245] Fuertes, M. B., Kacha, A. K., Kline, J., Woo, S. R., Kranz, D. M., Murphy, K. M., and Gajewski, T. F. (2011) Host type I IFN signals are required for antitumor CD8+ T cell responses through CD8{alpha}+ dendritic cells, *The Journal of experimental medicine 208*, 2005-2016.
[246] Deng, L., Liang, H., Xu, M., Yang, X., Burnette, B., Arina, A., Li, X.-D., Mauceri, H., Beckett, M., Darga, T., Huang, X., Gajewski, T. F., Chen, Z. J., Fuemail, Y.-X., and Weichselbaumemail, R. R. (2014) STING-Dependent Cytosolic DNA Sensing Promotes Radiation-Induced Type I Interferon-Dependent Antitumor Immunity in Immunogenic Tumors, *Immunity 41*, 843-852.
[247] Woo, S. R., Fuertes, M. B., Corrales, L., Spranger, S., Furdyna, M. J., Leung, M. Y. K., Duggan, R., Wang, Y., Barber, G. N., Fitzgerald, K. A., Alegre, M. L., and Gajewski, T. F. (2014) STING-Dependent Cytosolic DNA Sensing Mediates Innate Immune Recognition of Immunogenic Tumors, *Immunity 41*, 830-842.
[248] Baird, J. R., Friedman, D., Cottam, B., Dubensky, T. W., Jr., Kanne, D. B., Bambina, S., Bahjat, K., Crittenden, M. R., and Gough, M. J. (2016) Radiotherapy Combined with

Novel STING-Targeting Oligonucleotides Results in Regression of Established Tumors, *Cancer research 76*, 50-61.
[249] Sanchez, P. J., and Kedl, R. M. (2012) An alternative signal 3: CD8(+) T cell memory independent of IL-12 and type I IFN is dependent on CD27/OX40 signaling, *Vaccine 30*, 1154-1161.
[250] Schurich, A., Pallett, L. J., Lubowiecki, M., Singh, H. D., Gill, U. S., Kennedy, P. T., Nastouli, E., Tanwar, S., Rosenberg, W., and Maini, M. K. (2013) The third signal cytokine IL-12 rescues the anti-viral function of exhausted HBV-specific CD8 T cells, *PLoS pathogens 9*, e1003208.
[251] Starbeck-Miller, G. R., Xue, H. H., and Harty, J. T. (2014) IL-12 and type I interferon prolong the division of activated CD8 T cells by maintaining high-affinity IL-2 signaling in vivo, *The Journal of experimental medicine 211*, 105-120.
[252] Yanagida, T., Kato, T., Igarashi, O., Inoue, T., and Nariuchi, H. (1994) Second signal activity of IL-12 on the proliferation and IL-2R expression of T helper cell-1 clone, *Journal of immunology 152*, 4919-4928.
[253] Hu, H. M., Urba, W. J., and Fox, B. A. (1998) Gene-modified tumor vaccine with therapeutic potential shifts tumor-specific T cell response from a type 2 to a type 1 cytokine profile, *Journal of immunology 161*, 3033-3041.
[254] Au, G. G., Beagley, L. G., Haley, E. S., Barry, R. D., and Shafren, D. R. (2011) Oncolysis of malignant human melanoma tumors by Coxsackieviruses A13, A15 and A18, *Virol J 8*, 22.
[255] Sojka, D. K., Huang, Y. H., and Fowell, D. J. (2008) Mechanisms of regulatory T-cell suppression - a diverse arsenal for a moving target, *Immunology 124*, 13-22.
[256] Liu, C., Workman, C. J., and Vignali, D. A. (2016) Targeting regulatory T cells in tumors, *FEBS J 283*, 2731-2748.
[257] Whiteside, T. L., Schuler, P., and Schilling, B. (2012) Induced and natural regulatory T cells in human cancer, *Expert opinion on biological therapy 12*, 1383-1397.